UNIVERSITY OF TECHNOLOGY SYDNEY
Faculty of Science

DEVELOPMENT OF A REPORTER FOR PREDICTION OF MEMBRANE FOULING POTENTIAL AND APPLICATION OF NITRIC OXIDE FOR BIOFOULING CONTROL

By

THI TU UYEN BUI

A Thesis Submitted in Fulfillment of the Requirements for the Degree

Master of Science

Sydney, Australia

April 2019

CERTIFICATE OF AUTHORSHIP/ ORIGINALITY

I certify that the work in this thesis has not been previously submitted for a degree nor has it been submitted as a part of the requirements for other degree except as a fully acknowledged within the text.

I also certify that the thesis has been written by me. Any help that I have received in my research and in the preparation of the thesis itself has been fully acknowledged. In addition, I certify that all information sources and literature used are quoted in the thesis.

This research is supported by an Australian Government Research Training Program.

8 April 2019

Signature of candidate

Production Note:
Signature removed prior to publication.

Thi Tu Uyen Bui

ABSTRACT

DEVELOPMENT OF A REPORTER FOR PREDICTION OF MEMBRANE FOULING POTENTIAL AND APPLICATION OF NITRIC OXIDE FOR BIOFOULING CONTROL

By

Thi Tu Uyen Bui

Membrane fouling that results in increases in operational and maintenance costs is a major obstacle to the widespread application of membrane technology [2]. The concentration of assimilable organic carbon (AOC) is directly correlated with the growth of heterotrophic bacteria in water systems. AOC has been widely used as a biofouling indicator for the prediction of biofouling in reverse osmosis (RO) systems [3-5]. In addition to new methodologies to predict fouling, new membrane cleaning technologies are also being developed. One new cleaning method is the application of nitric oxide (NO), which is a biologically active signaling molecule that has been shown to induce biofilm dispersal at nanomolar concentrations [6-9].

In this study, potential AOC reporter strains were isolated for use in desalination RO systems. The results show that strains BLS2, CBSW3 and CBSW4 grew on seawater medium, with maximum cell densities of 5.1 x 10^5, 4.5 x 10^5 and 7.2 x 10^5 colony forming unit (CFU) ml^{-1}, respectively. In addition, all three strains were able to metabolise humic substances which are a major component of AOC in seawater, reaching maximum cell numbers of 5.0 x 10^4 - 2.1 x 10^5 CFU ml^{-1}. With *V. cholerae* A1552 (pUC19-*luxAB*), there was a linear relationship between bioluminescent intensity and glucose concentrations ranging from 0 to 100 µg C L^{-1}, with a coefficient (R^2) of 0.9761. The limit detection was 20 µg C L^{-1}. Our findings provide a more rapid AOC assay, which can quickly determine AOC concentrations within 10 min compared to 30 min performed by *V. fischeri* MJ1 [10, 11].

Pyrosequencing analysis revealed that there was a total of 1,372,739 16S rDNA gene V4 region reads obtained from 9 activated sludge and 10 biofilm samples. RDP Classifier identified 36 phyla, 101 classes and 527 genera of bacteria. The significant changes in relative abundance of the most dominant OTUs associated with the sudden TMP increases demonstrated that species of unclassified *Bacteroidetes*, *Saprospiraceae*, *Comamonadaceae*

and unclassified TM7-3 may play important roles in membrane fouling, and that *Saprospiraceae* and unclassified TM7-3 may be primary colonisers of the membrane. Unclassified *Bacteroidetes* and *Comamonadaceae* (*Comamonas* in particular) may be secondary colonisers of the biofilms on the MBR membranes. Treatment of the membranes with 40 μM DETA NONOate led to a reduction of the TMP by 35% compared to 21% obtained by control distilled water backwash (P value < 0.05), indicating that DETA NONOate was effective in delaying TMP increase.

Thesis directed by

Principle supervisor:
Associate Professor Diane McDougald
The ithree Institute, Faculty of Science

Co-supervisor:
Professor Saravanamuth Vigneswaran
School of Civil and Environmental Engineering,
Faculty of Engineering and Information Technology

ACKNOWLEDGEMENTS

I am especially thankful to my principle supervisor, Associate Professor Diane McDougald, for her direction, knowledge, patience, motivation and support throughout my study from the beginning to its completion. Her precious comments and suggestions helped me to develop my knowledge and skills of doing this research. I would like to thank Associate Professor Scott Rice and my co-supervisor, Professor Saravanamuth Vigneswaran for their valuable suggestions and support.

I am heartily thankful to my academic assistant, Dr. Shuyang Sun, for his ideas, guidance, assistance and continuous encouragement during my study. I was lucky to have him as my academic assistant. I would like to express my appreciation to Dr. Mohammed Johir for his direction and support working in the Environmental Engineering Laboratory.

In my daily work, I was really fortunate to be a member of a friendly and cheerful group. My appreciation goes to my dear colleagues, Gustavo, Parisa, Mozammel, William, Nireen and Yunju, for their generous help in various aspects of this research. I would like to thank Youngkwon for his assistance for providing fibre membranes for the membrane bioreactor. I also wish to thank the ithree Institute for providing a fantastic atmosphere for doing research.

I would like to thank my family for their love and support. I could not have completed my thesis without their support and encouragement.

TABLE OF CONTENTS

LIST OF TABLES

LIST OF FIGURES

ABBREVIATIONS

AFLP: Amplified fragment length polymorphism

AGRF: Australian Genome Research Facility

AOC: Assimilable organic carbon

ASW: Artificial seawater

Atm: Atmosphere

ATP: Adenosine triphosphate

BDOC: Biodegradable dissolved organic carbon

BFM: Berlin filtration method

BioEdit: Biological Sequence Alignment Editor

BLAST: Basic Local Alignment Search Tool

BOD: Biochemical oxygen demand

BOM: Biodegradable organic matter

cAMP: Cyclic adenosine monophosphate

C-di-GMP: Cyclic diguanylate monophosphate

CDOC: Chromatographable dissolved organic carbon

CFU: Colony forming unit

ChromCALC: Chromatography Calculator

COD: Chemical oxygen demand

Da: Daltons

DAP: Diaminopimelic acid auxotroph

DETA: Diethylenetriamine

DGGE: Denaturing gradient gel electrophoresis

DOC: Dissolved organic carbon

EBS: Environmental Business Specialists

EPS: Extracellular polymeric substances

F/M: Food to microorganisms

FISH: Fluorescent in situ hybridization

FMNH2: Flavin mononucleotide

HRT: Hydraulic retention time

KPa: Kilopascal

LB: Luria-Bertani

LC-OCD: Liquid chromatography - organic carbon detection

LMW: Low molecular weight

MAHMA NONOate: 6-(2-hydroxy-1-methyl-2-nitrosohydrazino)-N-methyl-1-hexanamine

MBR: Membrane bioreactor

MEGA: Molecular Evolutionary Genetics Analysis

MF: Microfiltration

MFI or $MFI_{0.45}$: Modified fouling index

MIC: Minimal inhibitory concentration

MLSS: Mixed liquor suspended solids

MLVSS: Mixed liquor volatile suspended solids

NCBI: National Center for Biotechnology Information

NF: Nanofiltration

NO: Nitric oxide

NOM: Natural organic material

NTU: Nephelometric turbidity unit

OCD: Organic carbon detection

OLR: Organic loading rate

OND: Organic nitrogen detector

OTU: Operational taxonomic unit

PAOs: Polyphosphate accumulating organisms

PAS: Per-Arnt-Sim

PBS: Phosphate buffered saline

PCoA: Principal coordinate analysis

PCR: Polymerase chain reaction

POC: Particulate organic carbon

PROLI NONOate: 1-(hydroxyl-NNO-azoxy)-L-proline, disodium salt

PVDF: Polyninylidene fluoride

QIIME: Quantitative Insights into Microbial Ecology

QS: Quorum sensing

RDP: Ribosomal database project

RLU: Relative light unit

RO: Reverse osmosis

ROC: Reverse osmosis concentrate

Rpm: revolutions per minute

SCELSE: Singapore Centre for Environment Life Science Engineering

SDI: Silt density index

SIMS: Sydney Institute of Marine Science

SMPs: Soluble microbial products

SNP: Sodium nitroprusside

SRT: Solids retention time

SWRO: seawater reverse osmosis

TMP: Transmembrane pressure

TOC: Total organic carbon

T-RFLP: Terminal restriction fragment length polymorphism

TSS: Total suspended solid

UF: Ultrafiltration

UV: Ultraviolet

UVD: Ultraviolet detector

VFM: VITO fouling measurement

VOCs: Volatile organic chemicals

CHAPTER 1

INTRODUCTION

1.1. Background

Water is considered to be one of the most fundamental resources on Earth and is necessary for economic, social and cultural development. It has been long thought to be plentiful. However, with the growth of the global population, the demand for clean water has increased and its scarcity is now an undeniable issue. Membrane technologies, for the conversion of seawater and wastewater into clean and potable water, play important roles in water sustainability. Membrane filtration is now competitive with conventional methods for water purification because of its advantages, including the production of high-quality effluent.

Australia occupies 5.6% of the world's landmass, but receives just over 1% of the global fresh water resources, and thus, is considered to be one of the driest inhabitable places on Earth [12]. Despite the limited water resources, Australia is the third largest consumer of water in the world. Agriculture and domestic use accounted for 67% and 9% of water consumption in 2001 - 2002, respectively. In the future, many capital cities in Australia will not have sufficient water to meet growing populations and economic development. Therefore, water treatment technologies, including desalination, membrane bioreactors and biofilters, play key roles in increasing alternative water resources. A considerable percentage of water in Australia comes from recycling or desalination processes. For example, in 2013 to 2014, 39% of Perth's and 41% of Adelaide's water was obtained by desalination and all cities consumed some recycled water, e.g. Canberra (8%), southeast Queensland (7%), Sydney (7%) and Melbourne (4%) [12].

Membrane filtration uses a filter that allows water to flow through, while retaining contaminants, such as suspended solids and other substances. There are two kinds of

membranes, low pressure (1 – 7 atmospheres (atm)) and high-pressure membranes (5 – 150 atm). Low pressure membranes include microfiltration (MF) (0.1 – 10 μm) and ultrafiltration membranes (UF) (10 – 100 nm) and are usually used for the removal of colloids and macromolecules. High pressure membranes are used for nanofiltration (NF) (~ 1 nm) and RO (~ 0.1 nm) processes which remove small organics and ions [1]. Membrane technologies have been widely applied in water treatment applications because they are efficient and cost-effective processes for producing municipal and industrial grade water.

Membrane fouling, which is the result of accumulation of foulants on the membrane surface, is a major problem for membrane technologies. There are numerous causes of membrane fouling, including the deposition of minerals, clay and organic matter as well as the growth of microorganisms on the membrane. The fouling caused by the deposition of substances can be reduced by decreasing the foulant concentration in the feed water. However, biofilm formation by bacteria on membrane surfaces is a complicated process that is harder to control, and is considered to be "the Achilles heel of membrane processes" [13]. Microorganisms growing on the membrane are encased within extracellular polymeric substances (EPS) and are therefore, less sensitive to chemical cleaning [14]. As a result, the use of chemicals to remove biofilms generally only has a temporary effect. Even if chemical treatment removes a large proportion of the attached biofilm, the remaining cells can regrow using biodegradable substances in the feed water [15, 16]. Furthermore, the application of oxidising biocides such as chlorine or ozone is incompatible with long-term use of polyamide membranes because of oxidative damage to the membrane [15]. Four factors that affect membrane fouling include the material used for the membrane, the characteristics of the biomass in the feed water, the feed water characteristics and the operating conditions [17].

Pre-treatment processes are applied to produce low fouling potential feed water. The pre-treatment of the feed water prior to membrane filtration removes some foulants like colloidal materials, microorganisms, organic matter, humics and fulvic acids [18]. Considerable research on the influence of organics in membrane fouling in RO systems revealed that assimilable organic carbon (AOC), a small portion of the dissolved organic carbon (DOC), is easily assimilated by bacteria and converted into biomass [3, 19]. Thus, AOC is largely responsible for the growth of heterotrophic bacteria in RO systems. The removal of AOC

compounds in feed water by applying appropriate pre-treatment processes is one way to control RO membrane fouling. Therefore, the AOC concentration is used as a standardised measurement to predict membrane fouling in RO processes. However, current available AOC assays are time-consuming and laborious. Furthermore, previous AOC studies focused on the quantification of AOC using the two strains *Pseudomonas fluorescens* P-17 and *Spirillum* sp. NOX, which are indigenous in drinking water and not appropriate for the quantification of AOC concentrations in seawater samples [4, 20]. Two marine bacteria used for AOC quantification are *Vibrio fischeri* and *Vibrio harveyi*, but these two species have metabolic limitations that leads to underestimation of the AOC concentration. Therefore, it is necessary to develop new AOC test strains to improve AOC assays for seawater samples. One of the objectives of this thesis was to develop a new rapid AOC detection method for seawater to allow prediction of the biofouling potential of the feed water. A more accurate and rapid AOC detection method will help to reduce or prevent biofilm formation in RO systems.

In addition to pre-treatment of feed water as a means to control membrane fouling, the induction of biofilm dispersal with nitric oxide (NO) may also reduce fouling on the membrane [6]. Bacterial biofilms are highly dynamic communities that undergo dispersal events which allow the attached bacteria to revert to free-living planktonic cells to allow colonisation of new surfaces [7]. The detachment of biofilm cells involves multiple inducers and signalling pathways, including the concentration of nutrients, oxygen and iron, presence of NO, D-amino acids, fatty acids, and cyclic adenosine monophosphate (cAMP) and cyclic diguanylate monophosphate (c-di-GMP) [21]. The application of NO as a biofilm dispersal cue is an attractive strategy for biofilm control in membrane technologies because of its short half-life, the lack of harmful residues and the ability to use low, non-toxic doses (picomolar to nanomolar range) [22]. Previous studies reported that NO donor compounds, such as sodium nitroprusside (SNP), 6-(2-hydroxy-1-methyl-2-nitrosohydrazino)-N-methyl-1-hexanamine (MAHMA NONOate) and 1-(hydroxyl-NNO-azoxy)-L-proline, disodium salt (PROLI NONOate) reduced bacterial biofilm biovolumes of *Pseudomonas aeruginosa* by 30 - 40% after 1 - 24 h of exposure [9, 23]. In this study, the potential for use of an NO donor to delay a rapid transmembrane pressure (TMP) increase in a laboratory-scale submerged membrane bioreactor (MBR) has been determined. In addition, the microbial community in

the MBR was characterised to provide information on the specific microorganisms responsible for biofouling, and those that remain after treatment of the membrane with NO. A better understanding of the microbial community in an MBR can help to prevent biofouling and to inform on proper cleaning procedures.

1.2. Research Objectives

It is essential that membrane fouling be controlled because of the considerable expense caused by downtime during cleaning and replacement of the membrane in membrane systems. In cases where membrane fouling is not controlled or prevented, there will be loss of productivity, low water quality and increased operating and maintenance costs due to the higher pressure needed to push water across the membrane and a lower permeate flow. For sizeable water treatment plants, these drawbacks can be prohibitive. Therefore, this thesis focuses on development of a biofouling prediction assay for RO systems, as well as the application of NO as a strategy to control biofouling in a laboratory-scale MBR. The thesis will thus address two aims:

i. Aim 1: Development of a sensitive bioluminescent reporter technology for AOC quantification.

ii. Aim 2: Characterisation of the microbial community in an MBR and efficacy of NO for reduction of TMP.

1.3. Thesis Organisation

This thesis includes five chapters. Chapter 1, the Introduction, describes the background information on the necessity of this study, as well as the targets of the study. The Literature Review discussed in Chapter 2 presents existing literature on membrane technologies, membrane fouling and fouling control strategies. In Chapter 3, the experimental design and the results and discussion on the isolation and selection of AOC test strains, the construction of AOC reporter strains and the development of bioluminescent AOC tests are demonstrated. Chapter 4 focuses on the efficiency of DETA NONOate for reduction of TMP and the

characterisation of bacterial community in a laboratory-scale submerged MBR. Chapter 5 presents the conclusions and recommendations for future work.

CHAPTER 2

LITERATURE REVIEW

2.1. Water Treatment Technologies

An understanding of the nature of incoming water sources is important for the selection of water treatment methods. The raw water coming in for treatment is either natural water (fresh or salt water) or wastewater (municipal and industrial wastewater). The characteristics of natural water are influenced by atmospheric conditions and seasonal variation, such as temperature and rainfall. The composition of natural waters includes colloidal and organic compounds (polysaccharides, proteins, amino sugars and polypeptides), humic compounds, inorganic substances (ammonia, nitrate, sulphides and salts) and microorganisms. Different sources of water are extremely variable in their composition. While municipal wastewater is generally similar in components, industrial wastewater varies and is dependent on production processes. The quality of wastewater refers to its physical (colour, odour, temperature and turbidity), chemical (organic and inorganic components) and biological characteristics (the microorganisms present). Different water treatment methods are used for different purposes, including production of drinking water or the removal of contaminants that are harmful to human health and/or the environment [24]. Natural water is used as a source for production of drinking water, whereas wastewater is treated to produce water for use in some industries, activities and other purposes.

2.1.1. Pre-treatment Processes

The objectives of pre-treatment processes are the removal of large particles hampering the downstream treatment processes and the production of low fouling potential feed water for RO water purification. Depending on the quality of raw water, the primary treatment may consist of all or some of the following steps; screening, coagulation, flocculation, sedimentation, filtration, chemical precipitation, adsorption, disinfection, MF and UF.

2.1.1.1. Pre-treatment Processes for Fresh Water

Fresh water, particularly surface water, contains suspended solids and larger objects including tree branches and aquatic creatures. The removal of these materials is required prior to treatment. In addition, depending on the geology of the drainage basin and contamination inputs, fresh water may have a wide range of pH values. Therefore, the incoming water is adjusted to a neutral value of pH 7 for further treatment processes [25].

2.1.1.1.1. Screening

Screening is the process of removing objects of different sizes, either large debris or large floating or suspended materials to protect downstream equipment from damage. This process is not necessary for groundwater treatment processes. Screening devices may consist of a vertical bar screen, a rotating perforated plate drum or microstrainers. The former is used to remove large objects, while the drum removes suspended solids and algae, while the microstrainer removes finer material around 2 mm in size [25].

2.1.1.1.2. Adjustment of pH

Typical methods used to neutralise the feed water include addition of acids (or bases) to alkaline (or acidic) wastewater. Limestone beds, lime slurries, caustic soda, sodium carbonate and ammonia are commonly used for the neutralisation of acidic wastewaters. For highly acidic waters, stripping dissolved carbon dioxide from the raw water using forced draft degasifiers is recommended. In contrast, to lower the pH, acids, such as carbonic acid, hydrochloric acid and sulphuric acid are added to alkaline waters [26].

2.1.1.2. Pre-treatment Processes for Seawater

Seawater contains a mixture of various inorganic salts, organic compounds, marine organisms and other small particles. The quality of seawater is determined by the concentration of inorganic and organic matters and the number of marine organisms [26]. Seawater undergoes a number of pre-treatment processes prior to RO treatment to minimise membrane fouling, as well as for improving the quality of effluent.

2.1.1.2.1. Screening

The process is described in 2.1.1.1.1.

2.1.1.2.2. Disinfection

To avoid membrane fouling, it is essential to remove microorganisms prior to RO treatment. Sodium hypochlorite or chlorine dioxide is generally used for treatment to prevent the growth of marine organisms, such as algae, mussels, clams and microorganisms. In addition to chemical disinfection, ultraviolet (UV) disinfection is also used to combat microbiological contamination. While chemical disinfectants inactive microorganisms by destroying their cellular structures or interfering with metabolism, UV light damages their nucleic acids which prevents replication [26].

2.1.1.2.3. Coagulation and Flocculation

Coagulation is a process where chemicals, such as aluminium sulphate, iron (III) chloride and lime are added to enhance sedimentation of suspended substances in feed water. After the addition of chemicals, coagulated particles flocculate which enhances sedimentation processes [26].

2.1.1.2.4. Sedimentation

The sedimentation process refers to a function of the particle settling velocity. The removal of flocs is based on the differences in specific gravity between suspended solids and the bulk of the liquid. Sedimentation basins or clarifiers are large tanks in which solids settle to the bottom by gravity [26].

2.1.1.2.5. Antiscalants

Typical seawater contains high concentrations of calcium, sulphate and bicarbonate ions which result in mineral scale that deposits on the membrane surface. Antiscalants are added into the feed water to prevent scaling by interfering with the reaction between calcium and bicarbonate [18].

2.1.1.2.6. MF or UF

MF or UF are used as pre-treatment processes in desalination due to their effectiveness in removing potential foulants in RO feed water. In membrane filtration pre-treatment, seawater

is forced through a membrane to remove particles, which are larger than the pore size of membrane [26].

2.1.1.3. Pre-treatment Processes for Municipal Wastewater

Typical urban wastewater is composed mainly of organic materials, either in soluble or colloidal form or as suspended substances. These organic compounds consist of proteins (40 – 60%), carbohydrates (25 – 50%), fats and oils (10%) and a small percentage of phenols, pesticides and surfactants [27]. The pre-treatment of domestic wastewater may include some of the processes described in 2.1.1.2, such as screening, coagulation, flocculation and sedimentation. However, flotation may be required to remove low gravity solids which are usually present in domestic wastewater.

In a flotation process, suspended solids, which have low specific gravities, such as fats, oils, grease and emulsions that are difficult to settle, can be removed by dissolved air floatation. In this process, gas is dissolved into the feed water under pressure to create tiny bubbles which attach to the solids and float them to the top when the pressure drops [26].

2.1.1.4. Pre-treatment Processes for Industrial Wastewater

The primary treatment of industrial wastewater includes the same processes as those applied for urban wastewater. Industrial sewage is highly variable in volume and composition. Depending on its specific characteristics, extra steps, including neutralisation, the reduction and oxidation of inorganic substances and the precipitation of cations and anions may be required [24]. Industrial wastewater containing high concentrations of salt must be pre-treated if used as RO feed water to minimise biofouling.

2.1.2. Filtration

Filtration is the process of removing contaminants by passing raw water through a semi-permeable fabric (membrane) or porous material (granular). The media filtration systems refer to slow and rapid sand filtration, diatomaceous earth filtration, direct filtration and packaged filtration, while membrane filtration is either low or high membrane pressure filtration.

2.1.2.1. Membrane Filtration

A membrane is a thin sheet of semi-permeable material that retains certain substances when pressure is applied across the membrane. Solids naturally flow from areas of high concentration to low concentration. By the application of external pressure, these substances can be forced to move from areas of low to high concentration. There are four different membrane groups based on the size of retentates (Figure 2.1), i.e. MF, UF, NF and RO. Because NF and RO membranes have much smaller pore sizes than MF and UF membranes, the pressures required for RO and NF (5 – 150 atm) are much higher than for MF and UF (1 - 7 atm). Due to the application of higher pressure, the overall yield of NF and RO is much lower compared to MF and UF filtration systems [1].

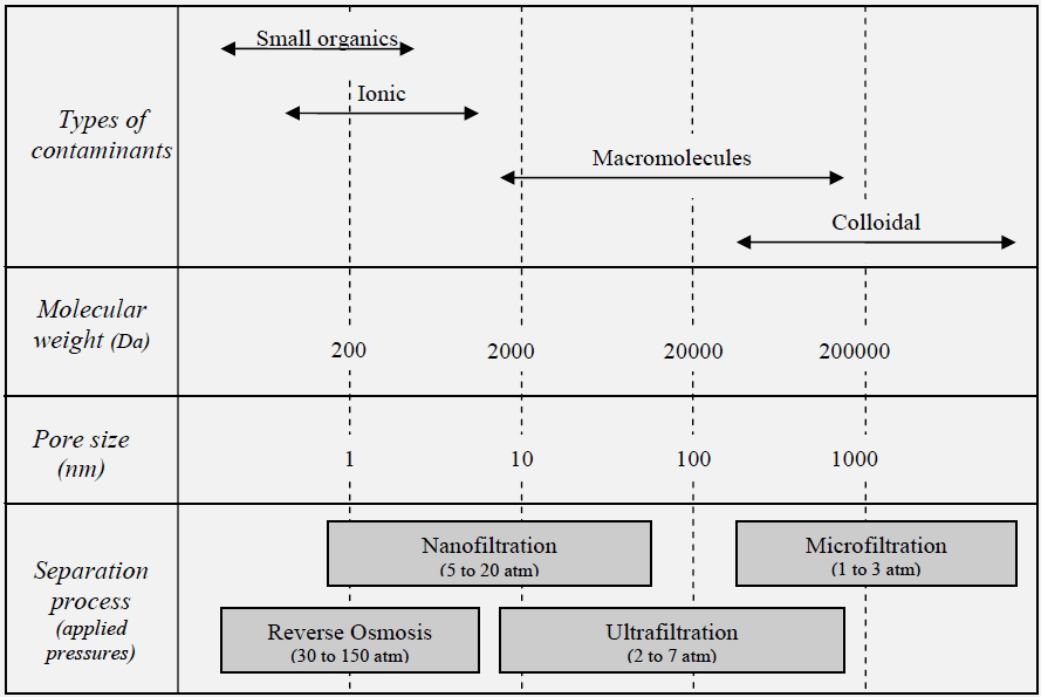

Figure 2.1. Types of membrane filtration based on membrane pore sizes. The different categories from smallest to largest pore size, including RO, NF, UF and MF. Pressure required for separation process decreases as membrane pore size increases [1].

Filtration membranes are made from a wide range of materials, including cellulose, polyamides, polysulfones, charged polysulfones, polyacrylonitrile, polyvinylidene difluoride, polyethersulfone, polyethylene and polypropylene. These polymeric materials have different properties including surface charge, degree of hydrophobicity, pH and chemical and physical resistance. However, these hydrophobic membranes have a higher

fouling propensity compared to hydrophilic membranes because the interaction between the membrane and foulants is mainly hydrophobic. Therefore, some modifications like chemical oxidation, organic chemical reactions and plasma treatments, are applied to achieve more hydrophilic surfaces [28].

The pore sizes of MF membranes range from 0.1 to 10 μm. MF is mainly used in the removal of large particles, including sand, silts, clays, colloids and microorganisms, while small materials, such as ions, dissolved organic matters, bacteria and viruses are able to cross the membranes. This technology has been widely applied in food, beverage and bio-processing industries for treating wastewater before discharging it to receiving waters [1].

UF membrane have pore sizes of 0.002 – 0.1 μm. The process of UF, similar to MF, does not require high pressure to remove high molecular-weight substances, but with the smaller pore sizes, UF is able to reject smaller particles, polypeptides, humic materials and viruses which may pass through MF membranes. The application of UF is frequently used in the pre-treatment of surface water, seawater and industrial sewage upstream of RO treatment [1].

NF membranes have a thin-film composite layer (1 – 10 nm) on the top of a membrane having pore sizes of 50 – 150 μm. In NF treatment, multivalent ions and uncharged solutes are removed, while some smaller hydrated monovalent salts, such as sodium and chloride ions, can pass through the membrane. NF is frequently applied in the treatment of wastewater from production of pharmaceuticals, fine chemicals and flavour industries and in particular water softening which refers to the process of removing calcium, magnesium and other cations in hard water [1].

RO purification technology can remove up to 99% of contaminants including dissolved salts, particles, colloids, organics and bacteria. The pore sizes of RO membranes are smaller than NF. RO membranes are designed to allow only water molecules pass through the membrane while rejecting nearly all salts, either multivalent salts or monovalent ions. The pressure required for RO is from 15 – 74 atm, but in some applications where there is a high salt concentration the pressure required may be up to 150 atm. This technology has been widely used for purification of seawater for the production of drinking water and for the removal of salts and other materials from industrial sewage [1]. MF and UF can also be used in cases

where NF and RO are used because the two formers are more conventional and have cost savings, either from the operation or the maintenance costs.

2.1.2.1.1. Desalination

Desalination is a process for producing clean water by removing salts, bacteria and pollutants from salty water. This advanced membrane technology is used in a wide range of applications including the production of drinking water from seawater, desalting water for agriculture, mining and the removal or recovery of heavy metals from saline wastewater [29]. Desalination is mainly divided into two categories, membrane processes and thermal processes. Both of them require energy for operation.

RO is a membrane filtration system for desalination processes. In the RO process, a portion of feed water passes through the membrane, while the retained water, the reverse osmosis concentrate (ROC) increases in salt content and is discharged without passing through the membrane. Without the discharge, the ROC continues to increase in salinity content, which results in super-saturation of salts. There are several systems involved in RO desalination plants, including pre-treatment systems, high pressure pumps, membrane systems and post-treatment systems [30]. The components of an RO desalination plant are illustrated in Figure 2.2.

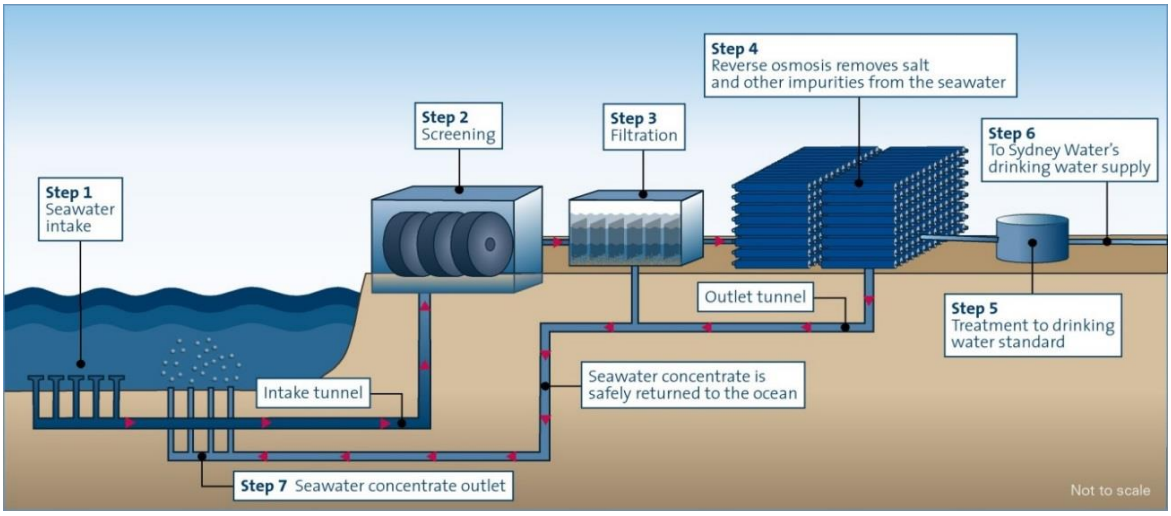

Figure 2.2. Sydney RO desalination plant (*Sydney Water*, 2007). The RO plant consists of four major systems: seawater intake (step 1), pre-treatment (steps 2 and 3), desalination (step 4) and post-treatment (steps 5, 6 and 7).

Pre-treatment processes used in desalination include screening, coagulation, sedimentation and MF or UF for removal of contaminants which are responsible for membrane fouling. High pressure pumps supply the pressure needed to pass feed water through the RO membrane. Depending on the characteristics of raw water, the pressure ranges from 10 atm for normal brackish water to 68 atm for seawater. The membrane system is composed of a pressure vessel and a semi-permeable membrane. RO membranes are either spiral wound or hollow fibre. The former is more widely used for desalination than the latter. Spiral wound RO membranes are constructed from flat sheet membranes wrapped around a central collecting tube. The feed water flows into the flat sheet membrane under pressure and the treated water is collected in the central tube. In a hollow fibre configuration, hollow fibre membranes are placed in a pressure vessel. The feed water is introduced into the vessel along the outside of the membrane. Under applied pressure, the feed water passes through the membrane and into the hollow centre. Post-treatment is the final step in desalination which prepares the treated water for distribution. The treatment frequently involves adjustment of the pH and disinfection. If the effluent is discharged to a receiving source, it is essential to ensure the same water quality in both the discharge and the receiving source [30].

Thermal desalination or distillation technologies are the processes of generating steam from saline water by the application of heat. The steam is then condensed to low salinity water which can be used for municipal and industrial purposes or irrigation. In thermal treatment, inorganic salts and high molecular-weight substances are not volatile and thus are not removed from the feed water, but some volatile petroleum chemicals can contaminate the condensed vapour.

2.1.2.1.2. MBRs

MBRs have the combined advantages of activated sludge and membrane filtration processes, typically either MF or UF. MBRs are widely used in the treatment of municipal wastewater produced in households, such as kitchen, shower and laundry wastewater. These types of wastewater contain suspended substances and limited chemicals that are easily treated by activated sludge processes. Previous studies showed that MBRs can effectively reduce biochemical oxygen demand (BOD), total organic carbon (TOC) and completely remove total suspended solid (TSS) [31]. Some industrial sewage can be treated by MBRs as well,

but feed waters containing toxic chemicals and heavy metals require more advanced treatments like NF or RO [29].

There are many variations of MBR systems, but the two most popular configurations are submerged and external membrane MBRs. In a submerged MBR (dead-end mode) membrane modules are installed in the activated sludge reactor vessel (Figure 2.3), while in an external MBR (side-stream MBR) the membrane modules are located outside the reactor (Figure 2.4). The wastewater is pumped through the membranes and then the retentate returned to the bioreactor [32]. The submerged configuration is more widely used due to the lower energy consumption of the dead-end design. Both designs provide a shear force over the membrane surface that promotes permeation flux and prevents fouling. The shear is supplied by the pumping of fluid in a side-stream MBR, while an air diffuser system is used in a submerged MBR. The latter design consumes less energy [28]. A significant obstacle in the application of MBRs for wastewater treatment is the flux decline over time as a result of membrane fouling. The external membranes need to be cleaned more frequently than the submerged membranes because the fouling is partly removed by aeration in the dead-end MBR. In general, submerged MBRs must be cleaned after 6 – 8 months of operation while external MBRs are cleaned after 2 months of operation.

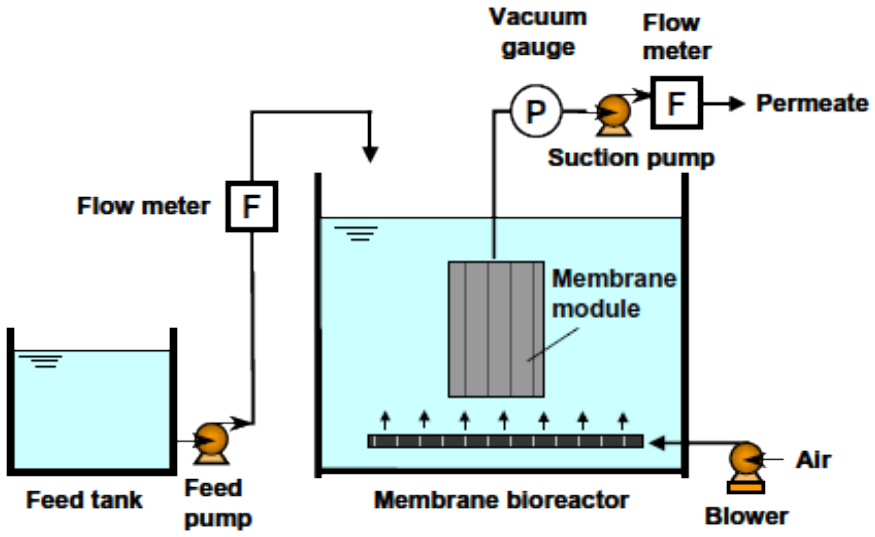

Figure 2.3. Submerge membrane bioreactor (*Trident Innovations*, 2012). The configuration consists of a mixed aeration tank in which membranes are immersed. The influent is fed to the bioreactor by using a feed pump. The aerobic condition is maintained by an air blower. A suction pump is used to extract permeate from the membranes.

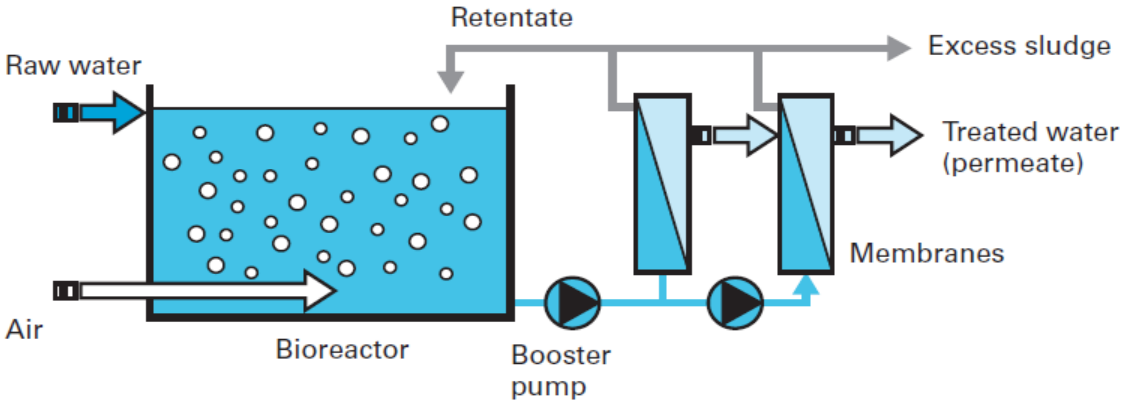

Figure 2.4. External membrane bioreactor (*SUEZ' degremont® water handbook*). The mixed liquor is circulated outside of the bioreactor to membrane modules enclosed in castings, where water is separated from the sludge by pressure. The concentrated sludge (retentate) is recycled back into the reactor.

Activated sludge is composed of sludge particles produced in wastewater by the growth of microorganisms. These particles are complex mixed microbial communities of approximately 95 percent bacteria and the remaining 5 percent made up of other organisms, including fungi, protozoa, rotifers, nematodes, invertebrates and viruses. The activated sludge process refers to biological treatment of organic and some inorganic matters by microorganisms which is then converted into cell biomass. In activated sludge processes, the mixed microbial communities use organic matter (carbon, nitrogen and phosphorus source) in feed water as food and energy sources for survival and reproduction. This is referred to as the BOD, which is the measure of how much oxygen is needed for the digestion of waste by the microbial community. Therefore, the aeration in the bioreactor needs to be maintained to allow the digestion of waste as well as to facilitate contact between the waste and the microorganisms. High BOD concentrations in wastewater stimulates the activity of microorganisms and increases oxidation rates. Insufficient oxygen results in the death of aerobic organisms and the production of foul-smelling by-products of anaerobic processes. For the system to work properly, the balance between the bacterial biomass and the BOD is important. Because BOD in wastewater is frequently stable, the mass of microorganisms in the system is stable. One adjustment is removal of the excess organisms from the system to maintain balance for effective treatment of wastewater [33].

Microorganisms in treatment systems secrete adhesive substances that bind them together in three-dimensional aggregated structures called flocs. Flocs are able to absorb not only soluble substrates but also colloids and macromolecules. The microbial species within the activated sludge are very diverse. Bacteria, which play an important role in the degradation process, are the dominant organisms found in MBRs with over 300 species commonly occurring. The majority of these are heterotrophs that are responsible for the removal of most of the organic matter in the waste. In contrast, autotrophs account for a small proportion of the bacterial community and use inorganic compounds for synthesising organic compounds. The most important group of autotrophic bacteria in MBRs is nitrifying bacteria that play a key role in removing ammonia from wastewater. Under aerobic conditions, ammonia is converted to nitrite (NO_2) and then to nitrate (NO_3) by nitrification. Nitrate is reduced to nitrogen gas (N_2) during denitrification which occurs under anaerobic conditions. To stimulate the denitrification process, an anoxic tank is frequently installed upstream from the aerated tank.

In MBRs, heterotrophic groups having high growth rates dominate the less abundant autotrophs. The removal of phosphate is achieved by removing biomass that has accumulated high concentrations of polyphosphates [28].

Forward osmosis MBR (FO-MBR) is the combination of FO and MBR processes to produce clean water from wastewater. In contrast to RO membranes that require intensive hydraulic pressures to operate, FO membranes require only osmosis pressure. In the FO-MBR process, the driving force of water for water separation is measured by the osmosis pressure difference between solutions on either side of the FO membrane and the direction of water diffusion is from low concentration to high concentration [1].

2.1.2.2. Biofilters

Biofilter treatment is a combination of biological and physical processes for the removal of suspended substances and colloidal particles from feed water. The water is passed through a filter media, such as silica sand, activated carbon or anthracite coal. Biofilter treatment is frequently used for the removal of residual substrates in the effluent from secondary treatments. The filter system can be gravity or pressure driven. In pressure filters, the filter media is contained in a pressure vessel where the feed water is delivered under pressure, while in gravity filters, the feed water passes through the bed by gravity. The design of the filter is determined by the hydraulic loading rate and the treatment capacity of the filters. The system may run at either low hydraulic loading rates ($0.1 – 0.2$ m h^{-1}) for biological processes or high hydraulic loading rates ($2.4 – 24.4$ m h^{-1}) for producing larger amounts of water [26].

The design of a typical biofilter column is illustrated in Figure 2.5. Feed water is introduced to the biofilter system through the distribution radials, which open at the bottom. Therefore, the effluent flows upward through the media bed, which may consist of either single, dual, or multimedia filters. The contaminants are captured in or on the moving granular bed, while the treated water rises into the filtrate pool above the bed [26]. Within the filter bed, the capture of organic or inorganic contaminants onto the surface of adsorbents allows microorganisms (aerobic, anaerobic, and facultative bacteria, fungi, algae and protozoa) to grow leading to the formation of a biofilm. This process may take days or months depending on the quality of wastewater. The performance of the biofilter system mainly relies on the

microbial activity for degradation of pollutants in the feed water. Therefore, it is important to maintain a healthy biomass on the surface of the media by supplying a constant source of substrates.

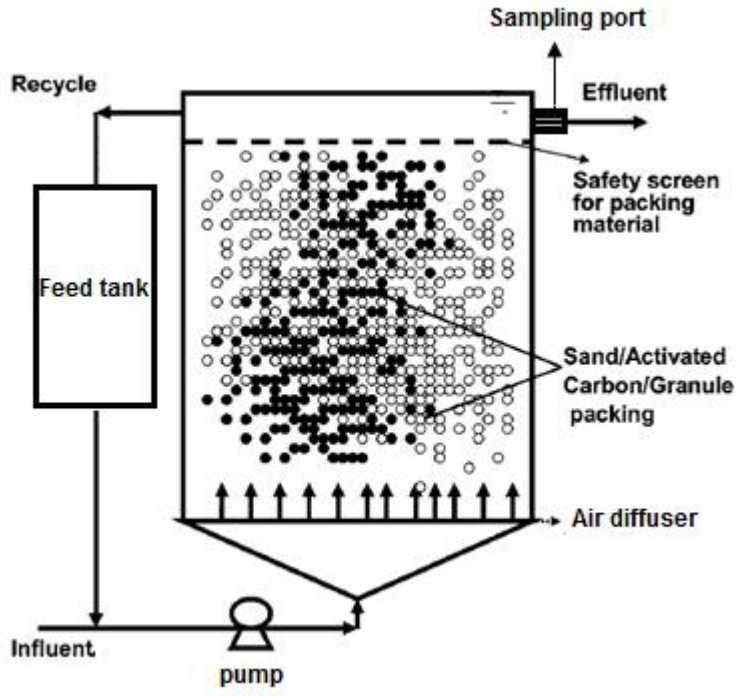

Figure 2.5. Schematic of the column filter system setup. Influent is fed to the biofilter column by a pump. The aerobic condition is maintained by air diffusers and the biofilm is grown on 0.4 - 0.5 mm particles of media. The effluent is collected from a sampling port [34].

There are the three main biological processes occurring in the system; microbial attachment, microbial growth and biofilm detachment. Initial adhesion occurs as soon as the organisms reach the surface of media. Attachment can be reversible or irreversible depending on the interaction energy, which depends on the sum of Van der Waals and electrostatic forces. Attachment is necessary for the development of a biofilm on the surface. These processes are determined by the characteristics of the feed water and the surface properties of the filter media. Biofilm detachment results either from fluid shear or filter backwashing, or the lack of organic substrates.

The removal of non-biodegradable metals which remain after secondary treatment involves the conversion these metals from soluble forms to less soluble or insoluble forms through

oxidation or reduction by microorganisms. These less soluble or insoluble metals are then adsorbed on the surface of the media. In addition, adsorbents like ferric oxide or activated alumina may be used to improve the removal of inorganic contaminants like arsenic, manganese, fluoride and other ions [35, 36].

2.2. Membrane Fouling

Membrane fouling is a consequence of interactions between particles in wastewater and the membrane (Figure 2.6). There may be multiple causes of fouling, including pore narrowing, pore clogging and cake formation. Fouling leads to an increase in TMP required to maintain a constant permeable flux. Membrane fouling leads to the loss of membrane performance and decreases the lifespan of the membrane. There have been a considerable number of studies on addressing these drawbacks so that these membrane technologies can be more widely used for wastewater treatment [2]. The four main causes of membrane fouling are the adsorption of colloids and macromolecules on the membrane, the growth of microorganisms on the membrane surface, the precipitation of inorganic substrates on the membrane and membrane aging. Depending on their biological and chemical characteristics, these foulants can be divided into three groups as biofoulants, inorganic foulants and organic foulants.

Biofouling is caused by the growth of microorganisms and the deposition of suspended flocs on the surface of the membrane. The first step in membrane biofouling is the attachment of microorganisms on the membrane surface. EPS secreted by microorganisms act to bind the cells together and anchor them on the surface of the membrane. Biofilms are highly dynamic communities which generally develop three-dimensional structures [37]. Bacteria living in this three-dimensional matrix become highly tolerant to antibiotics, disinfectants and nutrient-deficient conditions [38-41]. Therefore, it is difficult to remove the biofouling layer using physical and chemical membrane cleaning methods [32]. Chemical cleaning with acidic or alkaline chemicals and antimicrobials is the most popular method for biofouling control. However, overuse of these chemicals can damage the polymeric membrane structure, resulting in shorter membrane life. Furthermore, previous studies have shown that bacteria in biofilms can be 10,000-fold more resistant to antimicrobials than free-swimming cells [14].

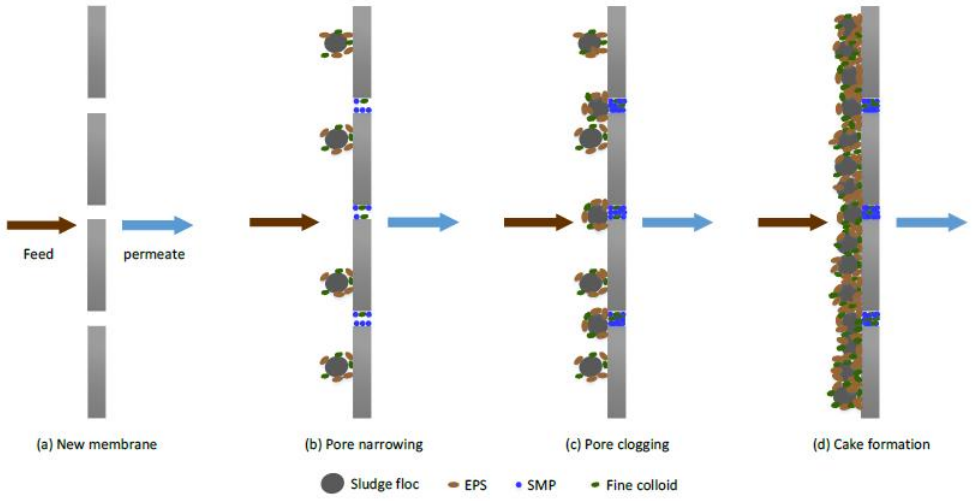

Figure 2.6. The mechanism of membrane fouling in MBRs. The physico-chemical interactions between foulants, such as sludge flocs, EPS, soluble microbial products (SMPs) and fine colloids and membrane material result in membrane fouling. Fouling results in pore narrowing, pore clogging and cake formation [2].

There are a variety of organic compounds found in feed water, including biopolymers and metabolic products from microbial activities. The major components of these organic substrates are polyphenols, proteins and polysaccharides, which directly affect the membrane fouling due to their role in the cohesion of colloidal particles leading to the formation of a cake layer on the membrane surface. Analysis of the composition of the fouling cake showed that the porous upper layer has a composition similar to sludge flocs. The middle layer contains high levels of polysaccharides, while bound proteins are dominant components in the lower layer [17].

Inorganic fouling or mineral scale is the precipitation of inorganic salts (Ca^{2+}, Mg^{2+}, Fe^{2+}, Al^{3+}, SO_4^{2-}, PO_4^{3-}, CO_3^{2-} and OH^{1-}) into the pores of the membrane or onto the membrane surface. Inorganic fouling is due to crystallisation (precipitation of ions) and particulate fouling (deposition of colloidal particulates) on the membrane or in membrane pores. Inorganic fouling is mainly attributed to carbonates due to the high concentration of carbon dioxide caused by aeration and bacterial metabolism. These affect the super-saturation of

carbonate salts, particularly Ca^{2+}, Mg^{2+} and Fe^{2}. Chemical cleaning is frequently adopted to treat inorganic fouling [17].

2.2.1. Fouling indicators

Fouling indicators are mainly used to measure the fouling potential of feed water prior to membrane filtration. Biofouling prediction plays an important role in the improvement of membrane performance and the reduction of operating costs, e.g. cleaning, maintenance and replacement costs. Therefore, rapid and accurate assays for the prediction of membrane fouling are needed so that plant operators have time to implement fouling controls.

2.2.1.1. AOC Concentration

Biofouling is the major problem affecting the use of RO systems. Biofilm formation can be controlled by removing or limiting conditions which support bacterial growth. Organic substrates are considered to be the primary determinant for bacterial regrowth in RO systems. Biodegradable organic matter (BOM) are nutrients needed for the growth of microorganisms and is composed of AOC and biodegradable dissolved organic carbon (BDOC) (Figure 2.7). The growth of microorganisms is limited at an AOC concentration of < 10 to 20 µg L^{-1} and BDOC at less than 200 µg L^{-1} [3, 19]. Furthermore, a study of Weinrich (2011) reported that the RO biofouling occurred when the median AOC concentration was 50 µg L^{-1} (Figure 2.8) [13] . Both AOC and BDOC are widely used as parameters for estimating the potential for undesirable bacterial growth in water systems [5, 19, 42, 43]. Most AOC assays use bacterial growth as a proxy for the measurement of the AOC concentration. BDOC assays measure DOC before and after incubation with a microbial community [19]. While BDOC is comprised of higher molecular weight compounds, AOC is composed of lower molecular weight carbon compounds [11, 43].

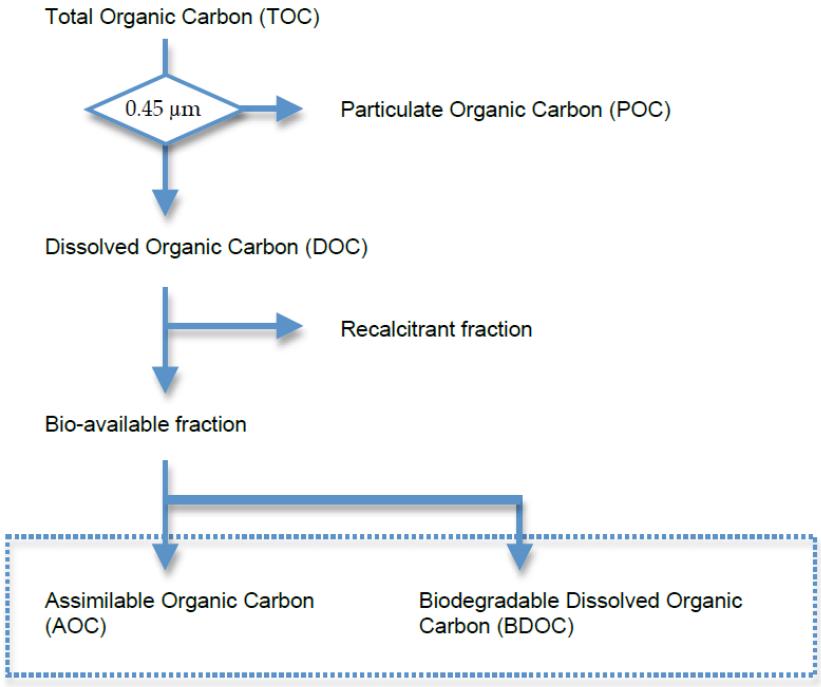

Figure 2.7. Schematic overview of the different organic carbon fractions. DOC is able to pass through a membrane pore size of 0.45 µm, which removes particulate organic carbon (POC). Recalcitrant carbon is a fraction of DOC that is not bioavailable to microorganisms. AOC is bioavailable carbon having molecular weight of less than 1000 Daltons (Da) [44].

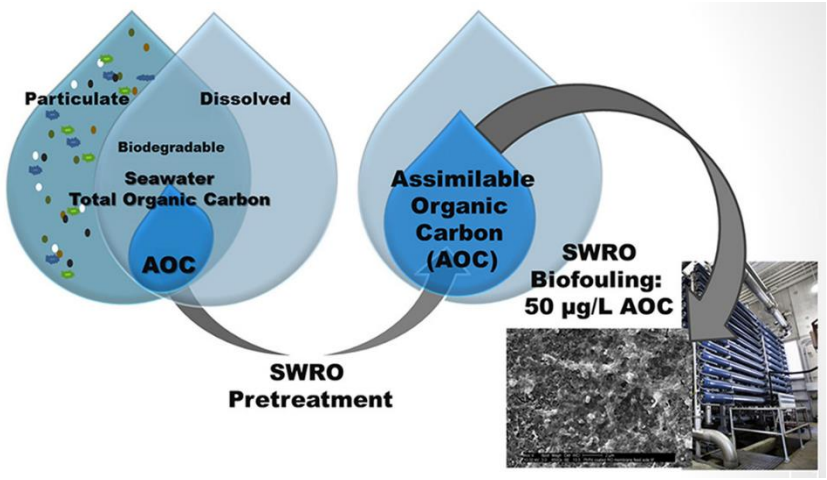

Figure 2.8. Correlation between AOC concentration and seawater reverse osmosis (SWRO) biofouling. RO biofouling occurred when the median AOC was 50 µg L^{-1} [13].

During desalination, feed water is pre-treated prior to RO treatment. BDOC is frequently removed by coagulation in pre-treatment processes while AOC is only marginally affected by coagulation. NF may also be used as a pre-treatment. The NF membrane removes 90% of the BDOC while low molecular weight AOC frequently passes through [44]. As a result, the concentration of these AOC compounds determines the growth potential of microorganisms and is considered as a standardised measurement to predict biofilm formation [3-5]. AOC is the fraction (0.1 - 9.0%) of TOC which can be easily assimilated by bacteria and converted to biomass [4]. AOC compounds are generally less than 1000 Da in size and include sugars, fatty acids, amino acids, humic acids, fulvic acids, hydroxycarboxylic acids, carbohydrates and peptides [4, 5, 19, 42]. It is difficult to quantify AOC by chemical methods because there are many small molecular weight compounds present at low concentrations. Therefore, microbiological methods have been developed to measure AOC concentration.

The original AOC assay developed by Van der Kooji et al. (1982) was based on plate counts. Two bacterial strains, *P. fluorescens* P-17 and *Spirillum* sp. NOX, are inoculated into water samples and incubated for several days until the AOC is fully converted into biomass. Colony forming units (CFUs) are measured daily to determine the maximum cell yield, which is correlated with the AOC concentration [45]. The AOC concentration can then be calculated from a standard curve representing the correlation between carbon concentrations (acetate or oxalate) and CFUs [20]. *P. fluorescens* P-17 can utilise a wide range of carbon compounds, including amino acids and carbohydrates, but cannot assimilate carboxylic acids or oxalate. In contrast to *P. fluorescens* P-17, *Spirillum* sp. NOX can metabolise carboxylic acids, including oxalate, but is unable to use carbohydrates, alcohols, amino acids and aromatic acids [44]. Thus, the two strains are used simultaneously to detect AOC compounds.

Other studies have used natural microbial communities to measure AOC instead of a single species. One of the advantages of this method is that in general, communities can assimilate a wider range of carbon compounds than a single strain [46]. However, it is difficult to enumerate CFUs when using a community as not all organisms will grow on the same agar medium. In addition, the plate count method is time-consuming and labour-intensive and results in the delay of control measures being taken. In 1993, a more rapid AOC assay was introduced which measures adenosine triphosphate (ATP) content rather than CFUs. The

ATP measurement is based on the production of light from luciferin-luciferase (Figure 2.8). The bacterial culture is filtered through a polyvinylidene difluoride membrane filter (0.22 µm). The filter then is placed into a buffer with an ATP releasing agent and luciferin-luciferase is injected into the sample. The emitted light intensity is determined using a luminometer and the results are described as relative light unit (RLU). The AOC concentration is measured from a standard curve showing the relationship between ATP, RLU and CFUs [3, 10, 44]. Since this method measures AOC concentrations based on ATP luminescence rather than CFUs, it is less time consuming as bacterial growth is not necessary, thereby reducing the assay time by three days [3]. However, this method involves expensive and complicated procedures, including injection of reagents (luciferin-luciferase), flow-cytometric enumeration and filter concentration of cells [3, 10].

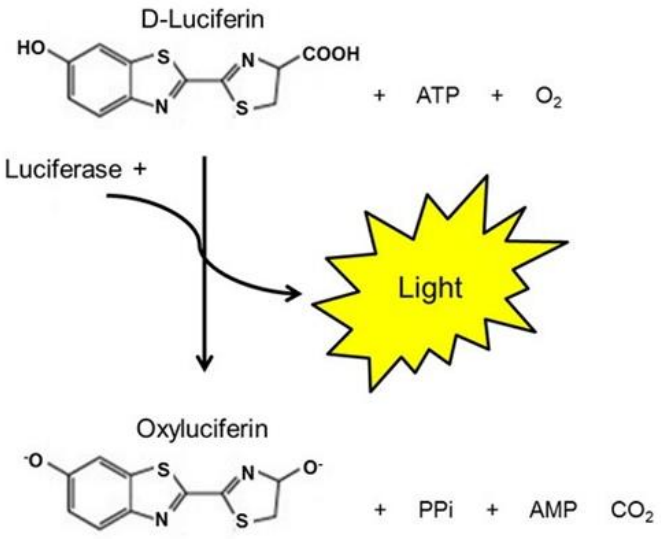

Figure 2.9. Luciferin-luciferase reaction. In the presence of ATP, luciferase oxidises luciferin leading to light production [47].

Haddix modified the AOC test strains (*P. fluorescens* P-17 and *Spirillum* sp. NOX) to produce luminescence by integrating the *lux* operon which encodes genes needed for bioluminescence (*luxCDABE*) into the genome. These modified strains constitutively produce luminescence so the RLUs produced are directly proportional to biomass. In the luminescence-based AOC assay, the AOC concentration is determined by a standard curve describing the linear relationship between bioluminescence and bacterial numbers [4, 20].

However, these strains are only marginally effective when low-sensitivity analog luminometers are used [13].

For quantifying AOC in seawater, naturally luminous marine microorganisms such as *V. fischeri* and *V. harveyi* have been used [11, 13]. Unlike other AOC measurement methods, the luminescence AOC assay gives an immediate luminescence response rather than being reliant on the growth of bacterial cells [44]. Thus, these newer AOC methods can determine the AOC concentration within hours. The AOC concentration in seawater samples is calculated based on a standard curve representing the linear correlation between bioluminescence and carbon concentration (acetate or glucose) and the final results are given as acetate/glucose-C-equivalents [11, 13]. However, bacterial growth on complex carbon mixtures (AOC compounds) may be different to growth on single substrates [48] and thus, this method may underestimate AOC concentrations in seawater.

To overcome this problem, sensitive bioluminescent reporter strains with broad metabolic potential will be developed in this study, to measure AOC in seawater samples. The AOC levels are determined according to a standard curve showing the linear relationship between bioluminescence and AOC compounds rather than a single carbon source (acetate or glucose). Therefore, this method is expected to give better estimation of the AOC concentration rather than an AOC-equivalent concentration.

2.2.1.2. TMP

Membrane filtration is usually operated at a constant flux. When membrane fouling occurs, the TMP increases to maintain a constant permeable flux. A sudden TMP increase, or TMP jump, occurs when membrane fouling increases beyond a certain level. The sudden TMP jump is attributed to the changes in the structure of the fouling layer and importantly the concentration of EPS. A number of studies have indicated that higher TMP values are associated with an increase in EPS concentration. For mature biofilms, oxygen becomes limited in the lower fouling layers leading to the increase in EPS concentration. The increase in TMP occurs in three stages, namely, an initial conditioning fouling, a gradual TMP increase and a rapid TMP rise. The first stage is associated with initial pore blocking by

fouling components. The next stage is due to secondary blocking or biofilm formation, while the last stage refers to serious membrane blockages where cleaning is required [28].

2.2.1.3. Filtration Resistance

Resistance parameters are important for the prediction of a pressure drop in filtration membranes. In MBRs, the determination of fouling tendency of individual activated sludges is essential for the optimisation of membrane performance. There are several methods for assessing filterability, including the Berlin Filtration Method (BFM) and the MBR VITO Fouling Measurement (MBR-VFM). The former method uses a test cell with a flat sheet membrane to measure fouling propensity through a flux step protocol with relaxation steps. For MBR-VFM, a tubular membrane is used to filter the sludge at a constant permeable flux and the filterability is assessed through the increase of TMP filtration resistance. The increase in filtration resistance is associated with the rise of pressure [49].

Filtration resistance is due to three components; membrane resistance, fouling resistance and cake resistance. The fouling layer resistance depends on the interaction between the properties of the membrane and the characteristics of foulants. Membrane fouling can be categorised as pore clogging caused by the deposition of tiny particles in the membrane pores and is referred to as fouling resistance, while the second is due to the accumulation of suspended solids forming a cake layer on the membrane surface and is referred to as cake resistance. Cake formation accounts for 80% of the total filtration resistance and is a major cause of membrane fouling in MBRs, while pore blocking and adsorption are negligible. Before filtration tests, membrane resistance is determined by measuring the permeable flux at a range of TMP from 7 – 10 kilopascal (kPa). The measurement of membrane resistance is carried out with clean water, while the total filtration resistance is measured with activated sludge [28].

2.2.1.4. Other Fouling Indicators

Other indicators that can also be used to determine fouling potential include the silt density index (SDI) and the modified fouling index (MFI) also called $MFI_{0.45}$ [14, 50]. Both of these two indexes are used for the prediction of colloidal fouling potential of feed water and the efficiency of pre-treatment processes in RO systems. SDI is a measure of contaminants in

feed water. In practical terms, a feed SDI < 5 indicates a lower fouling propensity. SDI is determined by calculating the time required for a fixed volume of feed water to flow through a 0.45 μm filter under a constant pressure (2 atm). The difference between the initial time and the time of second measurement after silt build-up (normally 15 minutes) represents the SDI value. The SDI is different from the turbidity value, which is a measurement of suspended particles. Previous studies showed that solutions with a low turbidity < 1 Nephelometric Turbidity Unit (NTU) may have a high SDI value [51]. The MFI is determined using the same procedures as for SDI measurement, except that the volume of filtered water is measured in 30-second intervals over a 15 minute filtration [51].

The two methods have limitations for predicting biofilm formation in RO systems because they are used to measure particulate fouling potential, and do not provide information on the nature of foulants and the risk of biofouling [10, 42, 52]. Previous studies indicate that there is a very weak linear correlation between the two indexes and RO fouling. The fouling rates based on these indexes are frequently too low because the filters are not able to capture colloidal particles smaller than 0.45 μm, which are the main cause of membrane fouling in RO filtration [53].

2.2.2. Membrane Fouling Control

There are several factors affecting membrane fouling, including the membrane properties, operational conditions, the composition of the microbial community and the quality of feed water. Strategies to reduce fouling are the use of pre-treatment processes, operation optimisation, membrane modification and periodic membrane cleaning.

2.2.2.1. The Application of NO Compounds for Induction of Biofilm Dispersal

Chemical cleaning with acidic or alkaline chemicals and antimicrobials is the most popular method for biofouling control. However, overuse of these chemicals can damage the polymeric membrane structure, resulting in shorter membrane lifespan. Furthermore, previous studies have shown that bacteria in biofilms can be 10,000-fold more resistant to antimicrobials than free-swimming cells [14]. To address problems related to either biofilm resistance due to the utilisation of antibiotics or the damage of membrane lifespan by strong oxidising agents, newer studies on biofilm control have focused on signalling molecules that

induce the transition from a biofilm mode of growth to a motile mode of growth. The utilisation of dispersal signals is one potential way to trigger biofilm dispersal. Previous studies have shown that NO, a ubiquitous biological signalling molecule, is a key mediator of biofilm detachment and is conserved across prokaryotic and eukaryotic species [22].

2.2.2.1.1. The Characteristics of Microorganisms in Biofilms

Physico-chemical characteristics (surface charge, structure, flocculation and adsorption) of microbial biofilm communities is mainly determined by EPS, the major foulant in membrane filtration. EPS is composed of polysaccharides, proteins, nucleic acids and other components. Polysaccharides and proteins account for a considerable proportion of EPS. EPS can be categorised as bound EPS and soluble EPS. The former is located around the cell surface and functions to protect and aggregate microorganisms. EPS affects fouling by altering flocculation ability, hydrophobicity, surface charge and sludge viscosity. The latter refers to soluble microbial products that are released into the solution and derives from metabolic activities and biofilm detachment. Previous studies indicated that soluble EPS has a higher propensity for fouling because it penetrates into sludge flocs and membrane pores more easily. EPS contains many charged hydroxyl, carboxyl, sulfhydryl, phosphoric, phenolic and polar groups, which make them amphoteric. This characteristic allows EPS to deposit on either hydrophobic or hydrophilic membranes [2].

There are five stages in the process of biofilm formation. In the first stage, bacteria leave the suspension and attach to a surface. The second stage involves the synthesis of EPS that leads to irreversible attachment. During stage 3, the continued growth of bacteria gathered in the matrix leads to the development of mature biofilms containing multi-layered clusters of millions of tightly packed cells. In stage 4, the formation of three-dimensional structures and further maturation of the biofilm occurs. The final stage is the detachment of cells from biofilms. When biofilms reach a critical mass, biofilm bacteria change from surface-associated cells to free-swimming cells that colonise new surfaces and restart the biofilm cycle. This complex dispersal process, which may vary in different species, involves numerous molecular signals and effectors [21, 54].

The mechanism of bacterial dispersal can be passive or active. Passive dispersion results when external forces such as shear forces cause parts of the biofilm to dislodge. Active detachment is initiated by the bacteria in response to environmental changes, including nutrient starvation, antimicrobial stress and unfavourable oxygen levels [55]. This active detachment plays a significant role in the expansion, reproduction and survival of microorganisms. Biofilm dispersal is considered to be a selective advantage that bacteria use to respond to changing surroundings. Many studies have demonstrated that the mechanism of biofilm detachment involves multiple cues and signalling pathways, including nutrients, oxygen, iron levels, NO, D-amino acids, fatty acids, quorum sensing (QS), cAMP and c-di-GMP.

2.2.2.1.2. The Removal of Biofouling by NO Compounds

C-di-GMP is a second messenger that is conserved across species and plays a key role in biofilm formation and maintenance. Intracellular levels of c-di-GMP regulate the planktonic to biofilm mode of growth in range of eubacteria [21, 56-63]. Elevated c-di-GMP levels are associated with an increase in EPS production and a decrease in motility, while decreased c-di-GMP levels leads to biofilm dispersal. Therefore, agents that bind c-di-GMP may be potential dispersal signals.

A recently proposed strategy for controlling fouling is the induction of biofilm dispersal with NO. NO is a biologically active signalling molecule that has been shown to induce biofilm dispersal [6]. For example, low, non-toxic concentrations of NO (nanomolar range) induced the transition from the biofilm mode of growth to the free swimming planktonic state in *P. aeruginosa* [7]. The mechanisms underlying NO-induced dispersal is stimulation of phosphodiesterase activity that results in the degradation of c-di-GMP (Figure 2.9). When biofilms are exposed to NO, cells experience changes in gene expression that favour the planktonic mode of growth [64]. Diguanylate cyclase and phosphodiesterase, enzymes that produce and degrade c-di-GMP, respectively, are encoded by genes which are widely distributed among bacteria and are usually related to redox sensors, including Per-Arnt-Sim (PAS) domains capable of sensing NO [65]. At higher concentrations of NO (micromolar to millimolar range), activation of regulatory systems that control detoxification prevent nitrosative stress occurs [66].

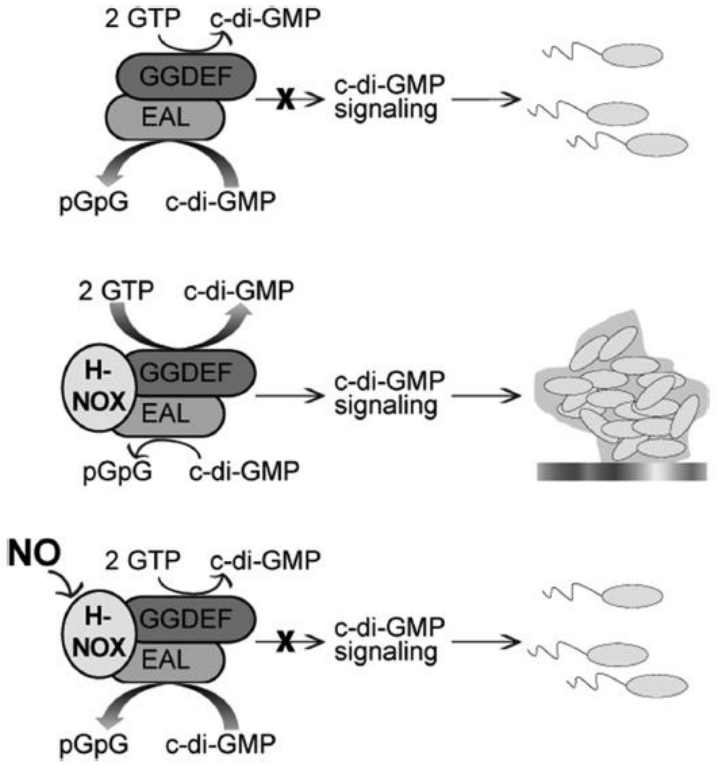

Figure 2.10. NO regulation of c-di-GMP synthesis in *Shewanella woodyi*. In the presence of NO, phosphodiesterase activity of the diguanylate cyclase gene (*swDGC*) is up-regulated resulting in the reduction in the biofilm formation. In the absence of NO, *swH-NOX* is associated with *swDGC* and maintains its basal phosphodiesterase activity while stimulating diguanylate cyclase activity. X indicates the production of c-di-GMP signaling does not occur and thick arrows indicate the direction of reaction [67].

NO donor compounds, such as SNP, MAHMA NONOate and PROLI NONOate, which have a short half-life, are used to generate NO in aqueous environments. Previous studies have demonstrated that these NO donors induce dispersal of biofilms of *P. aeruginosa* and other species, including mixed species biofilms [6-9]. PROLI NONOate, SNP and MAHMA NONOate reduced bacterial biofilm biovolumes of *P. aeruginosa* by 30 - 40% after 1 - 24 h of exposure [9, 23]. In addition, bacterial biofilms become more susceptible to antimicrobials after NO exposure. After NO exposure, the addition of various antimicrobials completely removed remaining biofilms cells of *P. aeruginosa* [6].

In this study, the influence of diethylenetriamine (DETA) NONOate on the reduction of TMP in a laboratory-scale submerged MBR has been investigated. In addition, specific bacterial communities responsible for the membrane fouling will be determined by measuring the changes in relative abundance of the most dominant bacterial populations associated with TMP jumps.

2.2.2.2. The Increase of the Quality of Feed Water through Pre-treatment Processes

Pre-treatment processes play an important role in the removal of foulants in feed water prior to membrane treatment, particularly in RO filtration. Insufficient pre-treatment results in frequent cleaning of the membrane. However, there are no fixed pre-treatment procedures for obtaining acceptable feed water. The pre-treatment processes are determined by the characteristics of raw water and the applied membrane systems. To address the need for timely fouling controls, fouling indicators, such as AOC concentration, SDI and MFI are adopted to assess the efficiency of pre-treatment processes. The speed and accuracy of fouling indicators are important for the selection and development of pre-treatment methods. In Table 2.1, SDI and turbidity values used to assess the quality of feed water in RO / NF filtration are presented. It has been shown that feed water with an SDI of 3 or lower and turbidity of 0.5 NTU or lower is acceptable for RO / NF treatment. In cases where feed water shows a high fouling potential, additional pre-treatment processes are required prior to the membrane treatment.

Table 2.1. Guidelines for acceptable RO / NF feed water [68].

Parameter	**Recommended Maximum Value**
Turbidity	0.5 NTU
SDI 15	3
TOC	2 mg/L
Iron	0.1 mg/L
Manganese	0.05 mg/L
Oil and grease	0.1 mg/L
Volatile organic chemicals (VOCs)	In µg/L range

2.2.2.3. The Modification of the Properties of Membrane

Membrane properties are determined by the material used, the charge of the membrane surface, the pore size and membrane roughness. Most membranes have negative surface charges. This results in the absorption of colloidal particles and cations in feed water to the membrane leading to organic fouling or mineral scale. Larger pore sizes have a greater tendency for pore blocking. Pollutants that are smaller than the pore sizes are trapped causing fouling. While particles larger than the pore sizes more easily form a layer on membrane surface, the layer can be easily removed by physical cleaning, normally air scouring. The optimal pore size of the membrane is different for membranes of different materials. For example, with polyvinylidene fluoride membranes, decreases in membrane fouling is the result of increases in membrane pore size, while cellulose acetate membranes with smaller pore sizes are less prone to the fouling. Another factor affecting membrane fouling is membrane roughness. Rough membrane surfaces are more prone to fouling than homogenous ones because the rougher membrane surface provides a structure allowing the accumulation of foulants on the surfaces [2].

Membrane materials can be polymeric, composite or ceramic materials. Polymeric membranes are the most popular membranes because of low cost and ease of manufacturing of the pores. Membranes made of polymeric materials have good physical and chemical resistance, but most of them are hydrophobic. Studies have indicated that the interactions between membrane materials, microorganisms and soluble substrates are mainly hydrophobic. Therefore, hydrophobic membranes adsorb hydrophilic substances leading to the formation of membrane fouling. In contrast, ceramic membranes not only have a high chemical resistance, inert nature and integrity, but also are hydrophilic. Therefore, ceramic membranes are more resistant to membrane fouling than polymeric membranes. However, the high cost of ceramic materials makes them economically prohibitive for application in membrane filtration. Composite membranes are the combination of two or more material in a final product to make the membranes more hydrophilic. As a result, composite membranes are more cost effective than ceramic membranes and are more resistant to membrane fouling than polymeric membranes. Most applications focus on the improvement of polymeric membranes, including air plasma treatment for polypropylene membranes, coatings of various forms of nanosilver on polyethersulfone membrane surfaces and production of photocatalytic nanocomposite membranes. These modified membranes have higher flux recovery and lower membrane cleaning frequency compared to unmodified membranes [2].

2.2.2.4. Determination of Sustainable Operating Parameters

Typical operating conditions like TMP, aeration and other parameters affect the membrane fouling. Therefore, the determination of suitable operating parameters that perform well with minimal membrane fouling is necessary. When a membrane system operates under a constant permeable flux, the increase in TMP indicates membrane fouling. It is necessary to determine an appropriate TMP for operation. This appropriate operational flux prevents excessive deposition of foulants on the membrane surface. Therefore, when membrane systems are performed at this sustainable TMP, chemical cleaning is unnecessary [2].

In MBRs, aeration provides oxygen to the microbial community as well as reducing fouling by the scouring effect it has on the membrane surface. However, high aeration leads to the breakage of sludge flocs, which may increase the membrane fouling because of the production of soluble microbial products. Furthermore, the operating cost increases due to

increased energy consumption. Therefore, it is necessary to find a suitable aeration intensity to balance between these factors [2].

Other parameters, such as solids retention time (SRT), hydraulic retention time (HRT), food to microorganisms (F/M) ratio and the organic loading rate (OLR) have an indirect effect on membrane fouling. At high SRTs (the average time the activated sludge solids remain in the system) and HRT (the average time a soluble compound remains in the system), there is a reduction in membrane fouling because of reduced production of EPS and sludge viscosity. However, an extreme SRT leads to an increase in fouling due to the high accumulation of biomass and an increase in sludge viscosity. In contrast, MBRs operated at high F/M ratio and OLR (amount of food per a volume of feed water) have higher fouling rates than those at low F/M ration and OLR. The increase in membrane fouling is attributed to the high EPS levels because of high food consumption by microorganisms [2].

2.2.2.5. Other Control Methods

Membrane fouling can be categorised as reversible, irreversible or irrecoverable fouling. Physical cleaning is only applied for the removal of fouling caused by deposition of inorganic or organic substances on the membrane surface, while chemical methods can remove either reversible fouling or irreversible fouling. However, irrecoverable fouling cannot be removed with any cleaning method. Therefore, membrane surfaces are cleaned periodically to prevent irrecoverable fouling.

2.2.2.5.1. Physical Cleaning

Backwashing is the most popular method used in physical cleaning for treatment of reversible membrane fouling. Backwashing is a reverse filtration process in which the direction of flow is reversed through the membrane for a short period of time (30 seconds to 3 minutes) every 15 – 60 minutes to remove foulants on the surface of membrane. This cleaning method leads to a reduction in productivity (5 to 10%) due to the amount of water used. Although backwashing can reduce TMP, it will begin to increase again during operation. To address severe fouling, backwashing is performed with chemicals [69].

2.2.2.5.2. Chemical Cleaning

Chemical cleaning is the most widely used cleaning method as it is more effective than physical methods. Chemical cleaning is applied in the cases where physical cleaning does not work, i.e. for irreversible fouling. Chemical cleaning is carried out by soaking the membrane in cleaning solution or by backwashing with chemicals. A typical cleaning process lasts 30 – 60 minutes. The selection of cleaning agents depends on the characteristics of foulants and membrane materials. These agents must be able to remove foulants on the membrane surface without damaging the membranes. Typically, alkaline agents (sodium hypochlorite and sodium peroxide) are used to treat organic foulants, while acidic compounds (phosphoric, hydrochloric, sulphuric and nitric) are used for the removal of lime or inorganic foulants [69]. However, the application of strong oxidising agents for fouling removal is incompatible for long term treatment of polyamide membranes because of oxidative membrane damage.

2.3. Summary

The main purpose of this literature review was to provide the background and context for the research problem. In this chapter, an overview of membrane filtration technologies and membrane fouling, which is considered to be a major drawback of this technology, was described. Two kinds of membrane systems, namely RO and MBRs, were introduced along with processes for cleaning for each system. In addition, fouling indicators and fouling control strategies, which relate to the main subject of this research, were introduced. Furthermore, a review of previous studies on membrane fouling controls including AOC detection to prevent membrane fouling in RO systems and NO treatment for reduction of TMP in MBR systems formed part of the research design process described here.

CHAPTER 3

DEVELOPMENT OF A SENSITIVE BIOLUMINESCENT REPORTER TECHNOLOGY FOR AOC QUANTIFICATION

3.1. Introduction

Development of a rapid and accurate indicator for AOC quantification is a novel strategy for biofouling control in RO technologies. However, most current AOC measurements use two AOC test strains, *P. fluorescens* P-17 and *Spirillum* sp. NOX, which are indigenous in fresh water and not suitable for seawater samples [45]. Currently, two marine luminescent bacteria, *V. fischeri* and *V. harveyi* have been used for the measurement of AOC in seawater. The principal behind this method is that there is a linear correlation between bioluminescent intensity of reporter organisms and carbon concentration. In this method, the AOC concentration in seawater is determined after 30 - 60 minutes incubation with luminescent test strains, compared to 7 days for the plate count method [11, 13]. However, the two marine species used to date have metabolic limitations in that they may not utilise a wide range of AOC compounds. As a result, the quantification of AOC is frequently underestimated. To address these problems, this chapter focuses on the following aims:

i. Isolation of new marine bacteria with broad metabolic potential
ii. Construction of luminescent AOC reporter strains
iii. Development of bioluminescent AOC tests

3.2. Materials and Methods

The experimental procedures for the development of AOC reporter strains are described in 3.2. To obtain potential strains with a broad metabolic capacity, marine bacteria were isolated by plating aliquots of seawater samples collected at the Sydney Institute of Marine Science (SIMS), 19 Chowder Bay Road, Mosman on seawater agar (15 g L^{-1} Bacto agar added to filtered seawater). Strains that grew quickly on seawater media were selected for further examination. These potential strains were identified based on 16S rDNA sequences. The transformation of the potential strains with a luminescent reporter plasmid was performed. These reporter strains were then tested for the quantification of AOC compounds, including glucose and humic acids.

3.2.1. Isolation of Microorganisms from Seawater

Seawater used in the aquaria at SIMS is passed through a series of filters of various pore sizes (100, 70 and 10 µm) to remove larger organisms and particles from the seawater before it is pumped into the aquarium. Seawater samples were taken after each successive filtration step and from the biofilms formed on the filters, as well as from unfiltered seawater. Samples were collected in 500 ml sterile bottles and transported to the laboratory. Biofilms from the 100 µm filter were collected by scraping the filter surface with sterile cell scrapers. The sample details are described in Table 3.1. To obtain marine bacteria able to grow under nutrient-poor conditions, 100 µl aliquots of seawater or biofilm suspensions (the biofilm suspended in sterile seawater) were plated on seawater agar plates that were incubated at room temperature for 24 and 48 h. Colonies that grew were transferred to Marine agar, (Marine Broth 2216 medium; BD, Difco, Sparks, MD) containing 15 g L^{-1} Bacto agar (BD). Single bacterial colonies were preserved at -80 ^{O}C in Marine broth containing 25% glycerol.

Table 3.1. Sample details

Sample code	Sample type	Sampling site	Collection date
CB	Unfiltered seawater	SIMS	31/08/2016
CB100	Seawater filtered through 100 µm filter	SIMS	31/08/2016
CB70	Seawater filtered through 70 µm filter	SIMS	31/08/2016
CB10	Seawater filtered through 10 µm filter	SIMS	31/08/2016
CBS	Biofilm collected from 100 µm filter	SIMS	31/08/2016
BLS	Unfiltered seawater	Brighton-Le-Sands (Rockdale, NSW)	31/08/2016
CBSW	Unfiltered seawater	SIMS	31/01/2017
CB10SW	Seawater filtered through 10 µm filter	SIMS	31/01/2017

3.2.2. Selection of Potential AOC Test Strains

Marine bacteria isolated in 3.2.1 were recovered on Marine agar and incubated overnight and then transferred to seawater agar plates and passaged three times to ensure no nutrient carried over from the Marine agar plates. The seawater plates were incubated at room temperature overnight and the biomass suspended into artificial seawater (ASW) (13.5 g L^{-1} NaCl, 1.96 g L^{-1} Na_2SO_4, 0.107 g L^{-1} $NaHCO_3$, 0.33 g L^{-1} KCl, 0.053 g L^{-1} KBr, 2.5 g L^{-1} $MgCl_2$. $6H_2O$, 0.55 g L^{-1} $CaCl_2$. $2H_2O$, 0.5 g L^{-1} NH_4Cl, 0.23 g L^{-1} K_2HPO_4, 0.0107 g L^{-1} $SrCl_2$. $6H_2O$ and 0.0107 g L^{-1} H_3BO_3 and pH 7.5) and adjusted to OD_{600nm} = 0.1 [11]. Ten ml of seawater was inoculated with the bacterial suspension at a final concentration of approximately 10^2 CFU ml^{-1}. The tubes were incubated at 28 ^{O}C for 168 h with shaking (200 revolutions per minute, rpm) and CFUs determined each day. *V. fischeri* MJ-1 was used as a control strain.

3.2.3. Identification of the Potential AOC Test Strains by 16S rDNA Sequencing

Strains that exhibited the fastest growth rates in sterile seawater were plated on Marine agar and incubated at room temperature overnight. DNA was extracted from colonies using the QIAamp DNA Mini Kit (Qiagen, Valencia, CA). The genomic DNA was amplified by polymerase chain reaction (PCR) using primers 27F (5'AGAGTTTGATCMTGGCTCAG3') and 1492R (5'TACGGYTACCTTGTTACGACTT3'). The PCR products were purified using QIAquick PCR Purification Kit (Qiagen, Valencia, CA). Purified 16S rDNA amplicons were sent to the Australian Genome Research Facility (AGRF; Westmead, NSW, Australia) for sequencing. The sequencing results were compared to the National Center for Biotechnology Information (NCBI) database using the Basic Local Alignment Search Tool (BLAST).

Phylogenetic trees of these strains with closely related strains based on 16S rDNA gene sequences were constructed by the neighbor-joining method using the Molecular Evolutionary Genetics Analysis (MEGA) software (version 5.05, the University of Pennsylvania State, USA) [70]. Multiple sequence alignments were made with the Biological Sequence Alignment Editor (BioEdit) software (version 7.2, Tom Hall) to remove sequence gaps and ambiguous bases [71]. The two-parameter method of Kimura (1980) was used to calculate distance matrices and the bootstrap analysis of Felsenstein (1985) based on 1000 replications was used to measure the confidence values of individual branches in the phylogenetic trees [72, 73].

3.2.4. Characterisation of Seawater

Seawater collected at SIMS was sent to the University of New South Wales for characterisation of Natural Organic Material (NOM) by Liquid Chromatography - Organic Carbon Detection (LC-OCD). LC-OCD has been widely applied in membrane-based water treatment processes to access the organic removal efficiency of treatment processes or to identify and characterise NOM in feed water. The principle of the technique is based on size exclusion, ion and hydrophobic interactions [74]. The system includes a chromatography column and three in-line detectors, namely, an organic carbon detector (OCD), a UV detector (UVD) and an organic nitrogen detector (OND). Chromatography is used to separate NOM

into different fractions according to their molecular size, ranging from larger than 20,000 to 350 Da, including biopolymers (polysaccharides, proteins, amino sugars, polypeptides, transparent exopolymer particles and EPS), aquatic humics (humic and fulvic acids), building blocks (weathering and oxidation products of humics), low molecular weight (LMW) neutrals (mono-oligosaccharides, alcohols, aldehydes, ketones and amino acids) and LMW acids (all monoprotic organic acids) (Figure 3.1). The relative signal response of organic carbon, UV, and organic nitrogen is measured continuously at different retention times. The concentrations of these fractions are calculated based on area integration of the fractional peaks using the Chromatography Calculator (ChromCALC) software package (DOCLabour, Karlsruhe, Germany). The technique detection limit was reported to be in the low-ppb range of individual fractions [75].

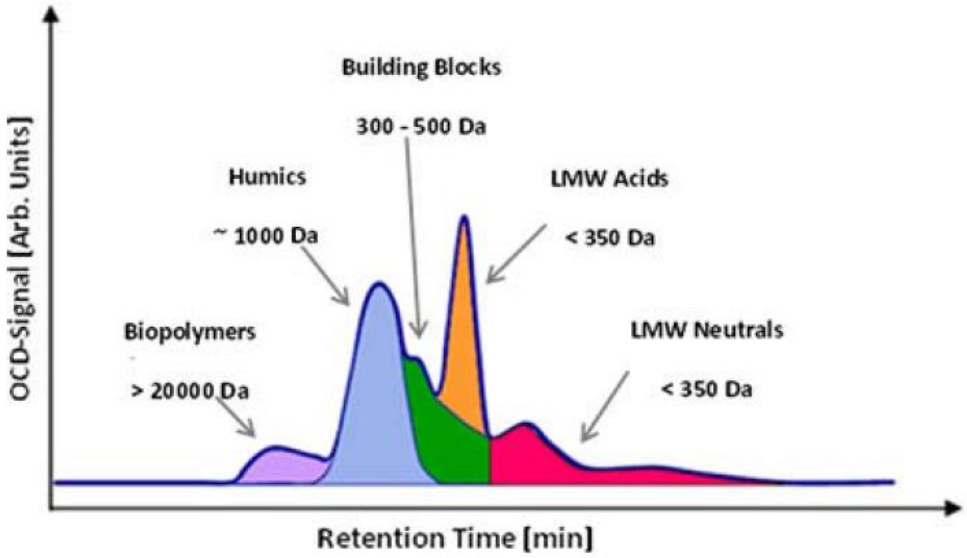

Figure 3.1. LC-OCD fractions identified by size-exclusion chromatogram using OCD. Organic substrates were fractioned according their molecular size from larger than 20000 Da to smaller than 350 Da [76].

3.2.5. Growth of Potential Test Strains on AOC Compounds

Potential test strains obtained in 3.2.2 were recovered on Marine agar overnight and transferred to ASW agar containing AOC compounds as determined in 3.2.4 and passaged three times to ensure no nutrient carried over from the Marine agar plates. These plates were

incubated at room temperature overnight and the biomass suspended in ASW and adjusted to OD_{600nm} = 0.1. Ten ml of ASW supplemented with AOC compounds were inoculated with the bacterial suspension at a final concentration of approximately 10^2 CFU ml^{-1}. The tubes were incubated at 30 ^{O}C for 48 h with shaking (200 rpm) and CFUs determined each day. *V. fischeri* MJ-1 and *V. cholerae* A1552 were used as control strains.

3.2.6. Development of Reporter Strains for AOC Quantification

A recombinant plasmid was constructed for the development of AOC reporter strains. The plasmid consisted of a pUC19 backbone containing *luxAB* genes and a strongly expressed promoter (*lacIQ*). The constructed plasmid, pUC19-*luxAB*, in which *luxAB* was under the control of the *lacIQ* promoter, was introduced into potential AOC test strains by electroporation.

3.2.6.1. Minimal Inhibitory Concentration (MIC) Tests

The MIC of the potential test strains was determined according to the agar dilution method of Singh et al. (2000) [77]. Potential strains were tested for their ability to produce visible colonies on a series of agar plates containing antibiotics (chloramphenicol, carbenicillin, ampicillin, kanamycin, gentamycin, spectinomycin, polymyxin B or tetracycline) at a range of concentrations (800, 400, 200, 100, 50, 25 and 0 µg ml^{-1}). The isolates were cultured in Luria-Bertani 20 (LB20; 10 g L^{-1} tryptone, 5 g L^{-1} yeast extract and 20 g L^{-1} NaCl; BD) at 30 ^{O}C overnight, with shaking at 200 rpm. The overnight cultures were adjusted to OD_{600nm} = 1.0 and diluted to obtain a final concentration of 10^6 CFU ml^{-1}. LB agar plates containing the antibiotics were inoculated with 10 µl bacterial stock (10^4 CFU/ spot). The plates were incubated at 30 ^{O}C for 48 h. The MIC refers to the lowest concentration of the antibiotics, which inhibited visible growth.

3.2.6.2. Construction of Bioluminescent Reporter Plasmids

Primers used in this study are described in Table 3.2. These primers were designed using the Genome Compiler software (Lucigen, USA). Plasmids and bacterial strains used in the construction of bioluminescent reporter plasmids are listed in Table 3.3. EconoTaq PLUS GREEN 2X Master Mixes (Lucigen) were used in PCR reactions in this study.

Table 3.2. Primers used in this study

Primers	**Sequences (5'-3')**	**Annealing temperature (^{O}C)**
F-LuxAB	TTC AGG GTG GTG AAT ATG AAG TTT GGA AAT ATT TGT TTT TC	65
R-LuxAB	GAT CCT CTA GAG TCG ACC TGC AGG CAT GTT ATG GTA AAT TCA TTT CGA TTT TT	
F-LacIQ	CTA TGA CCA TGA TTA CGC CAA GCT TGC ATG TGG TGC AAA ACC TTT CGC	65
R-LacIQ	ATT TCC AAA CTT CAT ATT CAC CAC CCT GAA TTG ACT	
FT4-LacIQ	ATG AGT CGA CTT ACG CCA AGC TTG CAT GTG GTG CAA AAC CTT TCG C	65
RT4-LuxAB	AGA GGT CGA CTC GAC CTG CAG GCA TGT TAT GGT AAA TTC ATT TCG ATT TTT	
FT4-CAT	ATG AGT CGA CCC CGG GAA TTA CGC CCC GCC CTG CCA	65
RT4-CAT	CAT AGT CGACGG GCA GGA GCT AAG GAA GCT A	

Table 3.3. Plasmids and bacterial strains used in the generation of bioluminescent reporter plasmids.

Plasmids or Strains	**Relevant Characteristics**	**Source or Reference**
Plasmids		
pUC19	2686 bp, Amp^R	Addgene
pKV34	8300 bp, Cam^R	[78]
pLG401	5442 bp, Cam^R, *mob*	[79]
pLS6	5485 bp, Cam^R, *mob*	[80]
Strains		
E. coli C2987	Chemical competent	BioLab
E. coli WM3064	Conjugation strain, DAP^-	[81]
V. cholerae A1552	Marine strain	[82]
V. fischeri MJ-1	*LuxAB* genes	[11]

Amp, ampicillin; Cam, chloramphenicol; DAP^-, diaminopimelic acid auxotroph

The sequence of the 2084 bp *luxAB* genes was obtained from *V. fischeri* MJ-1 (AF170104.1) by PCR using primers F-LuxAB and R-LuxAB. To obtain high levels of light production, a 66 bp highly expressed promoter, *lacIQ*, was cloned from pKV34 by PCR using primers F-LacIQ and R-LacIQ. pUC19 (NEB 5520, BioLabs, USA) was used as a backbone for the recombinant plasmid and was digested with *SphI* (NEB R3182, BioLabs) to linearise the plasmid. The two DNA fragments, the *lacIQ* promoter and the *luxAB* genes were cloned into the linear pUC19 using the NEBBuilder® HiFi DNA Assembly Cloning Kit (NEB 5520, BioLabs). The constructed plasmid containing an Amp^R marker was introduced into 5-alpha chemically competent *E. coli* (NEB C2987, BioLabs) by chemical transformation. Luminescent reporter plasmids were then extracted from *E. coli* C2987 and the confirmation of the plasmid sequence was carried out by PCR using primers F-LacIQ and R-LuxAB. The

DNA fragment was sent to AGRF for sequencing to confirm the successful construction. The procedures of bioluminescent reporter plasmid construction are described in Figure 3.2.

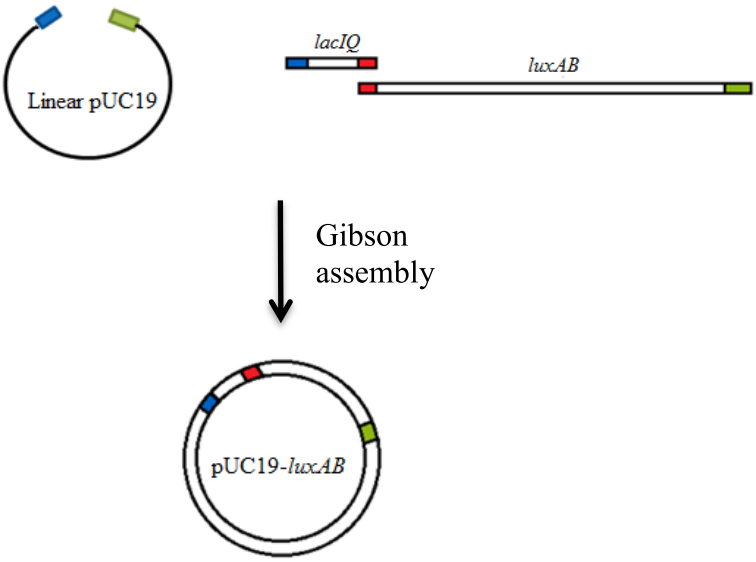

Figure 3.2. Steps in the construction of pUC19-*luxAB*. pUC19 was linearised by *SphI.* The *lacIQ* fragment possesses a 5' and 3' overhang complementary to linear pUC19 and *luxAB,* while *luxAB* has a 5' and 3' overhang complementary to *lacIQ* and the linear pUC19.

3.2.6.3. Transformation of the Recombinant Plasmid into the Potential Strains

Electroporation protocol. Electrocompetent cells in this study were prepared according to the method of Liu, 2006 [83]. Bacterial cultures were grown to an optical density at $OD_{600\ nm}$ = 0.5 for *E. coli* and 0.8 for *V. cholerae* and potential test strains. The cells were harvested by centrifugation at 3360 × *g* for 6 min at 4 ^{O}C and washed twice with ice cold 10% glycerol (*E. coli*) or ice cold 0.5 M sucrose (marine strains). The washed cells were resuspended in the same solution and stored at -80 ^{O}C until used. For electroporation, 50 µl aliquots of competent cells were mixed with 1 - 5 µl plasmids and transferred to ice cold 0.1 cm-gap electroporation cuvettes (Bio-Rad, Richmond, California) and inserted into the electroporation chamber of a Micropulser (Bio-Rad, Richmond, California) set at 1.8 kV. After the discharge, the cell suspensions were immediately mixed with 1 ml LB10 for *E. coli* or LB20 for marine strains and incubated at 37 ^{O}C or 30 ^{O}C, respectively for 1 h with shaking at 250 rpm. These suspensions were diluted and plated on LB10 or LB20 containing appropriate antibiotics and incubated at 37 ^{O}C or 30 ^{O}C for 24 to 48 h.

Conjugation protocol. The conjugation process was carried out using filter mating protocols [84]. Overnight cultures of *E. coli* WM3064 carrying reporter plasmids and AOC potential test strains were harvested by centrifugation at 7462 × *g* for 5 min at room temperature and washed twice with LB10 containing DAP (Sigma-Aldrich) and LB20, respectively. One hundred µl of *E. coli* WM3064 was mixed with 400 µl of the potential strains in 15 ml falcon tubes and the volume brought up to 5 ml with LB20 containing DAP. The mixtures were filtered through sterile 0.2 µm pore size membrane filters (Sigma-Aldrich) that were placed on LB20 containing DAP and incubated at 30 ^{O}C for 4 – 24 h. After the incubation, these filters were transferred to 5 ml phosphate buffered saline (PBS, Melford, UK). Appropriate dilutions were plated on LB20 containing chloramphenicol and incubated at 30 ^{O}C for 24 - 48 h.

3.2.7. Bioluminescent Experiments

Reporter strains were cultured in LB20 supplemented with appropriate antibiotics (100 µg ml^{-1} for carbenicillin or 25 µg ml^{-1} for chloramphenicol) and incubated at 30 ^{O}C overnight with shaking at 200 rpm. The cultures were diluted to OD_{600nm} = 0.4. Bacterial cells were collected by centrifugation 7462 × *g* for 5 min at room temperature and washed twice with ASW. The washed cells were resuspended in ASW containing appropriate antibiotics and incubated at room temperature for 30 min. For *E. coli* reporter strains, LB10 was used instead of LB20.

Bacterial cultures were added to a 24-well multiwell, tissue culture treated plate (BD Falcon^{TM}) containing carbon solutions at different concentrations ranging from 0 to 100 µg C L^{-1}. Bioluminescence was measured immediately after adding the substrate for 10 s using an integration time of 1 s with the Infinite 200 PRO plate reader (Tecan, Austria) using Magellan software (Tecan, Austria). For bioluminescent kinetic assays, bioluminescent output was measured automatically every 2.5 min for 20 - 30 min. The procedure is described in Figure. 3.3. For *V. fischeri* MJ1, the bioluminescent output was quantified without adding the substrate. The results were expressed as RLU. Each experiment was conducted in triplicate.

A 1% stock of aldehyde substrate, decanal (Sigma-Aldrich), was prepared in ethanol (Sigma-Aldrich). The stock solution was diluted with PBS to a final concentration of 6.4 mM. Carbon solutions, including glucose (BD) and humic acids (Sigma-Aldrich) were prepared in ASW as sole carbon sources at a range of concentrations (0, 20, 40, 60, 80 and 100 µg C L^{-1}). These solutions were sterilised by filtering through 0.22 µm pore size membranes.

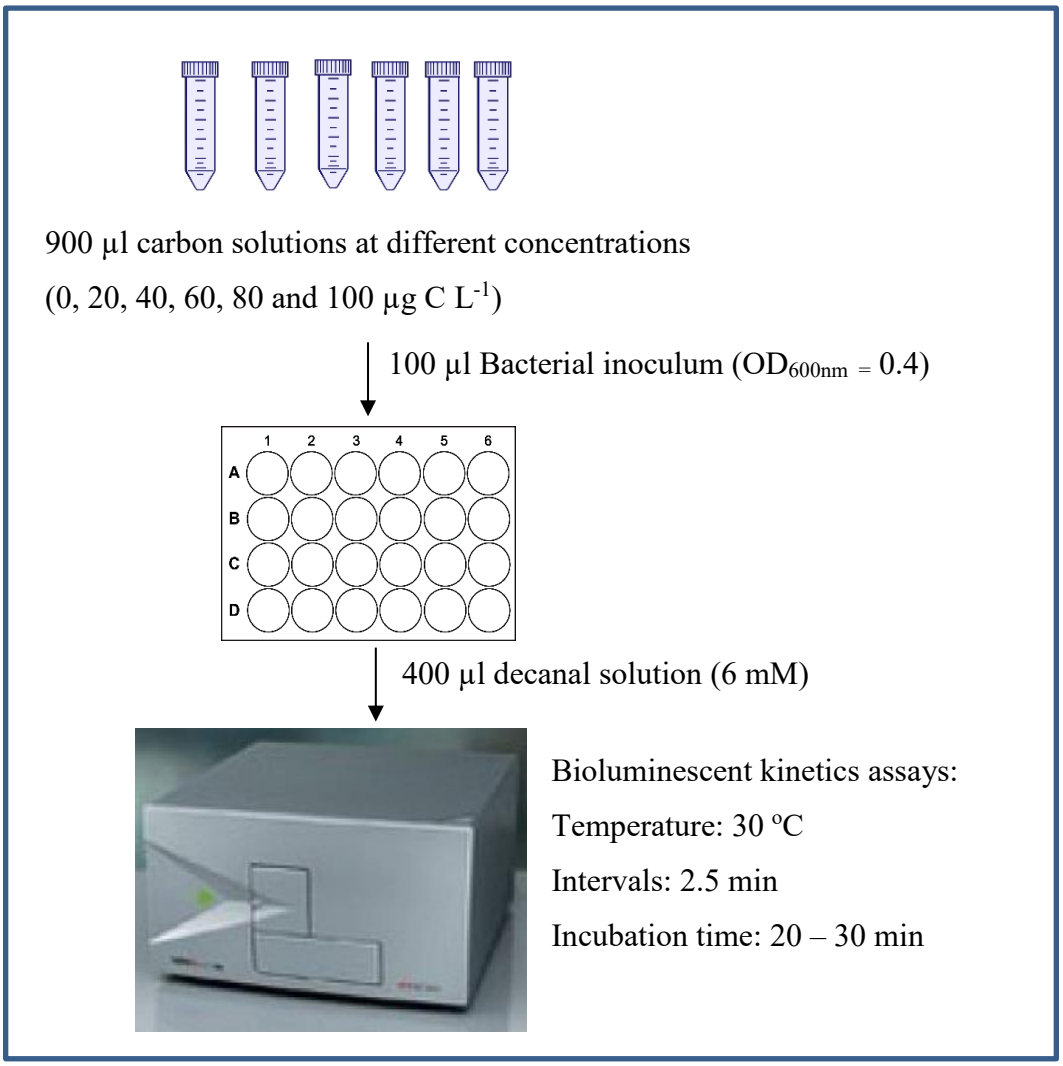

Figure 3.3. Schematic of bioluminescent experiment. Bioluminescence was measured automatically following the kinetics assays using Magellan software. For *V. fischeri* MJ1, PBS was used instead of the substrate solution.

3.3. Results

3.3.1. Isolation of Marine Bacteria with Broad Metabolic Potential

Representative marine microorganisms were investigated for their ability to grow in sterile seawater. Isolates obtained from seawater were used to develop bioluminescent reporter strains that will allow the quantification of AOC compounds in RO feed water.

3.3.1.1. Isolation of Marine Organisms from Seawater

In order to obtain strains with broad metabolic potential for use as an indicator strain for the quantification of AOC in seawater that will be used as feed water for desalination, we collected seawater and biofilms from the filtration system at SIMS, as well as seawater at Chowder Bay (SIMS) and Brighton-Le-Sands. These samples were plated onto seawater agar plates that were incubated at room temperature. This procedure led to the isolation of 15 colonies after 24 h and a further 20 colonies after 48 h incubation. The colonies were purified on Marine agar and preserved in Marine broth containing 25% glycerol, at – 80 ^{O}C. Images of marine strains showing different colony morphologies are presented in Figure 3.4.

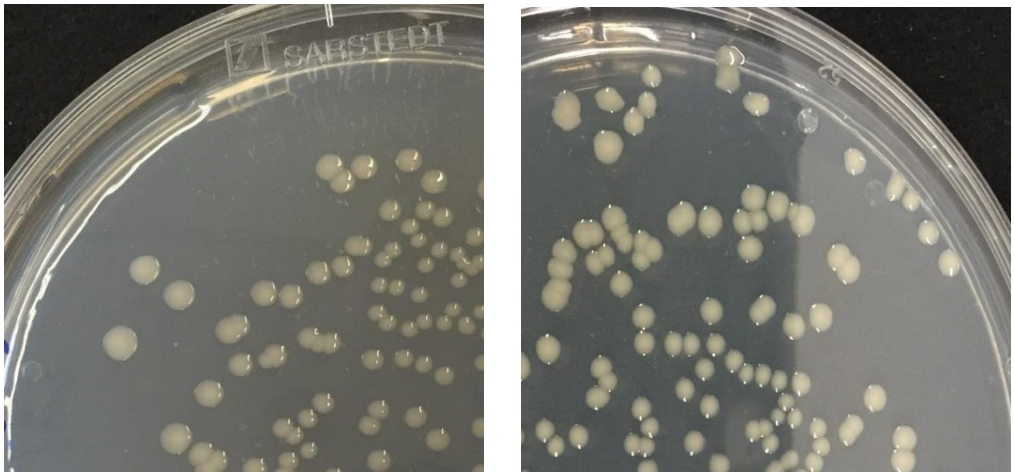

CB1a

CBSW4

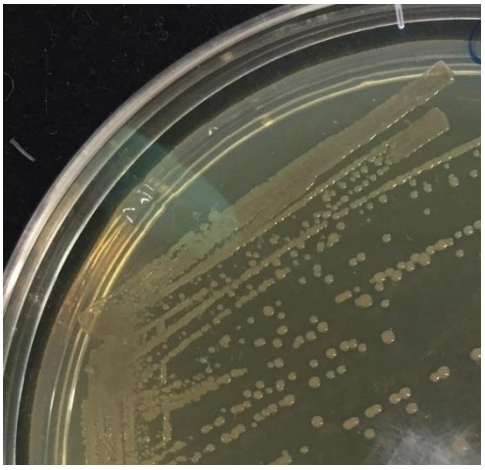

BLS2

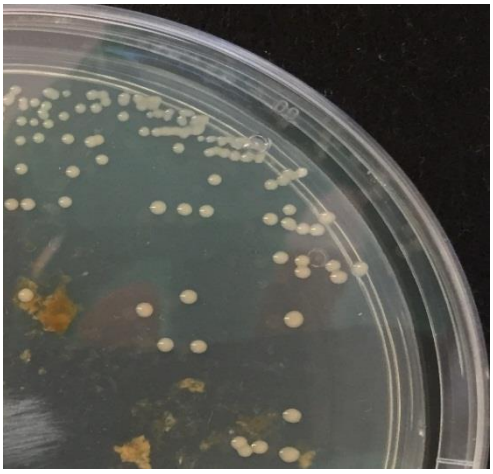

CBS2

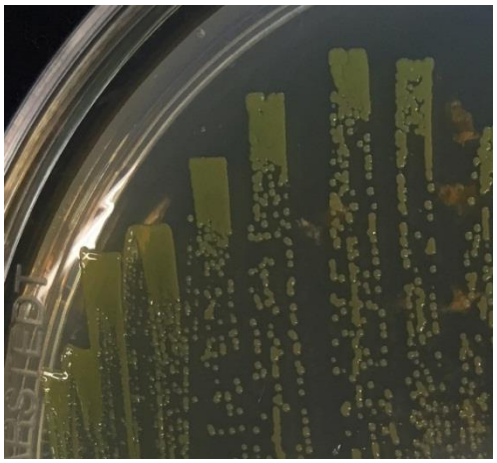

CBSW6

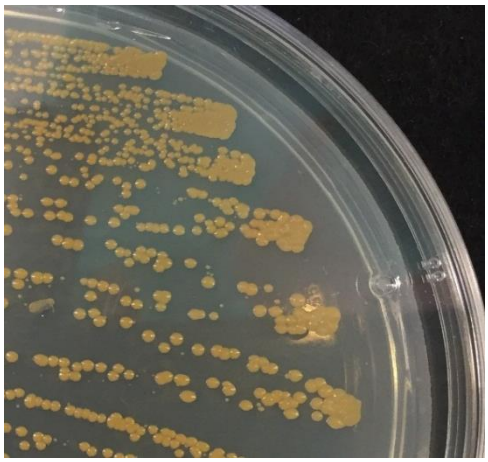

CBS5

Figure 3.4. Images of marine isolates (CB1a, CBSW4, BLS2, CBS2, CBSW6, CBS5). Isolates were cultured on Marine agar plates and incubated at 28 ^{O}C for 48 h.

3.3.1.2. Selection of Potential AOC Test Strains

Strains that are able to grow in low nutrient seawater may utilise AOC compounds in the RO feed water. The objective of this project is to utilise strains able to grow on AOC in seawater as indicator organisms for the quantification of AOC. Therefore, we isolated strains able to grow on seawater agar low nutrient media. Fifteen strains that grew after 24 h on seawater plates were selected for further investigation. *V. fischeri* MJ1 is used here as a control as this strain has been shown previously to accurately estimate glucose concentrations [11]. The strains were cultured in seawater and the CFUs were determined over 168 h of incubation. Isolates reached maximum numbers in 24 or 48 h (Table 3.4).

The results showed that the isolates BLS2, CBSW3 and CBSW4 reached higher CFUs than the other strains, reaching maximum cell densities of 5.1×10^5, 4.5×10^5 and 7.2×10^5 CFU ml^{-1}, respectively. The maximum cell densities of the three strains used here are similar to that of AOC test strains *Stenotrophomonas* sp. ZJ2 (1.2×10^6 CFU ml^{-1}), *Pseudomonas saponiphila* G3 (1.3×10^6 CFU ml^{-1}) and *Enterobacter* sp. G6 (7.7×10^5 CFU ml^{-1}) cultured in drinking water [85]. These results indicated that these three strains can utilise AOC for growth and thus were selected for further development as AOC test strains.

Table 3.4. The growth of 15 isolates (CFU ml^{-1}) in seawater over 7 days

Isolates	**Hour 0**	**Hour 24**	**Hour 48**	**Hour 72**	**Hour 96**	**Hour 168**
V. fischeri MJ1	$(6.7 \pm 8.9) \times 10^{2}$	$(1.3 \pm 0.4) \times 10^{3}$	$(5.3 \pm 5.2) \times 10^{3}$	$(1.1 \pm 1.8) \times 10^{4}$	$(1.7 \pm 2.8) \times 10^{4}$	$(5.3 \pm 9.2) \times 10^{4}$
BLS2	$(1.1 \pm 0.7) \times 10^{3}$	$(3.0 \pm 1.0) \times 10^{5}$	**$(5.1 \pm 1.9) \times 10^{5}$**	$(4.3 \pm 0.7) \times 10^{5}$	$(1.1 \pm 1.4) \times 10^{5}$	$(1.5 \pm 0.9) \times 10^{4}$
CB10-10	$(7.1 \pm 2.8) \times 10^{2}$	$(2.0 \pm 3.0) \times 10^{4}$	$(2.9 \pm 4.0) \times 10^{4}$	$(1.6 \pm 2.6) \times 10^{5}$	$(1.2 \pm 1.8) \times 10^{5}$	$(1.6 \pm 2.6) \times 10^{5}$
CB10-3	$(4.3 \pm 1.8) \times 10^{2}$	$(2.4 \pm 3.7) \times 10^{4}$	$(1.7 \pm 2.5) \times 10^{5}$	$(1.9 \pm 3.0) \times 10^{5}$	$(1.5 \pm 2.4) \times 10^{5}$	$(1.0 \pm 1.7) \times 10^{5}$
CB1b	$(5.5 \pm 1.1) \times 10^{2}$	$(1.9 \pm 1.7) \times 10^{5}$	$(2.1 \pm 1.9) \times 10^{5}$	$(5.7 \pm 4.8) \times 10^{4}$	$(2.1 \pm 1.6) \times 10^{4}$	$(8.0 \pm 3.5) \times 10^{2}$
CBS2	$(3.3 \pm 0.6) \times 10^{1}$	$(1.8 \pm 2.5) \times 10^{5}$	$(1.3 \pm 0.5) \times 10^{5}$	$(1.1 \pm 0.8) \times 10^{5}$	$(1.9 \pm 0.4) \times 10^{4}$	$(1.2 \pm 0.4) \times 10^{4}$
CB70-3	$(1.5 \pm 1.0) \times 10^{2}$	$(5.6 \pm 7.4) \times 10^{1}$	Not detectable	Not detectable		
CBS5	$(3.4 \pm 2.3) \times 10^{2}$	$(1.6 \pm 1.4) \times 10^{2}$	$(5.0 \pm 8.7) \times 10^{1}$	$(3.3 \pm 5.8) \times 10^{1}$	Not detectable	
CB10-8	$(8.2 \pm 13) \times 10^{2}$	Not detectable	Not detectable	Not detectable		
CBSW6	$(4.7 \pm 1.5) \times 10^{2}$	$(6.2 \pm 5.9) \times 10^{4}$	$(2.2 \pm 1.4) \times 10^{4}$	$(2.0 \pm 1.9) \times 10^{4}$	$(2.4 \pm 3.3) \times 10^{4}$	$(2.5 \pm 0.3) \times 10^{4}$
CB10SW1	$(3.0 \pm 0.6) \times 10^{2}$	$(5.9 \pm 4.2) \times 10^{4}$	$(3.0 \pm 2.4) \times 10^{4}$	$(8.6 \pm 14) \times 10^{4}$	$(6.9 \pm 11) \times 10^{4}$	$(1.0 \pm 1.6) \times 10^{4}$
CBSW3	$(2.3 \pm 1.6) \times 10^{2}$	**$(4.5 \pm 1.7) \times 10^{5}$**	$(2.4 \pm 2.1) \times 10^{5}$	$(2.3 \pm 2.7) \times 10^{5}$	$(1.7 \pm 2.5) \times 10^{5}$	$(1.8 \pm 3.0) \times 10^{5}$
CBSW4	$(1.8 \pm 0.8) \times 10^{3}$	$(1.6 \pm 0.9) \times 10^{5}$	**$(7.2 \pm 2.1) \times 10^{5}$**	$(5.1 \pm 6.0) \times 10^{5}$	$(3.0 \pm 3.5) \times 10^{5}$	$(2.3 \pm 3.2) \times 10^{5}$
CBSW5	$(2.1 \pm 2.2) \times 10^{2}$	$(1.1 \pm 1.5) \times 10^{5}$	$(1.1 \pm 1.8) \times 10^{5}$	$(1.0 \pm 1.7) \times 10^{5}$	$(9.3 \pm 15) \times 10^{4}$	$(3.4 \pm 6.1) \times 10^{4}$
CB10SW2	$(3.7 \pm 4.2) \times 10^{2}$	$(1.8 \pm 2.6) \times 10^{5}$	$(1.3 \pm 1.6) \times 10^{5}$	$(1.1 \pm 1.6) \times 10^{5}$	$(7.8 \pm 11) \times 10^{4}$	$(5.6 \pm 8.2) \times 10^{4}$
CB10SW4	$(1.7 \pm 2.1) \times 10^{3}$	$(3.5 \pm 0.7) \times 10^{5}$	$(1.4 \pm 1.2) \times 10^{5}$	$(1.2 \pm 1.0) \times 10^{5}$	$(4.6 \pm 2.2) \times 10^{4}$	$(3.2 \pm 2.1) \times 10^{4}$

3.3.1.3. Identification of Strains by 16S rDNA Sequencing

The three strains BLS2, CBSW3 and CBSW4 selected as potential test strains for AOC measurement of seawater were identified by sequencing of the partial 16S rDNA gene using 27F and 1492R primers. The resulting sequences were compared to sequences in the NCBI database using BLAST (Table 3.5). The BLAST results demonstrated that the sequence of strains BLS2, CBSW3 and CBSW4 shared 99% sequence identity to species of *Enterovibrio norvegicus*, *V. harveyi* and *Pseudoalteromonas nigrifaciences* and *Pseudoalteromonas lipolytica,* respectively. These genera are all common marine bacteria that have broad metabolic potential [86-88]. In a partial 16S rDNA gene sequence phylogenetic tree constructed by the neighbour-joining methods, BLS2 and the type strains of *Enterovibrio* sp. formed a cluster with the type strain of *E. norvegicus* at a bootstrap value of 91% (Figure 3.5). CBSW3 was related most closely to the type strains of *Vibrio ownensii*, *Vibrio communis*, *Vibrio campbellii* and *V. harveyi* with a bootstrap value of 54% (Figure 3.6). Similarly, CBSW4 clustered with *P. nigrifaciences* and *Pseudoalteromonas whanghaensis* with s bootstrap value of 100% (Figure 3.7). The data obtained indicated that BLS2 and CBSW3 were not closely related to *E. norvegicus* and *V. harveyi* respectively, while CBSW4 was closely related phylogenetically to *P. whanghaensis and P. nigrifaciens*.

Table 3.5. Bacterial isolates with the highest identity to BLS2, CBSW3 and CBSW4 on the basis of 16S rDNA sequence analysis.

Isolates	**Similarity**	**Sequence identity**	**Sequence Length**
BLS2	*Enterovibrio norvegicus* M4 (LK391520.1)	99%	1398 bp
CBSW3	*Vibrio harveyi* QH141026D (KU245732.1)	99%	1427 bp
CBSW4	*Pseudoalteromonas nigrifaciens* 1344 (GU726853.1)	99%	1386 bp
	Pseudoalteromonas lipolytica G3C (KM041116.1)		

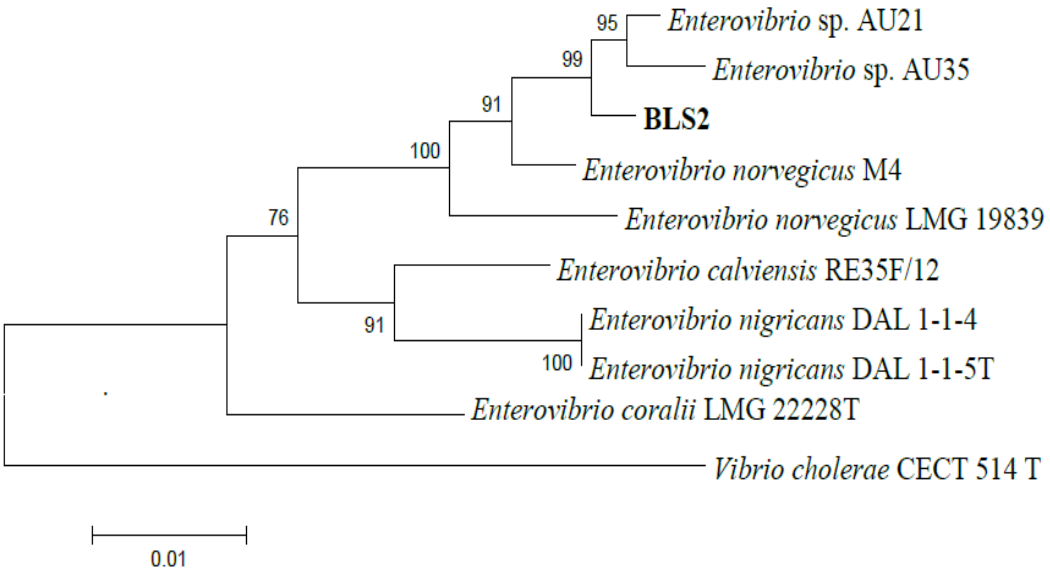

Figure 3.5. Phylogenetic relationship of BLS2 with closely related strains. The phylogenetic tree based on the partial 16S rDNA gene sequence was constructed by the neighbour-joining method. The type strain of *V. cholerae* was used as an outgroup. The numerals at the nodes of the respective branches indicate bootstrap values (%) derived from 1000 replications.

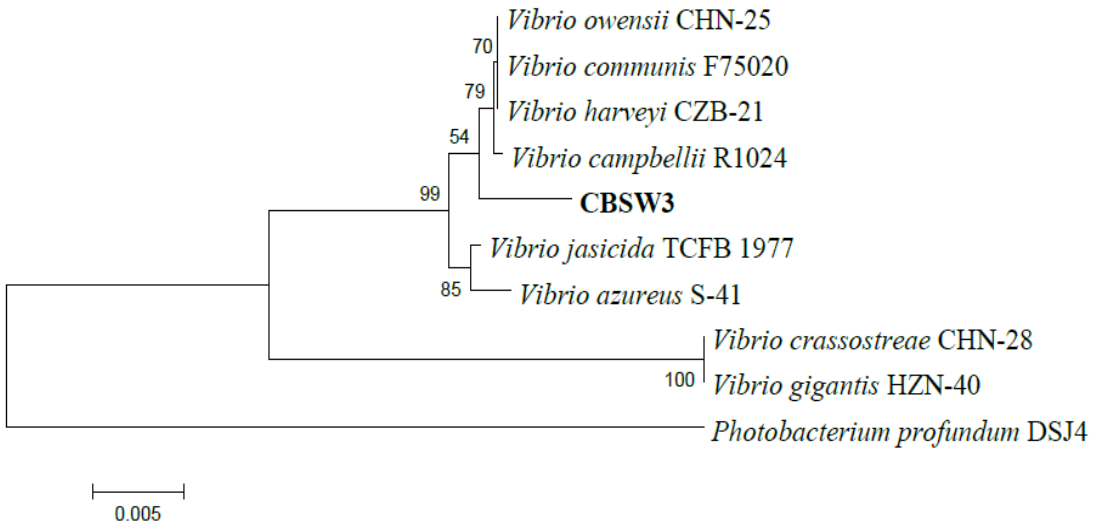

Figure 3.6. Phylogenetic relationship of CBSW3 with closely related strains. The phylogenetic tree based on the partial 16S rDNA gene sequence was constructed by the neighbour-joining method. The type strain of *Photobacterium profundum* was used as an outgroup. The numerals at the nodes of the respective branches indicate bootstrap values (%) derived from 1000 replications.

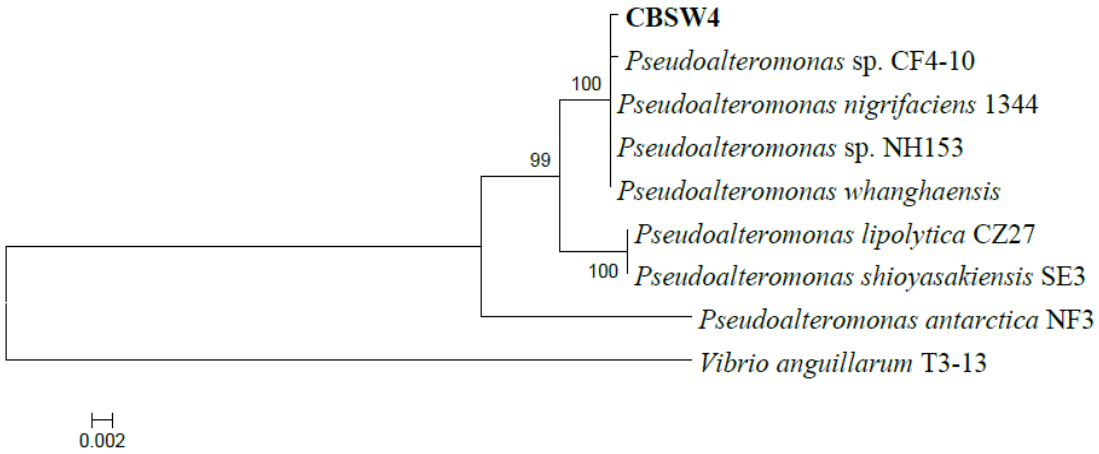

Figure 3.7. Phylogenetic relationship of CBSW4 with closely related strains. The phylogenetic tree based on the partial 16S rDNA gene sequence was constructed by the neighbour-joining method. The type strain of *Vibrio anguillarum* was used as an outgroup. The numerals at the nodes of the respective branches indicate bootstrap values (%) derived from 1000 replications.

It is difficult to confirm the identity of these three strains using partial 16S rDNA sequences due to high sequence similarity, especially for *Vibrio* spp. To confirm at the species level, further genomic analyses, i.e. the full 16S rRNA gene and multi-locus sequencing or analysis by amplified fragment length polymorphism (AFLP) would be required [87].

3.3.1.4. Characterisation of Seawater

According to LC-OCD analysis, humic substances, building blocks and LMW substrates, which have molecular weights less than 1000 Da, are common AOC compounds in seawater. DOC fractions and concentrations in seawater collected at Chowder Bay were determined by LC-OCD technology. The results presented in Table 3.6 show that humic acids and LMW neutrals account for 85% of the total chromatographable dissolved organic carbon (CDOC) in seawater, while building blocks and LMW acids comprised only 10% of the total CDOC. The results are consistent with findings from the study of Jeong et al. (2015) that indicated that humic acids and LMW neutrals were the main AOC compounds leading to membrane fouling [10].

Table 3.6. LC-OCD seawater organic fractions (µg C L^{-1})

Sample	Total CDOC	Bio-polymers	Humic substances	Building blocks	LMW neutrals	LMW acids
This study	2015	105	951	123	756	79
Jeong et al. (2013) [11]	1290	130	440	160	890	
Naidu et al. (2013) [89]	1850 ± 420	80 ± 20	350 ± 150	100 ± 40	730± 150	

3.3.1.5. Growth of Potential Test Strains on AOC Compounds

In this study, humic substances (Sigma-Aldrich) were used as AOC compounds due to their abundance in seawater. CBSW4, BLS2 and CBSW3 were cultured on ASW supplemented with humic substrates at the final concentration of 500 µg C L^{-1} and the CFUs determined over 48 h of incubation. Two common marine bacteria, *V. fischeri* MJ1 and *V. cholerae* A1552 were used as controls. The results presented in Table 3.7 indicated that all three marine strains were able to grow on humic acids, while there was no visible growth for *V. fischeri* MJ1 or *V. cholerae* A1552. Although both CBSW4 and CBSW3 showed good growth on humics with maximum cell densities of 2.1 x 10^5 and 1.6 x 10^5 CFU ml^{-1}, respectively, BLS2 CFUs increased slightly to 5.0 x 10^4 CFU ml^{-1} after 24 h incubation. Furthermore, the isolates were cultured onto either ASW agar plates (the control) or ASW agar plates with added humic acids. According to the data not shown in the text, CBSW4, BLS2 and CBSW3 were able to grow on ASW agar plates with humics, but not on the control.

Table 3.7. The growth of potential strains (CFU ml^{-1}) on humic acids over 48 h.

Isolates	**0 h**	**24 h**	**48 h**
CBSW4	$(7.1 \pm 0.8) \times 10^3$	$(2.1 \pm 0.8) \times 10^5$	$(4.6 \pm 2.1) \times 10^4$
CBSW3	$(1.8 \pm 0.6) \times 10^3$	$(8.1 \pm 1.6) \times 10^4$	$(1.6 \pm 0.1) \times 10^5$
BLS2	$(1.4 \pm 0.3) \times 10^2$	$(5.0 \pm 1.4) \times 10^4$	$(2.8 \pm 1.1) \times 10^4$
V. fischeri MJ1	$(1.1 \pm 0.1) \times 10^2$	Not detectable	
V. cholerae A1552	$(3.4 \pm 0.6) \times 10^3$	$(1.6 \pm 0.2) \times 10^3$	$(9.5 \pm 3.5) \times 10^2$

3.3.2. Development of Luminescent AOC Reporter Strains

In this study, bioluminescent reporter strains for the quantification of AOC were constructed by introducing plasmids containing *luxAB* genes obtained from *V. fischeri* MJ1 to potential AOC test strains. One of the main drawbacks to the use of bioluminescence for the quantification of AOC is the achievement of reporter protein expression levels high enough to produce a signal that can be detected externally. Therefore, promoter *lacIQ*, a mutated promoter of the *lacI* gene (a C -> T change in the -35 region) which causes a 10-fold increase in *lacI* expression compared to the wild type promoter was used. The pUC19 plasmid that has a high copy number of between 500 and 700 copies per cells was also used to optimise the expression levels of the bacterial luminous genes *luxAB* [90].

3.3.2.1. MIC Tests

To determine which antibiotics could be used for selection of recombinant plasmids, MICs of the strains were determined for chloramphenicol, carbenicillin, ampicillin, kanamycin, gentamycin, spectinomycin, polymyxin B and tetracycline. The results showed that BLS2 and CBSW4 were susceptible to all antibiotics tested, while CBSW3 was sensitive to chloramphenicol at a concentration of 25 µg ml^{-1}, but was resistant to the remaining antibiotics at all tested concentrations (Table 3.8). The MIC values of BLS2 and CBSW4 were found to be 25 µg ml^{-1} for chloramphenicol, carbenicillin, ampicillin, kanamycin, gentamycin, spectinomycin, polymyxin B and tetracycline.

Table 3.8. MIC values of antibiotics for BLS2, CBSW3 and CBSW4.

Isolates	**BLS2**	**CBSW3**	**CBSW4**
Antibiotics		**µg ml^{-1}**	
Chloramphenicol	25	25	25
Carbenicillin	25	-	25
Ampicillin	25	-	25
Kanamycin	25	-	25
Gentamycin	25	-	25
Spectinomycin	25	-	25
Polymyxin B	25	-	25
Tetracycline	25	-	25

'-' indicates no inhibition.

3.3.2.2. Construction of Bioluminescent Reporter Plasmids

To construct the bioluminescent reporters, DNA fragments encoding the *luxAB* genes and *lacIQ* promoter were amplified by PCR using primers designed using Genome Compiler software. The PCR products were electrophoresed on 1.0% agarose gel (Figure 3.8).

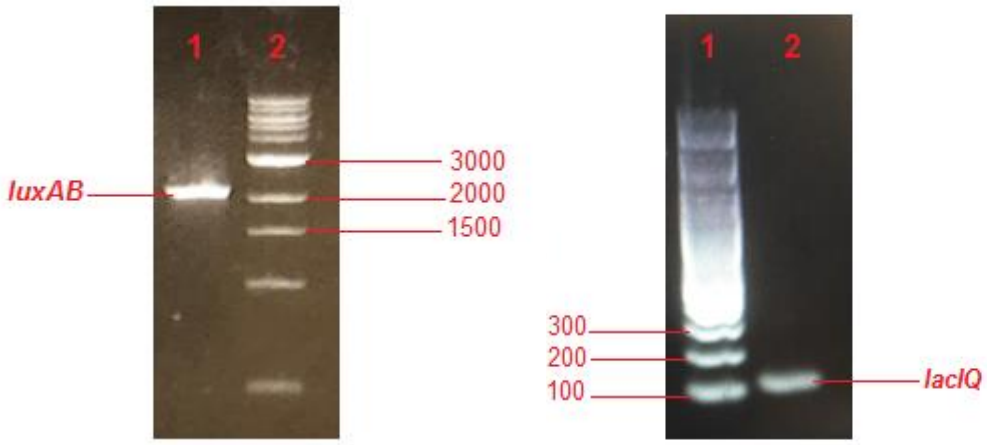

(A) **(B)**

Figure 3.8. PCR amplification of (A) *luxAB* using primers forward *luxAB* and reverse *luxAB*. Lane 1 is the PCR product (2127 bp); lane 2 is 1 Kb DNA ladder and (B) *lacIQ* using forward *lacIQ* and reverse *lacIQ* primers. Lane 1 is 100 bp DNA ladder; lane 2 is the PCR product (111 bp).

These DNA fragments were cloned into a linear pUC19 vector by Gibson Assembly (NEB, Ipswich, MA USA). The pUC19-*luxAB* reporter plasmids were transformed into *E. coli* C2987. These recombinant vectors were confirmed by restriction digestion using *EcoRI* (Figure 3.9). The confirmation of the DNA fragments was carried out by sequencing using primers F-laqIQ and R-luxAB. The sequencing results indicated that *luxAB* genes downstream of promoter *lacIQ* were successfully cloned into pUC19. pUC19-*luxAB* reporter plasmids were transformed into BLS2 and CBSW4 by electroporation. According to MIC results obtained in 3.3.2.1, CBSW3 was susceptible to chloramphenicol, but resistant to ampicillin, which is the antibiotic selection marker of pUC19. Therefore, the *cat* gene encoding chloramphenicol acetyltransferase obtained from pKV34 by PCR using primers FT4-CAT and RT4-CAT was inserted into pUC19-*luxAB* by T4 ligation using *SalI*. The T4 ligation products were introduced into *E. coli* C2987. The recombinant plasmid pUC19-*luxAB-cat* was extracted from *E. coli* C2987 and confirmed by restriction digestion, followed by transformation into CBSW3 by electroporation. *V. cholerae* A1552 was used as a positive control for the electroporation. The electroporation results showed that although electrotransformation efficiency of *V. cholerae* A1552 was 10^6 CFU ml^{-1} using 100 ng of plasmid DNA, all three strains BLS2, CBSW3 and CBSW4 were unable to take up the reporter plasmids.

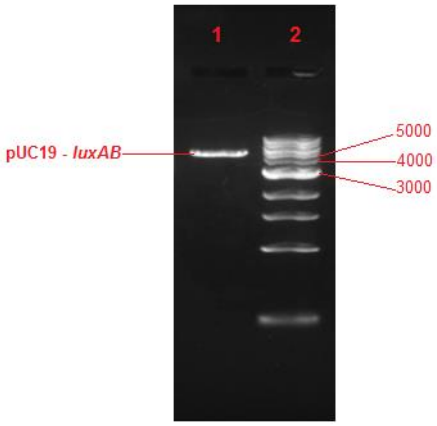

Figure 3.9. Restriction digestion of pUC19-*luxAB* with *EcoR*I. Lane 1 is the product of digestion with *EcoR*I (4836 bp); lane 2 is 1 Kb DNA ladder.

Failure to introduce pUC19-*luxAB* into these three AOC potential strains by electro-transformation led to the use of conjugation as an alternative method. Thus, conjugative plasmids, including pLG401 and pLS6 were used for the generation of reporter plasmids, which were introduced into these three potential strains by conjugation. The DNA fragment *lacIQ-luxAB* obtained from pUC19-*luxAB* by PCR using primers FT4-laqIQ and RT4-luxAB was inserted into pLG401 and pLS6 with T4 ligation. The products of the ligation reaction were transformed into *E. coli* WM3064 by electroporation. pLG401-*luxAB* and pLS6-*luxAB* were confirmed by restriction digestion with *EcoRI* and *lacIQ-luxAB* was confirmed by PCR with primers FT4-laqIQ and RT4-luxAB (Figure 3.10). pLG401-*luxAB* and pLS6-*luxAB* were conjugated into BLS2, CBSW3 and CBSW4. The results indicated that pLG401-*luxAB* and pLS6-*luxAB* were successfully introduced into BLS2 and CBSW3, but not into CBSW4.

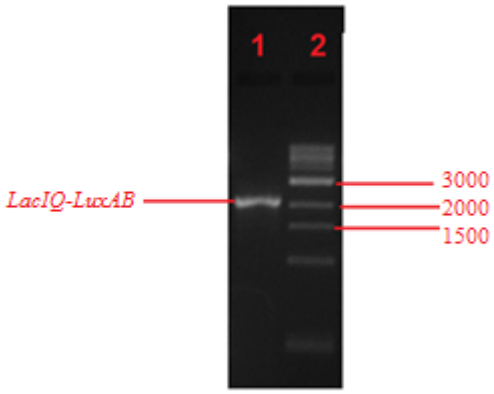

Figure 3.10. PCR amplification of *lacIQ-luxAB* using FT4-laqIQ and RT4-luxAB primers. Lane 1 is the PCR product (2238 bp); lane 2 is 1 Kb DNA ladder.

3.3.3. Bioluminescent Measurements

Conjugative plasmids pLG401 and pLS6 were used in an attempt to construct bioluminescent reporter strains for AOC quantification due to the inability to introduce the high copy number reporter plasmid pUC19-*luxAB* into three potential test strains CBSW4, BLS2 and CBSW3. Modified test strains, including BLS2 (pLG401-*luxAB*/ pLS6-*luxAB*) and CBSW3 (pLG401-*luxAB*/ pLS6-*luxAB*) were cultured in LB20 supplemented with 25 µg ml^{-1} chloramphenicol, incubated at 30 ^{O}C overnight, shaking at 200 rpm. The bioluminescence of these reporter strains was analysed by adding 400 µl substrate solution to the 1 ml overnight bacterial cultures (OD_{600nm} = 1.0). The results showed that all reporter strains were able to produce bioluminescence. However, the bioluminescence produced by these reporter strains were only slightly above background levels of bioluminescence (≈ 3 x 10^1 RLUs). Therefore, these reporter strains are not yet suitable for AOC quantification. To investigate the bioluminescence of pUC19-*luxAB,* the reporter plasmid was introduced into a common marine bacterium, *V. cholerae* A1552, for further studies.

The bioluminescence levels of *V. cholerae* A1552 (pUC19-*luxAB*), *E. coli* C2987 (pUC19-*luxAB*) and *V. fischeri* MJ1 are presented in Figure 3.11. The control, *V. fischeri* MJ1, is used here because it has been successfully used as an AOC test strain. Although *V. cholerae* A1552 and *E. coli* C2987 carry the same reporter plasmid, the bioluminescence output produced by these reporter strains were different. The light production of *V. cholerae* A1552 (pUC19-*luxAB*) was 3.3 x 10^4 RLU compared to 3.7 x

10^5 RLU of *E. coli* C2987 (pUC19-*luxAB*). This result indicated that the expression level of *luxAB* genes in *E. coli* C2987 were significantly higher than that in *V. cholerae* A1552. The light production of these two reporter strains was much lower than for *V. fischeri* MJ1 (1.1 x 10^6 RLU). The results are consistent with the findings of previous studies that bioluminescence of reporter strains expressing *luxAB* ranges from 3.6 x 10^3 to 3.9 x 10^5 RLU [91, 92]. This indicated that luciferase was successfully expressed in *E. coli* C2987 and *V. cholerae* A1552.

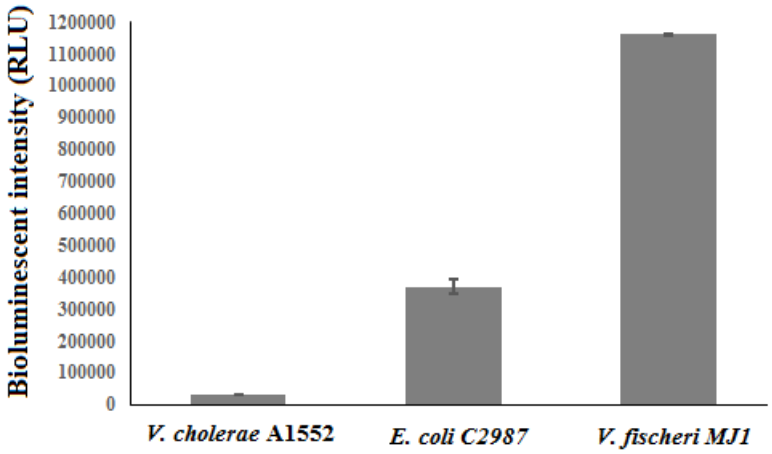

Figure 3.11. The bioluminescent levels of *V. cholerae* A1552 (pUC19-*luxAB*), *E. coli* C2987 (pUC19-*luxAB*) and the control strain *V. fischeri* MJ1 in LB. The bioluminescent signals are for bacterial cultures (OD_{600nm} = 1.0) after addition of the substrate. For *V. fischeri* MJ1, no substrate was added. The error bars represent standard deviation of the means.

The production of bioluminescence by *V. cholerae* A1552 (pUC19-*luxAB*) and *V. fischeri* MJ1 in diluted LB media was investigated at different carbon concentrations ranging from 0 to 11.2 mg C L^{-1} for 20 min (Figure 3.12 and 3.13). The results showed that at low carbon concentrations ≤ 1.4 mg C L^{-1}, *V. cholerae* A1552 (pUC19-*luxAB*) reached the maximum signal production after 5 min incubation and 7.5 min incubation at high carbon concentrations from 2.8 – 11.2 mg C L^{-1}, while *V. fischeri* MJ1 produced the greatest bioluminescent signal after 10 min incubation at carbon concentrations ≤ 1.4 mg C L^{-1} and became saturated when carbon concentrations exceeded 2.8 mg C L^{-1}. These results demonstrated that at low nutrient concentrations, bacteria required shorter incubation times to utilise all available carbon in the solution. When carbon concentrations were too high, there was no correlation between carbon concentrations and bioluminescent

intensity. The bioluminescence of the modified strain decreased suddenly after reaching the peak, while the bioluminescence of *V. fischeri* MJ1 remained for 10 min after reaching the maximum level. This rapid reduction that occurred in the modified strain was attributed to nutrient limitation. In an appropriate concentration range, bioluminescence intensity increased with increases in carbon concentration. At a low concentration of 0.7 mg C L^{-1}, the maximum bioluminescence of the modified strain and the control strain was 3.1 x 10^3 RLU and 1.4 x 10^4 RLU, while at a high concentration of 2.8 mg C L^{-1}, the bioluminescent response was 4.5 x 10^3 RLU and 2.1 x 10^4 RLU, respectively.

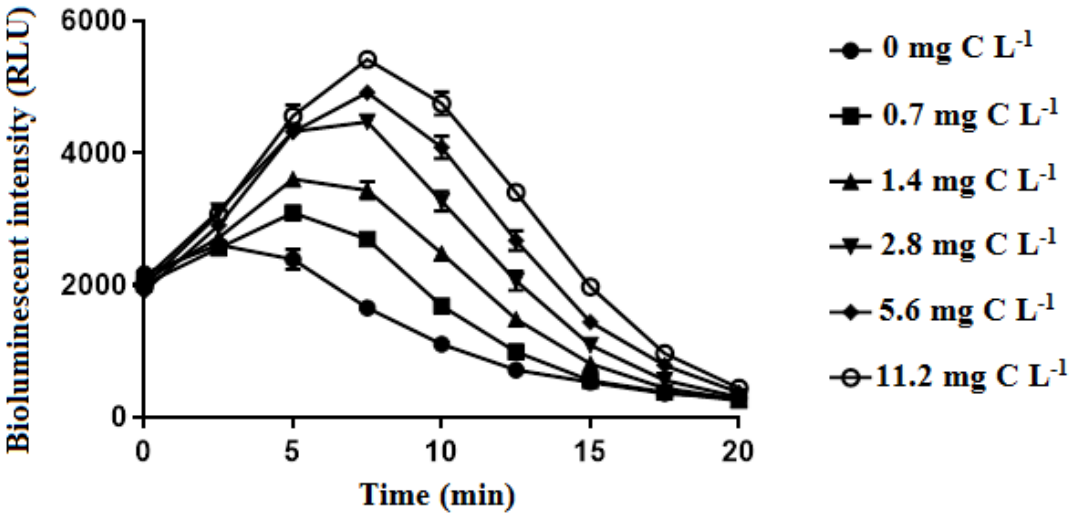

Figure 3.12. Bioluminescent intensity of *V. cholerae* A1552 (pUC19-*luxAB*) in response to different LB dilutions over 20 min. The bioluminescent signals are for bacterial cultures (OD_{600nm} = 0.4) after addition of the substrate. The error bars represent standard deviations of the means.

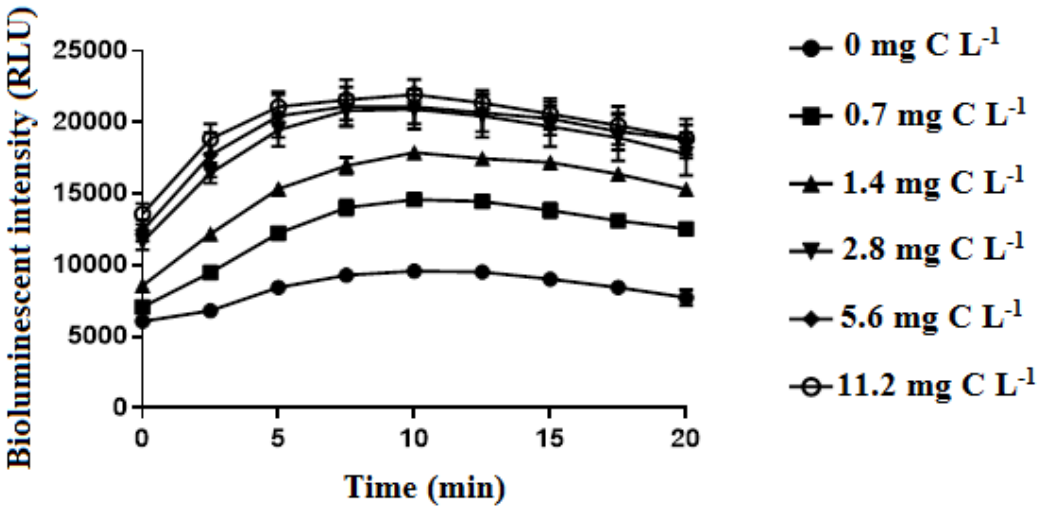

Figure 3.13. Bioluminescent intensity of *V. fischeri* MJ1 in response to different LB dilutions over 20 min. The bioluminescent signals were showed for bacterial cultures (OD_{600nm} = 0.4). The error bars represent standard deviation of the means.

Both *V. fischeri* MJ1 and *V. cholerae* A1552 are unable to utilise humic acids, which are a major component of AOC compounds in seawater. Therefore, a curve showing the relationship of bioluminescence intensity and humic concentration has not been constructed. The bioluminescence of *V. cholerae* A1552 (pUC19-*luxAB*) and the control strain *V. fischeri* MJ1 in the presence of glucose were measured at concentrations ranging from 0 to 100 µg mg C L^{-1} at 2.5 min intervals for 15 - 30 min to capture the maximum levels of bioluminescence (Figure 3.14). Glucose was used as it gave the greatest sensitivity for the detection of low amounts of carbon, expressed as glucose equivalent in µg C L^{-1} [93]. These results showed that the bioluminescence increased with increasing glucose concentration. The maximum bioluminescence of the modified and control strains at the highest carbon concentration (100 µg mg C L^{-1}) was 3.2 x 10^3 RLU and 5.3 x 10^5 RLU, while at the lowest concentration was 2.6 x 10^3 RLU and 2.8 x 10^5 RLU, respectively. At all tested glucose concentrations, bioluminescence intensity of *V. cholerae* A1552 (pUC19-*luxAB*) increased exponentially and reached the maximum after 5 min incubation compared to 7.5 min incubation in *V. fischeri* MJ1. The findings are different to those from a study of Jeong et al. (2013) where *V. fischeri* MJ1 obtained the maximum light emission after 30 min incubation [11]. The differences may be attributed to the higher initial cell density used in this study. The shorter incubation time to reach the maximum bioluminescence enables this to be a rapid AOC assay. After reaching the peak, the bioluminescence of the two tested strains sharply decreases over 70% by the

end of the experiment. The sudden reduction of bioluminescence indicates that all available glucose has been utilised by the tested strains.

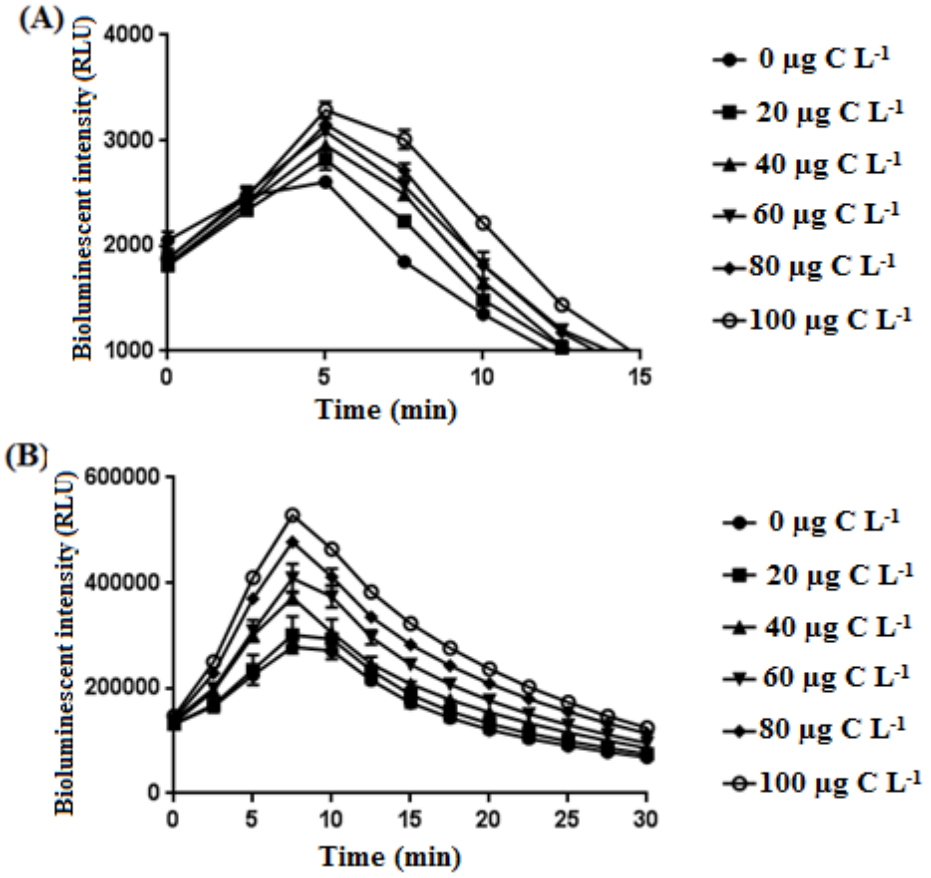

Figure 3.14. Bioluminescent intensity of (A) *V. cholerae* A1552 (pUC19-*luxAB*) and (B) control strain *V. fischeri* MJ1 in response to different glucose concentrations. The bioluminescent signals are for bacterial cultures at an OD_{600nm} = 0.4. The error bars indicate standard deviation of the means.

The maximum values of bioluminescence obtained after 5 min incubation of *V. cholerae* A1552 (pUC19-*luxAB*) and 7.5 min incubation of *V. fischeri* MJ1 plotted against glucose concentrations is presented in Figure 3.15. Results showed that the curve of *V. fischeri* MJ1 bioluminescence plotted against C concentration had R^2 of 0.9874 compared to 0.9761 for the modified strain. This result indicated that the linear relationship between bioluminescence and glucose concentration by *V. fischeri* MJ1 was better than that of the modified strain. In terms of variation, the findings from this study are consistent with the results obtained from previous studies of Jeong et al. (2013) and Ma et al. (2012) that showed a strong and linear correlation between bioluminescence and glucose

concentrations with $R^2 > 0.97$ [20, 93]. Therefore, it is possible to estimate the AOC concentration expressed in µg glucose-C L^{-1} in seawater samples by using the modified strain. Furthermore, the pUC19-*luxAB* was highly sensitive with a detection limit of 20 µg C L^{-1} (an increase of 2.2 x 10^2 RLU over background bioluminescence), demonstrating its usefulness for the quantification of AOC at low concentrations ranging from tens to several hundred µg C L^{-1} in seawater samples [20].

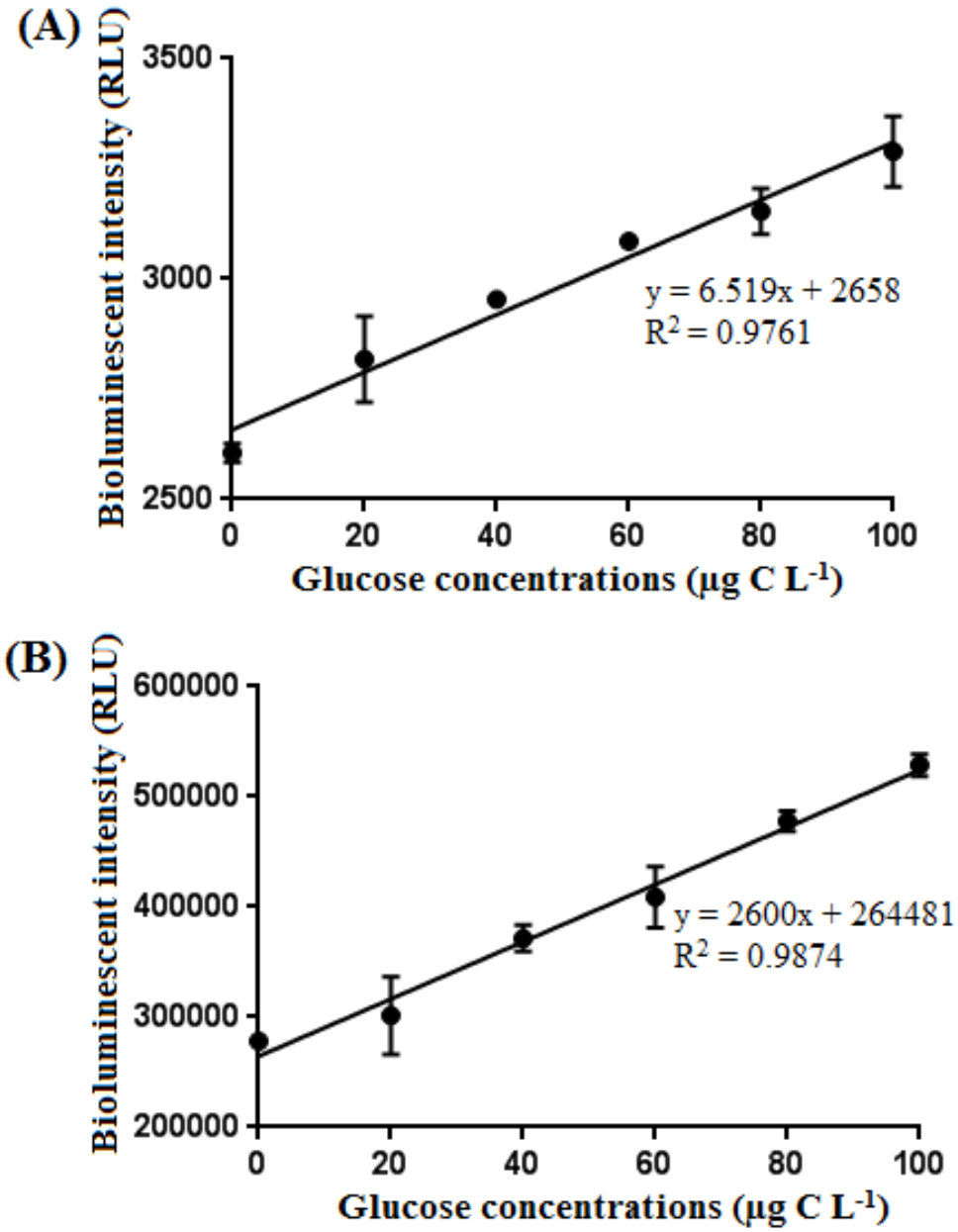

Figure 3.15. The linear relationship between the concentrations of glucose and the maximum bioluminescence in (A) *V. cholerae* A1552 (pUC19-*luxAB*) and (B) the control strain *V. fischeri* MJ1. The error bars indicate standard deviation of the means.

3.4. Discussion

AOC compounds, which are quickly metabolised by microorganisms are considered to be important sources of carbon and energy for bacteria. There is a significant correlation between AOC concentration and the growth of heterotrophic bacteria, which results in biofouling on RO membranes. Typically, the growth of microorganisms is limited when the AOC concentration is lower than 20 µg C L^{-1}, while at AOC concentrations greater than 50 µg C L^{-1}, there is a significant growth [20]. The AOC concentration is an important factor used to control the growth of microorganisms and microbial activity in aquatic environments. Therefore, understanding of the impact of desalination pretreatment processes on the removal of AOC is necessary to prevent or minimise membrane fouling. In general, the plate count assay for AOC measurement requires several days to complete. Conversely, bioluminescence-based AOC assays take only minutes to perform [3]. An added advantage of the bioluminescence-based AOC assay is the extreme sensitivity of detection, which permits the estimation of AOC at very low concentrations [94].

In previous studies, two marine strains *V. fischeri* and *V. harveyi* were widely used for the estimation of AOC concentration in seawater (expressed as µg glucose-C L^{-1}/ µg acetate-C L^{-1}) [10, 11, 13]. In this study, AOC potential test strains BLS2, CBSW3 and CBSW4 isolated from seawater exhibited better growth in seawater than the control *V. fischeri* MJ1, having maximal cell densities of 5.1 x 10^5, 4.5 x 10^5 and 7.2 x 10^5 CFU ml^{-1} compared to 5.3 x 10^4 CFU ml^{-1}, respectively. In addition, all three strains were able to grow on humic acids which are a major class of AOC compounds in seawater. For example, CBSW4 and CBSW3 reached high cell numbers of 2.1 x 10^5 and 1.6 x 10^5 CFU ml^{-1}, respectively, while *V. fischeri* MJ1 showed no growth over 48 h of incubation. Based on the analysis of the 16S rDNA, BLS2, CBSW3 and CBSW4 are closely related to species of *Enterovibrio*, *Vibrio* and *Pseudoalteromonas*, which are indigenous species frequently found in seawater. These results indicate that the three strains have potential for the development of more accurate AOC assays for seawater samples.

Bacterial luciferases are the most extensively used among the luciferase family members as reporter genes for biological and biotechnology applications. All bacterial luciferases are heterodimeric enzymes composed of two subunits each encoded by *luxA* and *luxB* genes sourced from luminous bacteria, including *V. fischeri*, *V. harveyi*, *Photobacterium*

phosphoreum, *Photobacterium leiognathid* and *Xenorhabdus luminescens*. In the presence of flavin mononucleotide (FMN) and oxygen, luciferase oxidises a long-chain aldehyde and releases energy in the form of visible light with an absorption maximum at 490 nm [94, 95]. The expression level of *luxAB* depends on the nature of the expression vector used, including the copy number, transcriptional and translational control and the promoter [91].

In the current study, we developed a *lux* system by integrating *luxAB* genes downstream of the strong promoter *lacIQ* into a high copy number pUC19 to maximise the expression levels. In previous studies it was reported that the *luxAB* genes from *V. harveyi* were transferred to different bacteria using a wide range of plasmids, but the luciferase activity of these modified strains was reduced up to 98% in comparison to the wild type [93]. In this study, the bioluminescence of the modified strains *E. coli* C2987 (pUC19-*luxAB*) and *V. cholerae* A1552 (pUC19-*luxAB*) were approximately 3-fold and 30-fold lower than that of the wild type, but the bioluminescence of these transformed strains was over 30000-fold and 3000-fold greater than the background bioluminescence, respectively. Therefore, the constructed *lux* system may be suitable as reporter plasmids for AOC quantification. However, the considerable decrease in the bioluminescent intensity of *V. cholerae* A1552 (pUC19-*luxAB*) compared to *E. coli* C2987 (pUC19-*luxAB*) demonstrated that although pUC19 was at high copy number in *E. coli*, it was not appropriate for the marine strains.

Previous studies reported that *Vibrio* species secrete DNases into the media culture that results in the degradation of circular DNA and plasmids [96, 97]. This may explain the failure to introduce pUC19-*luxAB* into the three potential strains BLS2, CBSW3 and CBSW4 by electroporation. For the majority of marine strains, conjugation with *E. coli* containing recombinant *lux* DNA has been required [97]. Therefore, in this study, the *lux* genes under the control of promoter *lacIQ* were integrated into conjugative plasmids PLG401 and PLS6, which has been previously used to transfer recombinant DNA into *Vibrio* species [79, 80]. The low levels of bioluminescence produced by the modified strains BLS2 (pLG401-*luxAB*/ pLS6-*luxAB***)** and CBSW3 (pLG401-*luxAB*/ pLS6-*luxAB*) may be attributed to low copy number conjugative plasmids affecting the expression level of *luxAB* genes. The bioluminescence was only 2-fold higher than the background signal. Therefore, the bioluminescence produced by these modified strains is not sufficient for the measurement of AOC concentration. Due to the failure to construct AOC reporter

strains from the three potential test strains, the linear relationship between bioluminescence and humic acids used as AOC compounds, which can be metabolised rapidly in seawater was not investigated.

The use of the maximum values of bioluminescence in the construction of the linear relationship to carbon concentrations ensures that all carbons are metabolised when bioluminescence reaches maximum intensity. The peak bioluminescence directly correlates to carbon concentration. In this study, the linear correlation between bioluminescence and glucose concentration was determined for the modified strain *V. cholerae* A1552 (pUC19-*luxAB*) and compared to the naturally luminous strain *V. fischeri* MJ1. The comparison of the two R^2 values (greater than 0.97) indicates that both the curves can be used as standard curves for quantification of AOC. Similar to *V. fischeri* MJ1, the modified strain responds to very low glucose concentrations (20 µg C L^{-1}). Therefore, these curves can be used for predicting AOC concentrations expressed in µg glucose-C L^{-1}. At low carbon concentrations (≤ 1.4 mg C L^{-1}), it took a shorter time to reach the maximum level of bioluminescence compared to higher carbon concentrations (≥ 2.8 mg C L^{-1}) (Figure 3.12 and 3.13). It is recommended that for AOC measurements based on a linear curve, reporter strains should take a similar amount of time to reach the maximum bioluminescence at all tested carbon concentrations. For a very high carbon concentration, to ensure a linear relationship between bioluminescence and substrate concentration, a sample needs to be diluted due to the saturation of bioluminescence. The downward trend after reaching maximal light output may be attributed to a decrease in metabolic activity and therefore the availability of FMN, which is oxidised to make energy required for the light reaction [94]. In the cases where LB and glucose were tested, *V. fischeri* MJ1 took a longer time to reach the maximum level of bioluminescence compared to the modified strains. Furthermore, the increase in density of the initial inoculum shortened the bioluminescence-based AOC assay time from 30 - 60 min to 10 min. Although attempts to introduce that reporter plasmids into the test strains were unsuccessful, the current research describes a rapid assay for AOC measurement which takes only minutes to perform. To minimise disadvantages caused by membrane fouling in RO systems, rapid monitoring assays are highly recommended to ensure prompt action is taken to control the AOC in feed water in time.

CHAPTER 4

CHARACTERISATION OF MICROBIAL COMMUNITY IN A LABORATORY SCALE MBR AND EFFICACY OF NO FOR REDUCTION OF TMP

4.1. Introduction

MBRs, which couple membrane filtration with biological activated sludge have been widely applied for the treatment and reuse of industrial and municipal wastewaters due to the production of excellent quality effluent. It has been known that degradation of organic substrates in the influent is the most important function of wastewater treatment systems. Microbial diversity and activity of activated sludge directly affects the stability and performance of MBRs [47]. Therefore, an understanding of microbial community composition in MBRs is necessary to achieve better removal of organic carbon, nitrogen and phosphorus present in the influent. Characteristics of microbial communities depend on operational conditions, characteristics of feed water and seed sludge. Among microorganisms in activated sludge, bacteria account for 95% of total microbial biomass and are mainly responsible for the removal of organics in feed water [47].

In this study, changes in bacterial community diversity of activated sludge samples collected at different time points from a laboratory scale MBR were investigated using Illumina high-throughput sequencing technology [68]. In addition, one of the biggest problems preventing the more widespread use of MBRs is membrane fouling, which results in an increase in operational pressure leading to increased costs, the frequency of membrane cleaning and a decrease in treatment process performance. Biofouling occurring in MBRs is more complicated than that in other membrane systems as the complex nature of activated sludge in MBRs is one of main factors affecting membrane fouling [17]. To address this issue, in this project, we investigate NO backwashing as a

membrane fouling control strategy. The efficacy of the treatment was measured in terms of TMP and microbial community changes. To achieve these objectives, the following investigations were performed in this chapter.

i. Characterisation of microbial communities in activated sludge in an MBR
ii. Efficacy of NO backwash for the reducing TMP increases

4.2. Materials and Methods

4.2.1. MBR Experiment

The laboratory scale submerged MBR used in this study is described in Figure 4.1. The system consisted of an aerobic sludge tank containing two hollow fibre membrane modules, pumps to transport feedwater from a feed tank to the bioreactor or withdraw effluent from the bioreactor to an effluent tank, air diffusers to maintain aerobic conditions in the bioreactor and pressure gauges used for TMP measurements. Hollow fibre membranes were provided by Prof. Vigneswaran at the University of Technology Sydney, Sydney Australia. The membranes were made of HF polyninylidene fluoride (PVDF) with a total effective membrane filtration area of 0.01 m^2 and a pore size of 0.1 µm. Each fibre is 17.5 cm long with an outer diameter of 2.0 mm and an inner diameter of 0.8 mm. The braid-reinforced hollow fibre MF (Cleanfil-S, Kolon, South Korea) is composed of polysulfone, polyethersulfone and polyvinlidene fluoride as a coating layer. One end of the hollow fibre membrane is sealed with a high-strength adhesive and the other end tied together with an acrylic tube that links the fibre to a suction pump for the withdrawal of effluent. MBR operating conditions are presented in Table 4.1.

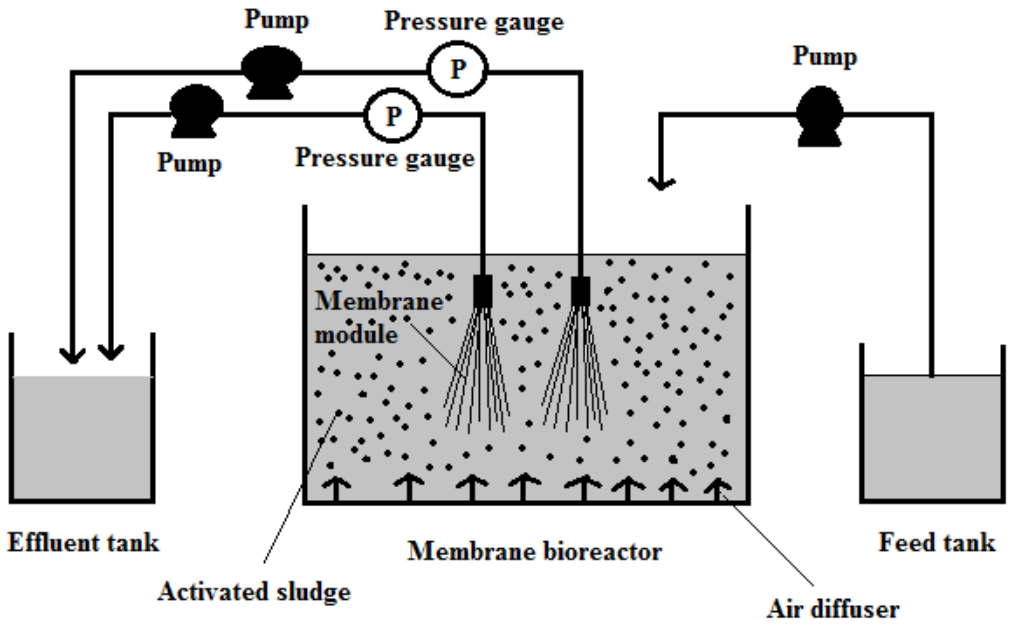

Figure 4.1. The submerged laboratory scale MBR. Influent from a feed tank was fed to the bioreactor using a feed pump. An aerobic condition was maintained by air diffusers. A suction pump was used to extract permeate from the membranes to an effluent tank. TMPs were measured by pressure gauges.

Table 4.1. MBR operating conditions

Parameters	**values**
Working volume (L)	10
Flux (L/m^2. h)	20.4
Sludge retention time (day)	No sludge withdrawn
pH	6.5 – 8.0
Mixed liquor suspended solids (MLSS, g L^{-1})	5.0 – 6.0
Mixed liquor volatile suspended solids (MLVSS, g L^{-1})	4.5 – 5.0
Aeration rate (L min^{-1})	6
OLR (kg chemical oxygen demand (COD)/m^3/day)	0.24

4.2.2. Components of Synthetic Feed Water

The components of the synthetic feed water are presented in Table 4.2.

Table 4.2. Components of synthetic feed water

Chemicals	**Value (mg L^{-1})**
$CaCl_2$. $2H_2O$	292
NaCl	750
KCl	90
KNO_3	35
NaF	7
$MgSO_4$. $3H_2O$	450
K_2HPO_4	15
$NaHCO_3$	70 - 80
Glucose	200
Yeast	300
COD	483.5

4.2.3. Acclimatisation Stage

Activated sludge was collected from a wastewater treatment plant (Mile End Rd, Rouse Hill NSW 2155, Australia). The seed sludge parameters (MLSS, MLVSS, TOC, COD, NO_2-N, NO_3-N, NH_4-N and PO_4-P) were measured and the microbial community composition determined. Five litres of the sludge combined with 10 L of tap water was fed to the MBR. During the acclimatisation period, mixed liquor samples were collected from the bioreactor after 1 and 3 days. The acclimatisation was carried out until the system stabilised in terms of TOC and ammonia removal.

4.2.4. Biofouling Treatment

After acclimatisation, two hollow fibre membranes were placed in the bioreactor. The effluent and the sludge were collected on day 1, followed by every 3rd day thereafter to measure nutrient parameters like TOC, COD, nitrate, nitrite, ammonia and phosphate, MLSS and MLVSS as well as for microbial community analysis. The TMP was recorded every 30 min using digital pressure gauges to evaluate the membrane fouling tendency. These data were saved in a data logger connected with a pressure transducer. When the TMP increased, one membrane was backwashed with 40 µM DETA NONOate solution (laboratory stock) for 60 min to remove biofouling on the membrane surface and another membrane was backwashed with distilled water as a control. Foulant samples removed from the backwash were collected for microbial community assessment. When the MBR experiment was completed, these membranes were collected and the microbial community which remained on the membrane surface was removed for analysis.

4.2.5. MLSS and MLVSS Measurements

MLSS and MLVSS were determined according to the protocol of Environmental Business Specialists (EBS). Ten ml of mixed liquor was filtered through Whatman glass microfiber filters (Sigma-Aldrich). The residue left on the filter was dried to a constant weight at 105 ^{O}C. The increase in the weight of the filter represents the MLSS value. The dried filter continued to be heated at 550 ^{O}C for 30 min. The weight lost on ignition represents the MLVSS.

4.2.6. Measurement of Nutrient Parameters

TOC was measured by using a multi N/C 3100 TOC analyser (Analytik Jena, Germany). Reagents (TNT 821, TNT 840, TNT 835, TNT 830 and TNT 843 (HACH, USA) were used to determine COD, NO_2-N, NO_3-N, NH_4-N and PO_4-P, respectively. These vials were read by spectrophotometry using the cell test method (DR9300, HACH). For mixed liquor samples, the samples were filtered through 1.2 µm pore sized membranes (Sigma-Aldrich) to remove the sludge before analysing.

4.2.7. pH Measurement

The pH in the bioreactor was maintained at the value of 6.5 – 8.0 by using $NaHCO_3$ (Sigma-Aldrich). pH was measured daily by using portable digital pH measurement meter

(model-HQ11D, HACH).

4.2.8. DNA Extraction

Samples, including mixed liquor and foulants, were stored at -20 ºC until DNA was extracted. After thawing, each sample was centrifuged at 18407 × *g* for 1 min to obtain approximately 0.5 g of biomass. DNA was extrated with the FastDNA® Spin Kit for Soil (MP Biomedicals, Illkrich, France). The DNA was purified by the use of the DNA purification kit (Qiagen, Valencia, CA). The quality of DNA was assessed by NanoDrop™ One Microvolume UV-Vis Spectrophotometer (Thermo Fisher Scientific, USA). These purified DNA samples were sent to the Singapore Centre for Environment Life Science Engineering (SCELSE) at Nanyang Technological University for Illumina sequencing.

4.2.9. Analysis of Microbial Community

DNA samples obtained in 4.2.8. were sequenced using Illumina sequencing (Solexa Ltd, UK). The forward primer (515F), 5'-GTGYCAGCMGCCGCGGTAA-3' and the reverse primer (806R), 5'-GGACTACNVGGGTWTCTAAT-3' were used to amplify the hypervariable V4 region of the 16S rDNA gene [108, 109]. The samples were individually barcoded to enable multiplex sequencing. The sequence results were analysed by Quantitative Insights into Microbial Ecology (QIIME) 2 to determine microbial community structure [110]. All the sequences were clustered at 97% sequence similarity with uclust. Each resulting cluster was considered to be a genus. A representative sequence from each OUT cluster picked by the software was assigned to taxonomic data using the Ribosomal Database Project (RDP) classifier. Some OTUs could be assigned to specific bacterial species, while others may only be assigned to general groups or the bacterial domain [111].

4.3. Results

4.3.1. Acclimatisation Stage

Activated sludge consists of inorganic and organic substances, in which MLSS is used to indicate the concentration of suspended solids and MLVSS exhibits the concentration of biomass. Therefore, the MLVSS/ MLSS representing the portion of active biomass is frequently used to estimate sludge activity [112]. Microbial diversity within the activated

sludge has a significant impact on stability and performance of MBRs. In MBR treatments, an acclimatisation phase is required to provide preferably suspended aerobic growth for microorganisms in wastewater. Microorganisms of the original sludge respond to operational conditions by altering microbial community structure or varying their metabolic processes to adapt to these altered environmental conditions [113, 114]. Therefore, in this project, activated sludge was acclimatised to the operational conditions before the MBR experiment commenced.

In this study, synthetic feed water was used for the MBR experiment to maintain consistency in the chemical and physical properties of the influent. Typically, when the MLVSS/ MLSS ratio reaches 0.8 and MLSS > 5 g L^{-1}, the acclimatisation is completed [112, 115]. Figure 4.2 demonstrates changes in MLSS and MLVSS of the raw sludge during the acclimatisation. On day 15, MLSS was 5.7 g L^{-1} and the ratio of MLSS and MLVSS was 0.8 indicating that the biomass concentration was appropriate for treatment. Table 4.3. describes the changes in the characteristics of the original and the acclimatised sludge.

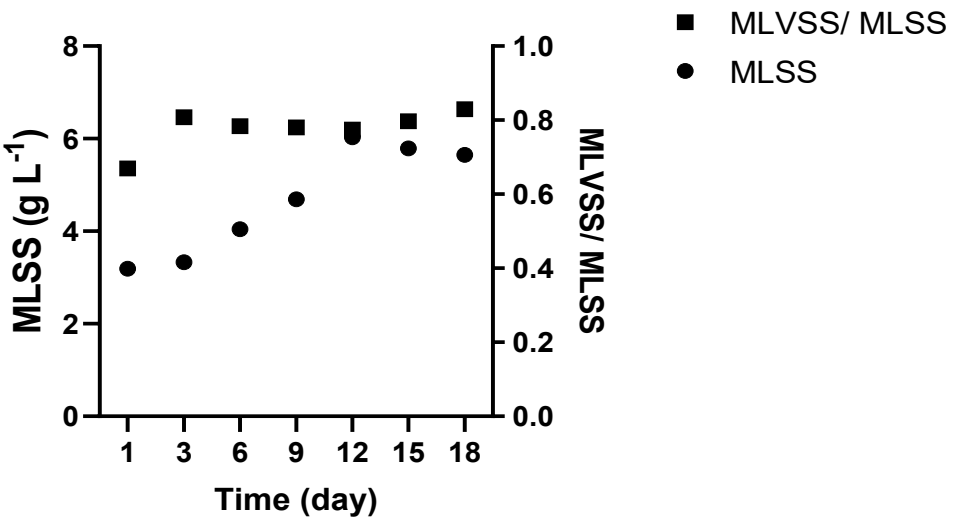

Figure 4.2. The variation of MLSS and MLVSS values in MBR with respect to time during acclimatisation. The measurements were performed in duplicate.

Table 4.3. Chemical analysis of the activated sludge and synthetic wastewater

Parameters	**Original sludge**	**Synthetic wastewater**	**Acclimatised sludge**
TOC (mg L^{-1})	13.7 ± 0.2	82.3 ± 0.7	31.2 ± 0.03
COD (mg L^{-1})	684 ± 2.8	483.5	200.5 ± 12.0
PO_4-P (mg L^{-1})	94.2 ± 1.5	16.3 ± 0.1	304 ± 4.2
NH_4-N (mg L^{-1})	73.2 ±2.4	4.9 ± 0.1	590.5 ± 4.9
NO_2-N (mg L^{-1})	0.088 ± 0.001	0.09 ± 0.01	121 ± 1.4
NO_3-N (mg L^{-1})	0.44 ± 0.06	5.4	81.6
MLSS (g L^{-1})	4.5 ± 0.1	-	5.7 ± 0.1
MLVSS (g L^{-1})	2.9 ± 0.1	-	4.7 ± 0.01

4.3.2. MBR Performance

After the acclimatisation stage, two hollow fibre membranes were directly installed into the bioreactor. The MBR was continuously operated at room temperature for 18 days, with HRT of 24.5 h and the OLR of 0.24 kg COD/m^3/day. Figure 4.3 depicts the variation in MLSS and MLVSS values with respect to time in the MBR. During the operation, the MLSS and MLVSS fluctuated between 5.5 – 6.0 g L^{-1} and the ratio of MLVSS to MLSS remained at 0.8 throughout the MBR experiment, indicating high bioactivity of the sludge. Furthermore, the high concentration of ammonia (600 mg/L) found in the acclimatized sludge may be attributed to the microbial degradation of the yeast extract to ammonia.

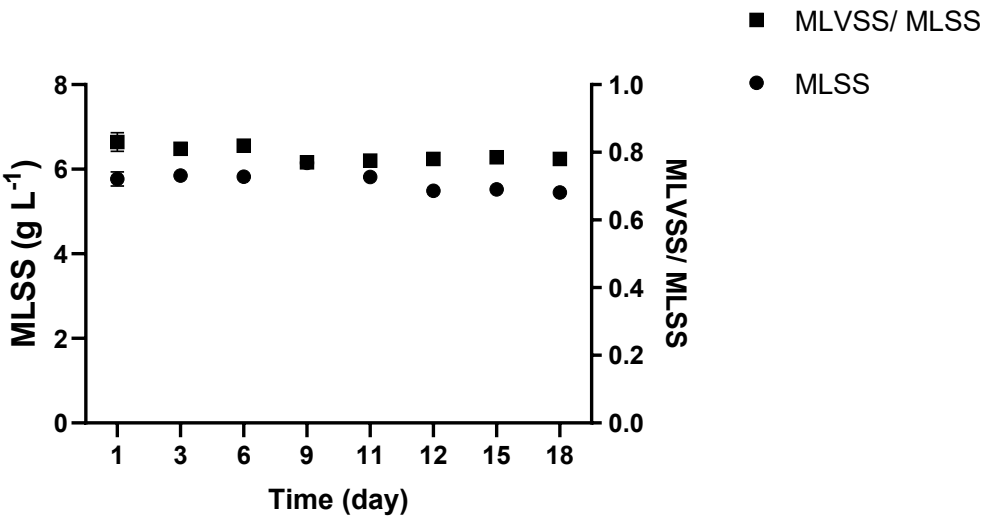

Figure 4.3. The variation in MLSS and MLVSS values in MBR with respect to time. The measurements were performed in duplicate and error bars indicate the standard deviation of the means.

During the operation of the MBR, the effluent was collected on day 1 and every 3rd day thereafter to measure the removal efficiency of organic matter as TOC and COD concentrations. Changes in the concentration of TOC and COD during the 18 days, indicated that the removal of TOC and DOC increased over time (Figure 4.4). The removal efficiency began to stabilise on day 9 and the concentration of COD was not further reduced. The percentage removal of TOC and COD on day 18 was 96.7% and > 99.4%, respectively. The MBR achieved higher removal efficiency of TOC and COD compared to previous studies reporting TOC and COD removal efficiencies of 76 – 95 % and 80 - 98%, respectively [114, 116]. The higher removal efficiency may be attributed to the low OLR used in this study. In addition, in terms of TOC and COD removal, the quality of effluent, which met the permissible level for TOC and COD in MBR's effluent (< 3 and < 30 mg L^{-1}, respectively), was recorded on day 18 as being 2.7 and < 3 mg L^{-1}, respectively [117, 118].

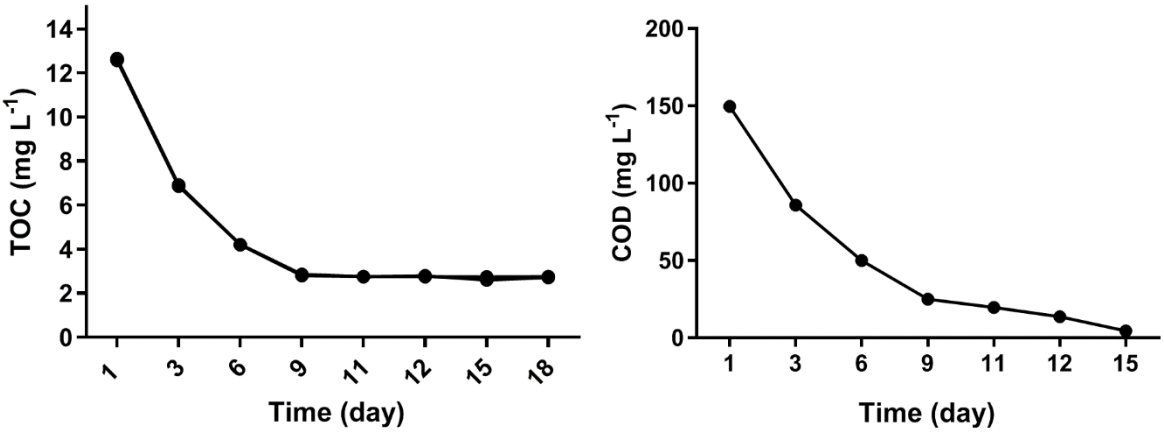

Figure 4.4. TOC and COD concentrations in the effluent over time. The measurements were performed in duplicate.

In MBRs, biological phosphorus removal is performed mainly by polyphosphate accumulating organisms (PAOs), which take up phosphorus and store it as biomass [119]. The changes in PO_4-P concentrations within the 18-day operation demonstrated that the removal of PO_4-P gradually increased for 9 days of operation and slightly decreased thereafter (Figure 4.5). For example, the concentration of PO_4-P in the effluent on day 9 was 21.6 mg L^{-1}, which was higher than that in influent was 16.3 mg L^{-1}. This may be attributed to the low COD/ PO_4-P ratio of 30 as the biodegradable carbon source is one of limiting factors for the uptake of phosphorus by PAOs [120]. Typically, to obtain high P removal efficiencies, the ratio of COD to P should be 100 [115, 121]. Thereafter, there was a slightly increase in the PO_4-P concentration from 21.6 to 31.2 mg L^{-1}. The increase in PO_4-P concentration indicated that the uptake capacity of the sludge for phosphorous may be limited.

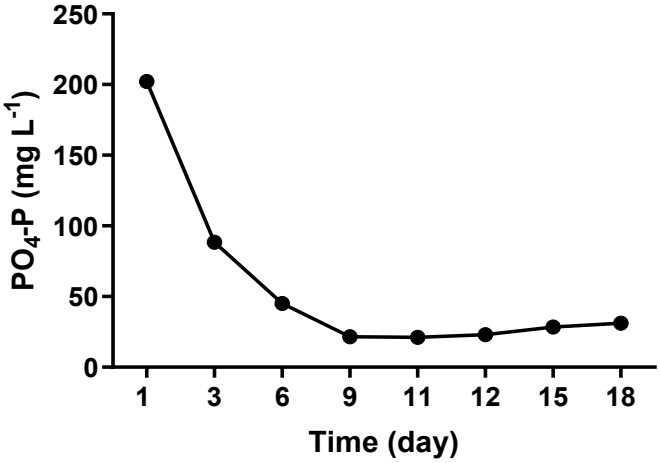

Figure 4.5. PO_4-P concentrations in the effluent over time. The measurements were performed in duplicate.

Biological nitrogen removal is carried out in a two-step process, nitrification and denitrification. In the first process of nitrification, NH_4-N is aerobically converted to NO_2-N and then to NO_3-N by *Nitrosomonas* and *Nitrobacter* bacteria, respectively. For the second process of denitrification, NO_3-N is anoxically converted to N_2O or N_2 by denitrifying bacteria. The N_2 produced will escape into the atmosphere as air bubbles [122]. The changes in NH_4-N, NO_2-N and NO_3-N concentration over 18 days of operation are shown in Figure 4.6. The concentration of NH_4-N, NO_2-N and NO_3-N in the effluent decreased from 359, 106.5 and 65.6 mg L^{-1} on day 1 to 1.52, 19.56 and 8.85 mg L^{-1} on day 9, respectively. At this time point, the NO_2-N concentration of > 1 mg L^{-1}, indicated that the nitrifying process was not fully completed [123]. The concentration of NH_4-N slightly increased to 2.65 mg L^{-1} at the end of the experiment and the concentration of NO_3-N sharply increased to 31.15 mg L^{-1}, while NO_2-N concentration decreased to less than < 0.6 mg L^{-1}. These results are consistent to findings from a study of Wen at el. (2015) that the low NO_2-N concentration (< 1 mg L^{-1}) indicates that all of the NH_4-N is oxidised to nitrite and the nitrite completely converted to nitrate [123]. The high concentration of NO_3-N was due to the inefficiency of denitrification under aerobic conditions.

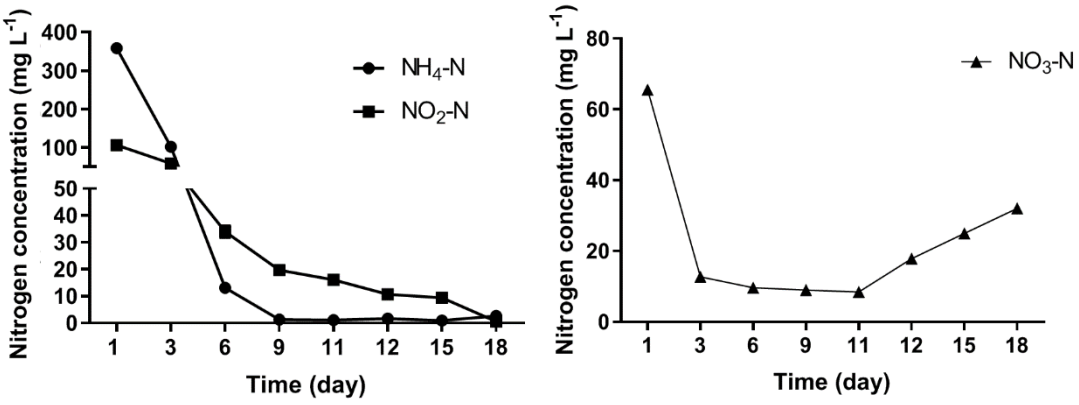

Figure 4.6. Concentrations of NH_4-N, NO_2-N and NO_3-N in the MBR effluent over time. The measurements were performed in duplicate.

4.3.3. Efficacy of NO Backwashing Treatment for Reduction of TMP

The MBR was operated at a constant membrane flux of 20.4 L/m^2. h throughout the experiment. Therefore, an increase in TMP values indicated that the membrane was fouling, as high TMP is an indication of serious membrane fouling. In this study, TMP values were automatically recorded every 30 min using digital pressure gauges. When the TMP increased significantly, backwashing was then performed periodically to remove the fouling layer covering the membrane surface. The TMPs of the two membranes were 3.3 kPa ± 0.7 in the first 7 days of operation (Figure 4.7). After 7 days, the TMPs increased rapidly to 6.7 kPa on day 9. To reduce the TMP, backwashing was applied periodically, and after the first backwash, the TMP of the NO-treated membrane remained at 6.3 kPa ± 0.4, while the TMP of the control membrane treated with distilled water continued to increase, reaching 9.4 kPa on day 11. Two more treatments were applied on days 11 and 15. The results indicated that the TMP of NO-treated membrane remained stable at 6.3 kPa ± 0.3 after the second backwash and reduced slightly to 6.1 kPa ± 0.3 when the third backwash was applied. Similarly, the TMP of control membrane showed a slight decrease from 9.4 kPa to 7.8 kPa ± 0.3 after the second backwash and 7.4 kPa ± 0.4 after the third treatment. The downward trend of TMPs after the treatments demonstrated that the backwashing could reduce the TMPs.

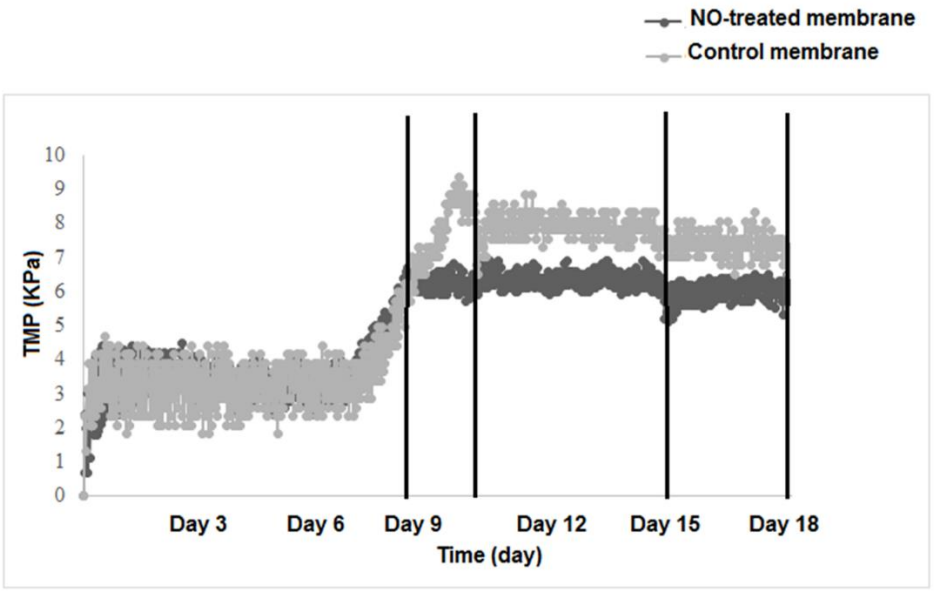

Figure 4.7. Efficacy of NO backwashing treatment on the TMP of control and NO-treated membranes. The vertical lines indicate the backwashing treatments.

4.3.4. Changes in Microbial Communities in the MBRs

Community composition is an essential factor affecting biofouling tendency of MBRs. Therefore, understanding shifts in bacterial communities in MBRs with respect to MBR operation and fouling will inform on targeted strategies to control biofouling. In this study, the microbial composition of activated sludge and biofilms were measured by Illumina sequencing. There was a total of 1372739 reads obtained from 9 aerobic activated sludge samples and 10 biofilm samples after removing low quality sequences, denoising and removing chimeras by QIIME 2. The sequence libraries used for downstream analysis ranged in size from 59827 – 95141 reads. OTUs were grouped at the 3% distance level (97% of sequence similarity) and assigned to taxonomy data using RDP Classifier. RDP Classifier identified 36 phyla, 101 classes and 527 genera of bacteria.

Changes in the bacterial community structures of activated sludge samples at the phylum level, indicating that *Bacteroidetes* (42.4 – 56.2%, average at 51.0%) and *Proteobacteria* (18.8 - 40.9%, average at 31.4%) were the most abundant phyla in the activated sludge samples (Figure 4.8). This is consistent with the results of other studies on microbial composition of activated sludge collected from MBRs, in which *Proteobacteria* and *Bacteroidetes* were the most abundant phyla [105, 124-126]. The microbial community

structure changed significantly after the acclimatisation stage. In the raw sludge sample, principle bacteria groups belonging to the phyla *Proteobacteria* and *Bacteroidetes* accounted for 50.7% and 28.8 % of the total sequences, followed by *Actinobacteria* (5.3%) and *Chloroflexi* (4.0%). Other phyla including *Firmicutes*, TM7 and *Verrucomicrobia* contributed approximately 1% to the total sequences. After the acclimatisation stage, the relative abundance of *Bacteroidetes* and TM7 increased to 56.2% and 10.8%, while *Proteobacteria* decreased in relative abundance to 18.8%. In addition, phyla *Actinobacteria* and *Verrucomicrobia* increased to 3.1% and 2.5%, respectively. Conversely, *Chloroflexi* and *Firmicutes* were reduced to 0.3% in abundance. During the MBR experiment, the relative abundance of *Bacteroidetes* showed a slight decrease of approximately 7%, while there was a significant upward trend observed in *Proteobacteria* from 18.8 to 40.9% on day 12 remaining stable until day 18. The changes in the relative abundance of the most dominant OTUs with at least 5% relative abundance at different classification levels are summarised in Table 4.4.

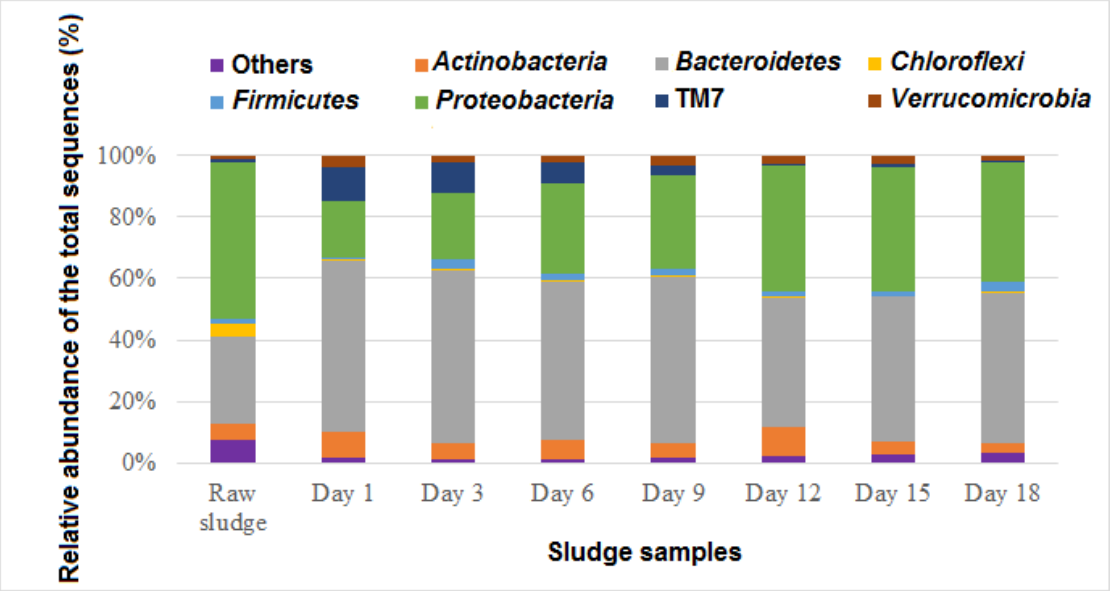

Figure 4.8. Changes in bacteria community structure of activated sludge at phylum level during the MBR experiment. Raw sludge collected from a wastewater treatment plant (Mile End Rd, Rouse Hill NSW 2155, Australia) was the seed sludge. Days 1 - 18 are sludge samples collected on day 1 and every 3rd day during MBR experiment.

Table 4.4. Changes in the relative abundance of the most abundance OTUs at different classification levels in sludge samples during the MBR experiment. The relative abundance threshold of ≥ 5% of out abundance is used for OTUs.

Description (% relative abundance)	Classification level	Phylum	Class	Family	Genus
		TM7 (0.6 – 10.8%)	TM7-3 (0.6 – 10.6%)	Unclassified TM7-3 (0.4 – 8.9%)	Unclassified TM7-3 (0.4 – 8.9%)
			Grammaproteobacteria (5.2 – 8.8%)	*Xanthomonadaceae* (3.5 – 6.7%)	< 5% relative abundance
		Proteobacteria (18.8 – 40.9%)	*Betaproteobacteria* (6.0 – 27.9%)	*Comamonadaceae* (4.4 – 27%)	*Comamonas* (0.3 – 18.7%)
					Rubrivivax (0.5 – 5.7%)
			Saprospirae (15.2 – 34.4%)	*Saprospiraceae* (8.4 – 27.9%)	unclassified *Saprospiraceae* (8.4 – 27.9%)
				Chitinophagaceae (4.6 – 7.2%)	unclassified *Chitinophagaceae* (4.3 – 6.7%)
		Bacteroidetes (42.2 – 56.2%)	Unclassified *Bacteroidetes* (16.6 – 24.7%)	Unclassified *Bacteroidetes* (16.6 – 24.7%)	Unclassified *Bacteroidetes* (16.6 – 24.7%)
			Sphingobacteriia (2.8 – 5.8%)	*Sphingobacteriaceae* (1.7 – 5.2%)	< 5% relative abundance
		Actinobacteria (3.2 – 9.3%)	*Actinobacteria* (2.9 – 8.8%)	< 5% relative abundance	< 5% relative abundance

4.3.5. Determination of Key Bacteria Involved in Membrane Biofouling

To investigate the impact of microbial communities on biofouling, changes in microbial community composition associated with the increase in TMPs were measured to identify specific bacterial populations that may have key roles in membrane fouling. The changes in the relative abundance of the most dominant families and average TMPs of the NO-treated and control membranes are demonstrated in Figure 4.9. At the beginning of MBR experiment, the most dominant families in the activated sludge were *Saprospiraceae,* unclassified *Bacteroidetes* and unclassified TM7-3 that accounted for 24.5, 16.6 and 8.9% of the total community, respectively. In addition, *Comamonadaceae, Chitinophagaceae, Xanthomonadaceae* and *Sphingobacteriaceae* contributed approximately 5% relative abundances. For the first and second increase in TMPs on days 9 and 11, changes were observed in *Saprospiraceae, Comamonadaceae*, unclassified *Bacteroidetes* and unclassified TM7-3. The relative abundance of *Saprospiraceae* and unclassified TM7-3 decreased to 14.2 and 2.2%, while the relative abundance of *Comamonadaceae* and unclassified *Bacteroidetes* increased to 18.7 and 8.1%, from 4.4 to 23.1% and 16.6 to 24.7%, respectively. Conversely, *Sphingobacteriaceae, Xanthomonadaceae* and *Chitinophagaceae* changed only slightly in relative abundance. *Sphingobacteriaceae* decreased from 5.2 to 3.8%, while the relative abundance of *Chitinophagaceae* and *Xanthomonadaceae* increased from 5.6 to 7.2% and 3.5 to 6.0%, respectively. After the second treatment, TMPs of the NO-treated membrane and control membrane remained stable at 6.3 kPa ± 0.3 and 7.8 kPa ± 0.3 until day 15, when the third treatment was performed.

The relative abundance of *Saprospiraceae* and TM7-3 continued to decrease to 8.4% and 0.8% compared to a significant increase in that of *Comamonadaceae* to 27% and slight increase of *Xanthomonadaceae* to 6.7%. In addition, there was a slight decrease of 1 – 2% relative abundance observed in unclassified *Bacteroidetes*, *Sphingobacteriaceae* and *Chitinophagaceae*. After the third backwash, the relative abundance of *Saprospiraceae* increased to 13.6%, while the remaining bacteria exhibited a decrease of 0.2 – 2.7%. The four families *Saprospiraceae, Comamonadaceae*, unclassified *Bacteroidetes* and TM7-3 contributing 59.2% of the total sequences showed significant changes in relative abundances associated with the TMP increases, indicating that these bacteria may play important roles in

the development of biofouling. The role of these bacteria in membrane fouling was determined by measuring their relative abundance in biofouling samples.

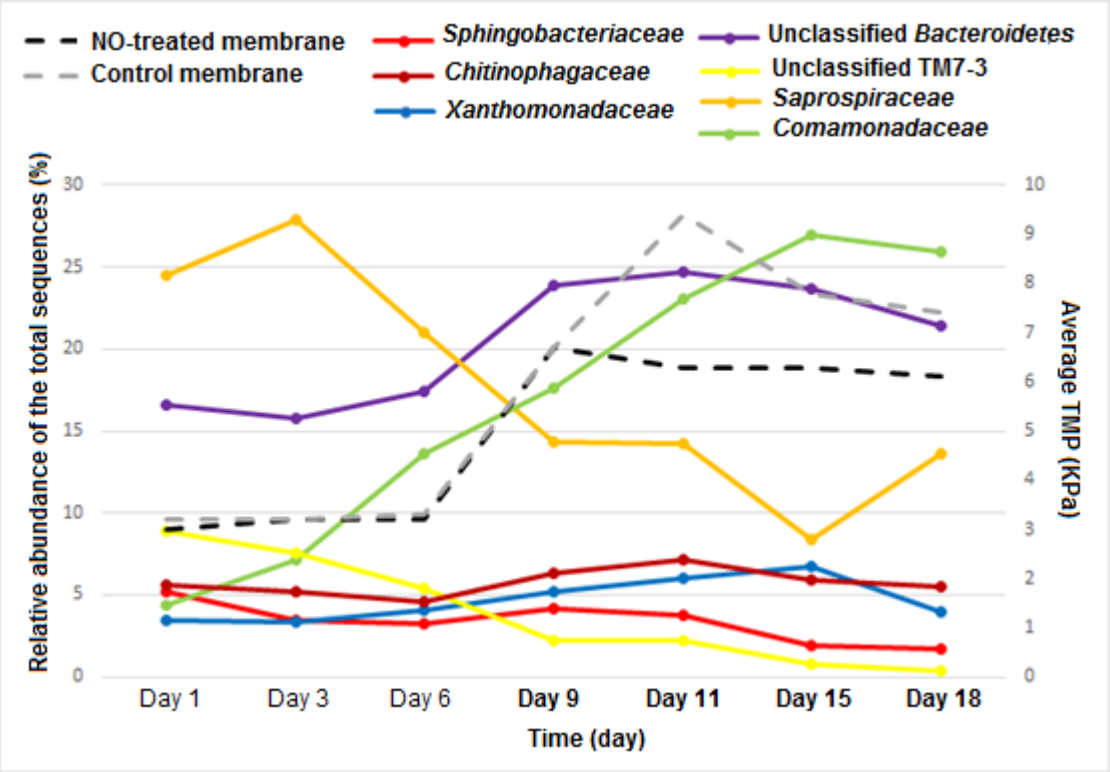

Figure 4.9. Changes in the relative abundance of the most abundant families (solid lines) in the activated sludge samples and the average TMPs (dash lines) during MBR experiment. The relative abundance threshold of ≥ 5% is used for OTUs. The days marked in bold indicate when backwashing treatments were performed.

Changes in relative abundances of the genus *Saprospiraceae* and TM7-3 in sludge, dispersed and attached biofouling samples are summarised in Figures 4.10 and 4.11. Results indicate that although the relative abundance of *Saprospiraceae* and TM7-3 was reduced in sludge samples, *Saprospiraceae* and TM7-3 were abundant (20.8 – 21.2% and 5.8 – 7.7%, respectively) in the first dispersed biofilm sample. However, the relative abundance of TM7-3 in biofouling samples gradually decreased to 0.2%, while that of *Saprospiraceae* remained high at an average of 20%. These results suggested that TM7-3 may be involved for the initial stage of biofilms, while *Saprospiraceae* are key communities in membrane biofouling layers. In addition, the high relative abundance of *Saprospiraceae* in the biofouling layer on

membranes demonstrated that the treatments were ineffective in dispersing these bacteria at the concentrations used here.

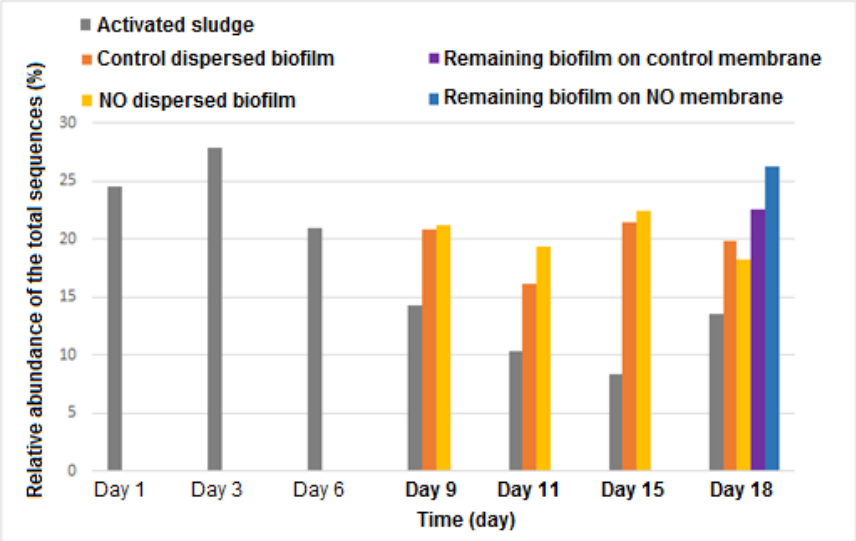

Figure 4.10. The relative abundance of *Saprospiraceae* in sludge, dispersed and membrane biofouling samples. The days marked in bold indicate when backwashing treatments were performed.

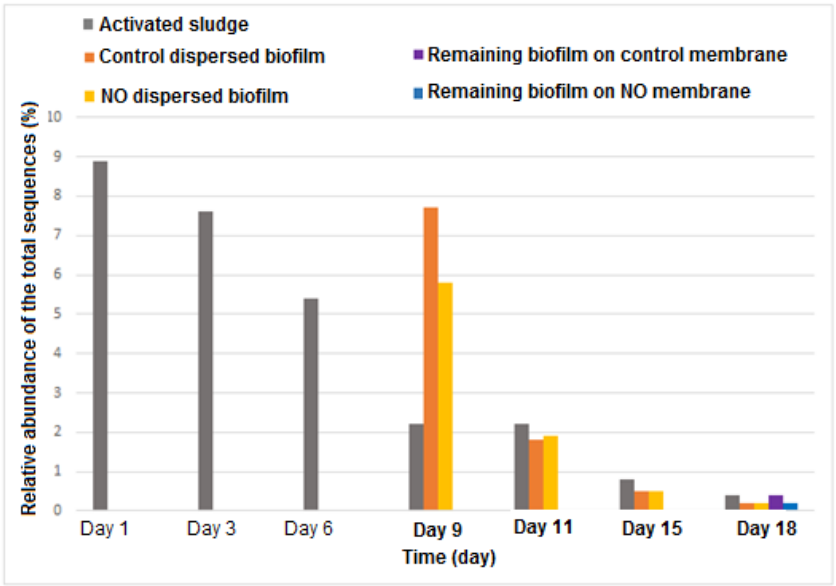

Figure 4.11. The relative abundance of TM7-3 in sludge, dispersed and remaining membrane biofouling samples. The days marked in bold indicate when backwashing treatments were performed.

Among the family *Comamonadaceae*, the most dominant genus was *Comamonas,* which accounted for 55% sequences, followed by *Rubrivivax* at 20%. The relative abundances of *Comamonadaceae* in sludge, dispersed and membrane biofouling samples are demonstrated in Figure 4.12 A. In contrast to *Saprospiraceae,* the relative abundance of *Comamonas* in the sludge samples increased over time from 0.3 to 18.7%. These bacteria also played an important role in biofouling as demonstrated by the high relative abundance in dispersed samples (control 9.6% ± 5.3 and NO backwash 10.4% ± 6.1). Interestingly, on day 18, the relative abundance of *Comamonas* was reduced both in the dispersed (2.8 – 3.2%) and membrane biofouling (3.1 – 3.5%) samples, although its relative abundance in sludge remained at 18.7%. These results indicate that the backwashing treatments effectively dispersed these bacteria. However, NO treatments showed no significant differences compared to the control.

The relative abundance of *Rubrivivax* was higher in the dispersed samples compared to the sludge samples, except on day 11 (Figure 4.12 B). The average relative abundance of *Rubrivivax* in the dispersed control and NO samples was 4.7% ± 1 and 5.1% ± 1.2, while in the sludge samples collected from day 9 to 18 was 4.3% ± 1.3. On day 18, the relative abundance in the membrane biofouling sample was approximately 2.6% compared to 3.5% in the dispersed sample and 2.8% in the sludge.

The relative abundance of the genus unclassified *Bacteroidetes* in sludge samples was high throughout the experiment (Figure 4.13). The average relative abundance of *Bacteroidetes* from day 9 to 18 was 23.4 ± 1.4 compared to 11.9% ± 2.8 in dispersed biofilms. These results demonstrated that *Bacteroidetes* species may play an important role in both in activated sludge and in the membrane biofouling community. In addition, on day 18, the relative abundance of these bacteria in dispersed biofilms (8.2%) and remaining biofilms (9.2% ± 2.5) was lower than that in previous dispersed biofilms (13.2% ±1.8), suggesting that the treatments partially reduced the relative abundance of these bacteria. However, there was also no significant difference between NO and control dispersal treatments.

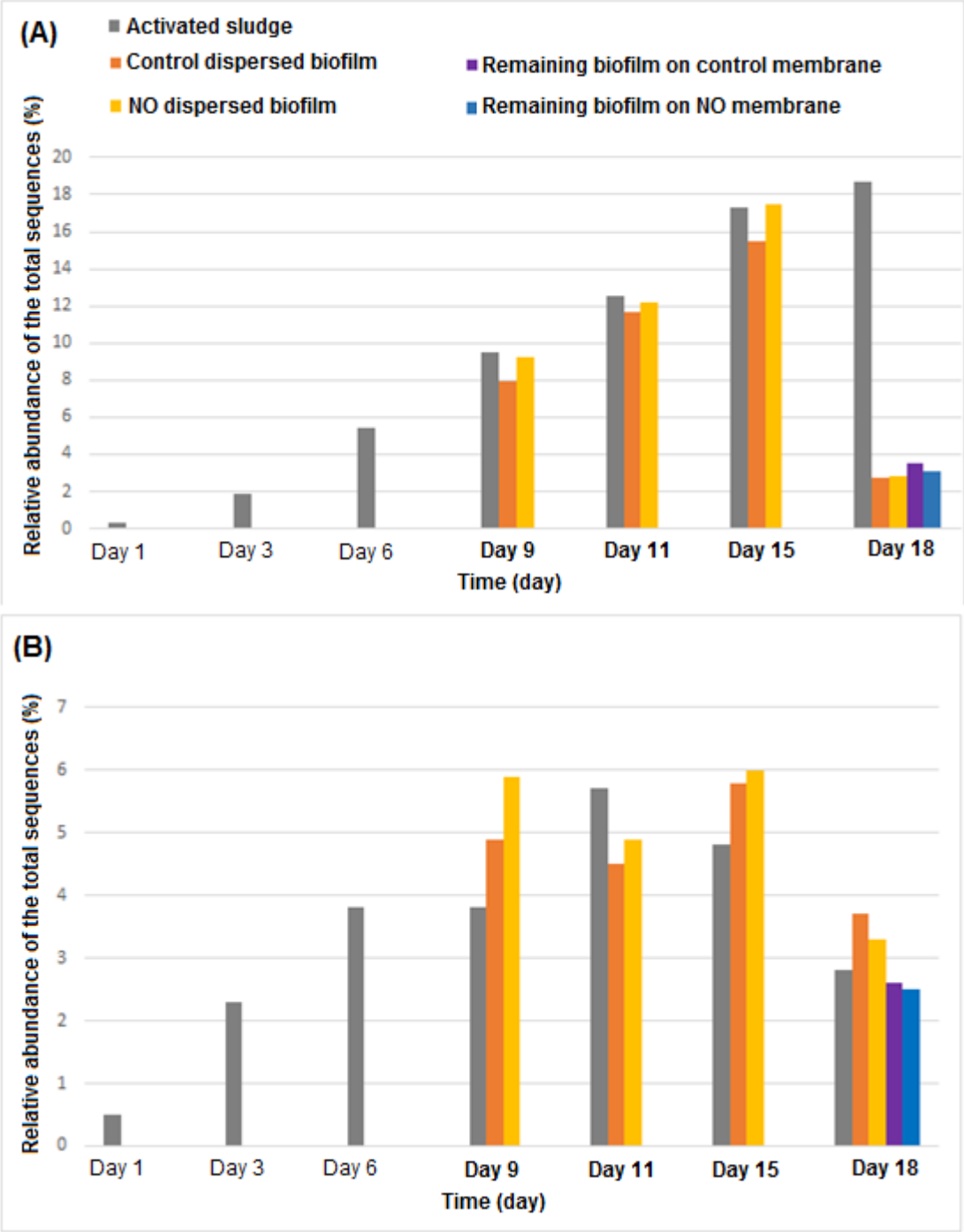

Figure 4.12. The relative abundance of the genera (A) *Comamonas* and (B) *Rubrivivax* in the sludge, dispersed and membrane biofouling samples. The days marked in bold indicate when backwashing treatments were performed.

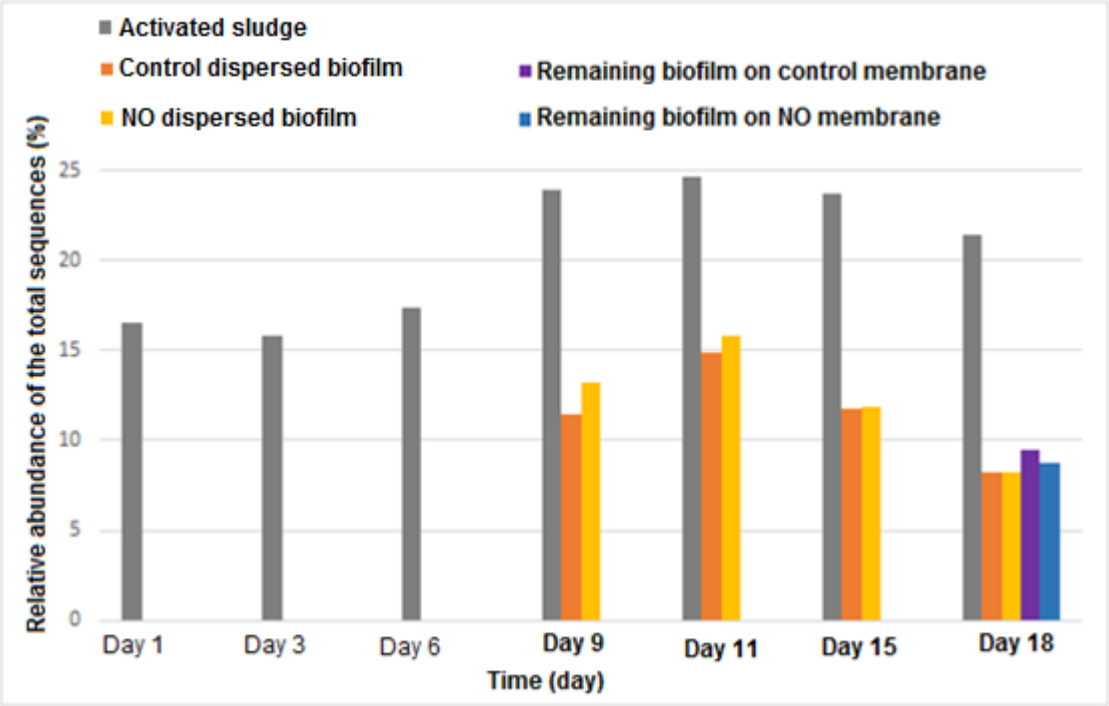

Figure 4.13. The relative abundance of the genus of unclassified *Bacteroidetes* in the sludge, dispersed and membrane biofouling samples. The days marked in bold indicate when backwashing treatments were performed.

A principal coordinate analysis (PCoA) plot based on the weighted UniFrac metric for abundance of observed OTUs was constructed by QIIME 2 to compare the dissimilarity in microbial communities between samples (Figure 4.14). The two axes of the PCoA plot explained 63% of the variation in the data set. The PCoA for the bacterial community structure of the raw sludge, MBR sludge, dispersed and membrane biofouling samples, indicated that there was no significant difference in microbial community structure in the MBR sludge, dispersed and membrane biofouling samples, while the raw sludge sample was significantly different. The results suggested that both NO treatment and the control did not affect the bacterial composition of the sludge, dispersed community or the membrane biofouling samples, while the acclimatisation resulted in the significant changes in microbial community structure.

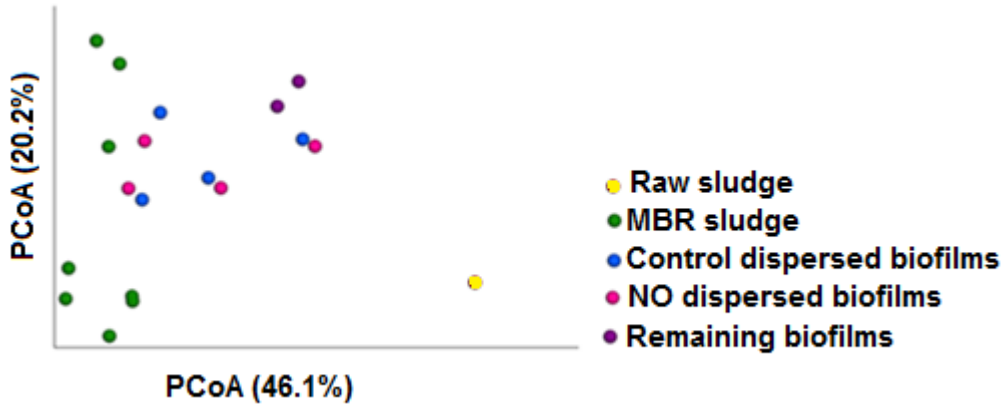

Figure 4.14. Principal coordinate analysis (PCoA) for bacterial community structure of the raw sludge, MBR sludge, dispersed and membrane biofouling samples. Axis values indicate percentage of variance.

4.4. Discussion

After the acclimatisation, the MLSS of the activated sludge was enriched to 5.7 g L^{-1}. In addition, the MLSS/ MLVSS ratio of 0.8 represented high sludge activity, which may be able to achieve stable operation of the MBR. These results exhibited that the acclimatised activated sludge was capable of degrading organics in feed water.

The efficiency of TOC and COD removal was 96.7% and > 99.4% (corresponding to 2.7 and < 3 mg L^{-1} in effluent, respectively), and thus removal of organics in the MBR was efficient. During the MBR experiment, the removal efficiency of TOC and COD gradually increased over time, reflecting the stability of the MBR. The high concentration of PO_4-P in the effluent may be attributed to the low concentration of COD after day 9. No accumulation of NO_2-N (< 0.6 mg L^{-1}) and the NO_3-N concentration of 32 mg L^{-1}, demonstrated that all NH_4-N was fully converted to NO_3-N, but the NO_3-N was only partially denitrified to N_2.

Removal of biofouling from membranes has been predominantly by chemical cleaning with acid or alkaline solutions. However, chemical methods have negative impacts, such as damaging membrane materials, inhibiting the microbial activity of activated sludge and posing an environmental and health risk. To overcome these drawbacks, biological strategies have been developed, one of which is the application of an NO donor, an intracellular signalling molecule that stimulates motility and biofilm dispersal at nontoxic concentrations

(typically at the low nanomolar range) [127]. In this study, DETA NONOate was used as the NO donor to treat the fouling of the membrane. It is interesting to note that after the first treatment, the TMP of the treated membrane remained at 6.3 kPa ± 0.4, while the TMP of the control increased to 9.4 kPa. Previous studies support the finding that DETA NONOate can constrain further increases in biofilm formation on the membrane surface [128]. After the three backwashing treatments, the TMP of DETA-treated membranes was reduced by 35% compared to 21% for water backwashing treatments (P value < 0.05).

MBR performance is determined by microbial hydrolysis, which is a process where macromolecules are broken down into oligomers and monomers before being further degraded. These hydrolysis processes are performed by exoenzymes, such as proteases, galactosidases, glucosidases, lipases, chitinases and phosphatases that are excreted by the microbial communities in the MBR. The properties of the feed water and operational conditions lead to selection for specific bacterial communities capable of growing on the macromolecules present. In this study, the acclimatisation resulted in significant changes in microbial community structure. *Bacteroidetes* increased in relative abundance from 28.8% to 56.2% and became the most dominant phylum in the MBR. The increase in the relative abundance of *Bacteroidetes* may be attributed to the high yeast extract concentration (0.3 g L^{-1}) in the feed water. Many previous studies reported that *Bacteroidetes* are responsible for the degradation of complex organic compounds, including polysaccharides and proteins [126, 129, 130]. During the MBR experiment, there were a slight decrease (approximately 8%) in the relative abundance of *Bacteroidetes*. Conversely, the relative abundance of *Proteobacteria* increased from 18.8% to 41%, which may explain the high COD removal efficiency (> 99.4%) as bacteria belonging to *Proteobacteria*, especially *Betaproteobacteria* are associated with organic substrate degradation [126]. Furthermore, *Bacteroidetes* and *Betaproteobacteria* were reported to be salt-tolerant, which may also explain their proliferation under the high salt concentration of feed water used in this study [131, 132]. The most abundant families (≥ 5% relative abundance) in the MBR were unclassified *Bacteroidetes*, *Comamonadaceae*, *Saprospiraceae*, *Chitinophagaceae,* unclassified TM7-3, *Xanthomonadaceae* and *Sphingobacteriaceae*, most of which belong to *Bacteroidetes* and *Betaproteobacteria.*

EPS and SMPs have been reported to be the main substances responsible for biofouling and the associated increase in TMP [133, 134]. Therefore, bacteria able to produce these biofouling metabolic products may contribute to membrane biofouling. In this study, species belonging to *Saprospiraceae, Comamonadaceae*, unclassified *Bacteroidetes* and unclassified TM7-3 showed changes in their relative abundance that correlated with the sudden increase in TMP, and had relatively high abundances in the dispersed biofouling samples. The results indicate that these bacteria may contribute to biofouling. These findings are supported by previous studies, suggesting that *Saprospiraceae, Comamonadaceae* and unclassified *Bacteroidetes* are successful biofilm community members [129, 130, 132, 134].

Unclassified TM7-3 and *Saprospiraceae* may play roles as pioneers or primary colonisers of the membrane, explaining the reduction in relative abundance of these bacteria in sludge samples associated with the TMP jumps. Previous studies support these findings and demonstrate that species of TM7 are filamentous bacteria that attach to surfaces. TM7 have been shown to hybridise with the FISH probe SAP309, which targets most members of *Saprospiraceae* in the phylum *Bacteroidetes* [129]. Filamentous bacteria belonging to TM7-3 had a relative abundance of 5.8 – 7.7% in the first dispersed sample, but were reduced subsequently, indicating that these filamentous bacteria may play a role only in initial attachment. However, *Saprospiraceae* were highly abundant at 20% of the community in all dispersed biofouling samples. These results suggested that species of *Saprospiraceae* are key members in the biofouling layer. Previous studies support the findings that most *Saprospiraceae* are protein-hydrolysing organisms that produce substrates (amino acids and oligopeptides), which are utilised by filamentous bacteria and others hydrolysate consumers [134, 135]. In addition, *Saprospiraceae* themselves were reported to be plastic-attached bacteria, which produce EPS and scavenge biofilm materials responsible for irreversible biofouling by attaching to other bacteria [129, 130, 136, 137]. The attachment of *Saprospiraceae* to filamentous and commensal bacteria resulted in the formation of three-dimensional biofilm structure, which was reported as irreversible biofouling [129, 138].

In this study, the unclassified *Bacteroidetes* were in high relative abundance in in both sludge (16.6 – 24.7%) and the dispersed biofouling samples (8.2 – 15.8%). The unclassified *Bacteroidetes* are capable of producing extracellular enzymes for degradation of

biopolymers, such as polysaccharides and proteins into oligosaccharides and amino acids, which are utilised by polyphosphate-accumulating organisms responsible for phosphorus removal and denitrification processes [126, 129, 139]. This makes them key microbial community members in both sludge and biofilms. Furthermore, species of *Bacteroidetes* were reported to harbor a large number of genes for adhesive exopolysaccharides and adhesion proteins [140], showing that these bacteria are successful biofilm organisms. In addition, *Bacteroidetes* are secondary surface colonisers affecting the structure, dynamics and function of mature biofilms [140]. *Bacteroidetes* are also involved in biofilm dispersal as they secrete EPS-degrading enzymes, which enable them to disperse from the biofilm and attach to new surfaces [140, 141]. The high relative abundance of *Comamonadaceae* in both sludge (average at 17%) and dispersed samples (average at 20%) are consistent with findings from other studies, indicating that these bacteria have versatile catabolic capabilities for degradation of a wide range of organic compounds. Further, the production of slime and capsular EPS contributes to them being among the most abundant microorganisms in activated sludge and biofilms [140, 142].

Species of *Comamonadaceae* (*Comamonas* in particular) were reported to be members of nitrate-removing microbial communities that play an important role in maintaining the viability of biofilm-cells in mature biofilms by increasing c-di-GMP concentrations through denitrification [143]. Although *Comamonas* species are obligate aerobic bacteria, most of them harbor NAR-type nitrate reductase systems that enable them to convert nitrate to nitrite under bulk aerobic conditions (biofilms) [143]. The high concentration of nitrate (32.2 mg L^{-1}) at the end of the MBR experiment may be attributed to the reduction in relative abundance of *Comamonas* in biofilm samples (2.8 – 3.5%), while being highly abundant in sludge sample (18.7%), suggesting that the denitrification mainly occurred in biofilms. Other dominant bacteria in the dispersed biofouling samples were *Chitinophagaceae* (average at 5.8%), *Xanthomonadaceae* (average at 5.3%), *Rubrivivax* (average at 4.4%) and *Sphingobacteriaceae* (average at 2.5%), which have been reported to be biofilm colonisers capable of producing EPS that enables attachment and utilisation of hydrolysates (oligopeptides, amino acids and oligosaccharides) [128, 130, 136]. The attachment of these bacteria to the biofilm resulting in the development of three-dimensional structure of biofilm,

which traps organic matter and facilitates the degradation of these substrates by other bacteria, including *Saprospiraceae* and *Bacteroidetes* [129, 138].

After three backwashing treatments, the relative abundance of *Comamonadaceae* and *Bacteroidetes* in the membrane biofouling community was reduced to 18.7 and 4%, respectively. However, the treatment unsuccessfully reduced the relative abundance of *Saprospiraceae,* which remained abundant in the membrane biofilm (24.4% ± 2.6). The results indicated that some bacterial members can be dispersed more easily than others. Furthermore, there was no significant difference in biofouling dispersal (in terms of microbial community structure and the reduction of relative abundance) between NO backwashing and the control, that may be attributed to the low concentration of DETA NONOate (40 μM) used in this study which is much lower than the 500 μM DETA NONOate used in the study of Hyun-Suk Oh et al. (2018), demonstrating that the dispersal efficiency for 500 μM DETA NONOate treatment was 22.4 – 55.4% higher than the control (10 Mm NaOH) [128].

CHAPTER 5

CONCLUSIONS AND RECOMMENDATIONS

5.1. Conclusions

5.1.1. Development of a Sensitive Bioluminescent Reporter Technology for AOC Quantification

In desalination systems, seawater is fed through a pre-treatment process, including screening, coagulation, sedimentation and microfiltration, to remove organic and colloidal substances before passing through the RO membranes where salts and impurities are removed under very high pressure (30 – 150 atm) [1]. Available carbon (AOC in particular) in RO feed water has been assumed to be the key determinant for microorganism growth leading to membrane fouling, and limiting the use of this technology [3-5]. This study has developed bioluminescent reporter strains for assessing AOC in feed water as a membrane biofouling control strategy in RO systems.

A luminous AOC test strain *V. fischeri* has been frequently used for measuring AOC in RO feed water [10, 11]. However, use of *V. fischeri* is limited because this bacterium grows on glucose as a sole carbon source but not on AOC mainly composed of humic substances and LMW neutrals. To improve the current AOC assay, marine bacteria having metabolic potential to utilise AOC were isolated from seawater. The selection of AOC test strains was based on the growth of the strains on seawater medium. Three isolates BLS2, CBSW3 and CBSW4 were selected as potential AOC test strains as they grew better than other strains, reaching maximum cell densities of 5.1 x 10^5, 4.5 x 10^5 and 7.2 x 10^5 CFU ml^{-1}, respectively. All three strains were able to grow on humic substances reaching high cell densities of 5.0 x 10^4 - 2.1 x 10^5 CFU ml^{-1}, while *V. fischeri* MJ1 did not grow. According to a partial 16S

rDNA gene sequence analysis, the three strains BLS2, CBSW3 and CBSW4 are species of *Enterovibrio*, *Vibrio* and *Pseudoalteromonas*, respectively.

The construction of bioluminescent reporter plasmids was done by integrating *luxAB* genes from *V. fischeri* MJ1 downstream of a strong promoter (*lacIQ*) into high copy number plasmids pUC19 and pUC19-*cat* or conjugative plasmids pLG401 and pLS6. These reporter plasmids pUC19-*luxAB,* pUC19-*luxAB*-*cat,* pLG401-*luxAB* and pLS6-*luxAB* were transferred into BLS2, CBSW3 and CBSW4 and a common marine strain, *V. cholerae* A1552, creating BLS2 (pLG401-*luxAB*/ pLS6-*luxAB*)**,** CBSW3 (pLG401-*luxAB*/ pLS6-*luxAB*) and A1552 (pUC19-*luxAB*). A reporter plasmid was not successfully transferred into CBSW4.

Bioluminescence of BLS2 (pLG401-*luxAB*/ pLS6-*luxAB*)**** and CBSW3 (pLG401-*luxAB*/ pLS6-*luxAB*) was approximately 3 x 10^1 RLU, which was only 2-fold greater than the background signal. In contrast, *luxAB* genes was successfully expressed in *V. cholerae* A1552, producing bioluminescent intensity of 3.3 x 10^4 RLU, which was 3000-fold greater than the background signal. The linear curve constructed by A1552 (pUC19-*luxAB*) with R^2 of 0.9761 showed that there is a strong correlation between bioluminescent intensity and glucose concentrations in a range of 0 – 100 µg C L^{-1}. The detection limit of this assay was 20 µg C L^{-1}. In the current study, the time needed to perform the bioluminescence-based AOC assay was 10 min rather than 30 – 60 min described in other studies.

Bioluminescent AOC tests developed in this study can be used as membrane fouling indicators to estimate fouling potential of RO pre-treated feed water. This early warning system can save on costs associated with RO membrane fouling, including additional energy costs, chemical cleaning and membrane installation. In comparison to previously developed AOC assays, the AOC assays performed in this study were faster and would allow for prediction of membrane fouling potential and prompt and effective remedial action. In addition, this simple bioluminescent detection can be used to assess the efficiency of pre-treatment processes allowing for development of more effective pre-treatment processes to improve RO feed water quality. Furthermore, the isolation of marine strains (BLS2, CBSW3 and CBSW4) able to metabolise main AOC compounds is promising for further development of more accurate AOC tests, which represent real AOC concentrations.

5.1.2. Characterisation of the Microbial Community in an MBR and Efficacy of NO for Reduction of TMP

MBRs have been widely applied for treatment of high COD wastewater using activated sludge and membrane filtration. Bacterial communities in activated sludge play essential roles in the degradation of organic substances in feed water, while the attachment of microorganisms and the accumulation of microbial products on membranes result in membrane biofouling. As a result, mechanisms of membrane fouling in MBRs is frequently complicated as activated sludge bacterial communities interact with each other and the membrane in different ways, making it difficult to determine the key foulants [17]. Characterisation of microbial communities in activated sludge and those members responsible for the membrane fouling were carried out in this study to identify appropriate biofouling control strategies.

The raw sludge was acclimatised for 18 days to obtain high sludge activity with the concentration of MLSS at 5.7 g L^{-1} and the ratio of MLVSS to MLSS of 0.8. The acclimatisation resulted in significant changes in the microbial community structure of the raw sludge. In the raw sludge, *Proteobacteria* was the most dominant phylum (50.7%), followed by *Bacteroidetes* (28.8%). After the acclimatisation, *Bacteroidetes* increased significantly to 56.2% and became the most dominant phylum in the MBR, while *Proteobacteria* was reduced to 18.8%.

The activated sludge showed strong microbial activity with high TOC and COD removal efficiency (96.7% and > 99.4%, respectively). However, a slight increase in phosphate concentration in the effluent after day 9 indicated the saturation of the sludge for phosphate uptake due to the low COD concentrations after day 9. Furthermore, the high nitrate concentration in the end of the experiment suggested the inefficiency of denitrifying processes. *Bacteroidetes* and *Proteobacteria* were the most dominant phyla in the MBR accounting for 82.4% average relative abundance of the total sequences. In addition, the most abundant classes (≥ 5% relative abundance) were *Saprospirae*, unclassified *Bacteroidetes*, *Betaproteobacteria*, *Gammaproteobacteria*, *Actinobacteria*, TM7-3 and *Sphingobacteriia*. Most of these classes belong to *Bacteroidetes* and *Proteobacteria*.

At family level, the most dominant OTUs belong to unclassified *Bacteroidetes*, *Comamonadaceae*, *Saprospiraceae*, *Chitinophagaceae,* unclassified TM7-3, *Xanthomonadaceae* and *Sphingobacteriaceae*, in which unclassified *Bacteroidetes*, *Comamonadaceae*, *Saprospiraceae* and unclassified TM7-3 showed significant changes in relative abundance associated with the rapid TMP increases. TM7-3 and *Saprospiraceae* may be primary colonisers of the biofilm, which are responsible for surface attachment, that may explain the significant reduction of their relative abundance in activated sludge. In addition, unclassified *Bacteroidetes* and *Comamonadaceae* (*Comamonas* in particular) are secondary colonisers of the biofilm, which may affect the structure, dynamic and function of mature biofilms.

Dispersal efficiency of different bacterial species by the backwashing treatments was significantly different. The treatment successfully dispersed species of *Comamonas* and partially reduced the relative abundance of *Bacteroidetes,* while species of *Saprospiraceae* were resistant to backwashing. However, DETA NONOate treatments showed no significant differences compared to the control (distilled water backwash). In addition, PCoA revealed no significant changes in the microbial communities of NO-treated biofilms and control either in dispersed biofilms or remaining biofilms. In terms of TMP recovery, NO backwashing reduced the TMP by 35%, while the control showed a reduction of 21% (P value < 0.05).

The analysis of activated sludge and biofilm microbial communities in this study complement our existing understanding of the structure and diversity of MBR membrane biofilm communities. Furthermore, the identification of specific microbial communities associated with the TMP increases will allow for targeted novel fouling control strategies against those specific organisms. In addition, the significant reduction of TMP by NO backwashing presented in the current study provides evidence for the application of DETA NONOate for delaying sudden TMP jumps in MBR systems.

5.2. Recommendations and Future Directions

For the first objective of the development of bioluminescent reporter strains for AOC measurement, the transfer of high copy number recombinant plasmids pUC19-*luxAB* into the

three potential AOC test strains (BLS2, CBSW3 and CBSW4) strains was not successful. While these strains were capable of utilising the main AOC compounds (humic substances) in feedwater further work needs to be done to increase their bioluminescence. To complement the current study, several suggestions for future directions are:

- Modification of transformation protocol is an attempt to introduce pUC19-*luxAB* into these potential AOC test strains. Conjugative plasmids, which replicate at high copy numbers in marine strains may be developed and other strong promoters tested for use in these strains.

In the MBR study, DETA NONOate treatments significantly delaying the rapid TMP increase compared to the control. However, there were no difference between the NO treatment and the control in terms of microbial community. In addition, one of the key questions of how DETA NONOate affects other biofilm constituents remains to be determined. Therefore, further experiments listed below are needed for the confirmation of the effectiveness of DETA NONOate against membrane biofouling.

- Improvement of the efficiency of the NO compound by optimising the dosing protocol.

- Confirmation the efficiency of the NO compound on the reduction of biofilm constituents (polysaccharides, proteins and total cells).

- Development of appropriate strategies to target these key bacteria communities responsible for biofouling.

- Replicates for the MBR experiment required to achieve statistical significance.

REFERENCES

1. Giwa, A. and Ogunribido, A. (2012). The applications of membrane operations in the textile industry: a review. *Br J Appl Sci Technol*; **2** (3): 296.

2. Iorhemen, O.T., Hamza, R.A. and Tay, J.H. (2016). Membrane bioreactor (MBR) technology for wastewater treatment and reclamation: membrane fouling. *Membranes*; **6** (2): 33.

3. LeChevallier, M.W., Shaw, N.E., Kaplan, L.A. and Bott, T.L. (1993). Development of a rapid assimilable organic carbon method for water. *Appl Environ Microbiol*; **59** (5): 1526-1531.

4. Haddix, P.L., Shaw, N.J. and LeChevallier, M.W. (2004). Characterization of bioluminescent derivatives of assimilable organic carbon test bacteria. *Appl Environ Microbiol*; **70** (2): 850-854.

5. Van Der Kooij, D., Visser, A. and Hijnen, W.A.M. (1982). Determining the concentration of easily assimilable organic carbon in drinking water. *AWWA*; **74** (10): 540-545.

6. Barraud, N., Hassett, D.J., Hwang, S.H., Rice, S.A., Kjelleberg, S. and Webb, J.S. (2006). Involvement of nitric oxide in biofilm dispersal of *Pseudomonas aeruginosa*. *J Bacteriol*; **188** (21): 7344-7353.

7. Barraud, N., Schleheck, D., Klebensberger, J., Webb, J.S., Hassett, D.J., Rice, S.A. and Kjelleberg, S. (2009). Nitric oxide signaling in *Pseudomonas aeruginosa* biofilms mediates phosphodiesterase activity, decreased cyclic di-GMP levels, and enhanced dispersal. *J Bacteriol*; **191** (23): 7333-7342.

8. Barnes, R.J., Low, J.H., Bandi, R.R., Tay, M., Chua, F., Aung, T., Fane, A.G., Kjelleberg, S. and Rice, S.A. (2015). Nitric oxide treatment for the control of reverse osmosis membrane biofouling. *Appl Environ Microbiol*; **81** (7): 2515-2524.

9. Barnes, R.J., Bandi, R.R., Wong, W.S., Barraud, N., McDougald, D., Fane, A., Kjelleberg, S. and Rice, S.A. (2013). Optimal dosing regimen of nitric oxide donor compounds for the reduction of *Pseudomonas aeruginosa* biofilm and isolates from wastewater membranes. *Biofouling*; **29** (2): 203-212.

10. Jeong, S. and Vigneswaran, S. (2015). Practical use of standard pore blocking index as an indicator of biofouling potential in seawater desalination. *Desalination*; **365**: 8-14.

11. Jeong, S., Naidu, G., Vigneswaran, S., Ma, C.H. and Rice, S.A. (2013). A rapid bioluminescence-based test of assimilable organic carbon for seawater. *Desalination*; **317**: 160-165.

12. Sivakumar, B. (2014). Water resources and environment in Australia. *Stoch Environ Res Risk Asses*; **28**: 1-2.

13. Weinrich, L.A., Schneider, O.D. and LeChevallier, M.W. (2011). Bioluminescence-based method for measuring assimilable organic carbon in pretreatment water for reverse osmosis membrane desalination. *Appl Environ Microbiol*; **77** (3): 1148-1150.

14. Brooun, A., Liu, S. and Lewis, K. (2000). A dose-response study of antibiotic resistance in *Pseudomonas aeruginosa* biofilms. *Antimicrob Agents Chemother*; **44** (3): 640-646.

15. Bereschenko, L.A., Prummel, H., Euverink, G.J.W., Stams, A.J.M. and Van Loosdrecht, M.C.M. (2011). Effect of conventional chemical treatment on the microbial population in a biofouling layer of reverse osmosis systems. *Water Res*; **45** (2): 405-416.

16. Nguyen, T., Roddick, F.A. and Fan, L. (2012). Biofouling of water treatment membranes: a review of the underlying causes, monitoring techniques and control measures. *Membranes (Basel)*; **2** (4): 804-840.

17. Meng, F., Chae, S.R., Drews, A., Kraume, M., Shin, H.S. and Yang, F. (2009). Recent advances in membrane bioreactors (MBRs): membrane fouling and membrane material. *Water Res*; **43** (6): 1489-1512.

18. Ning, R.Y. (2011). Pretreatment for reverse osmosis systems. *Expanding issues in desalination*. InTech: London (Ch. 2, pp 57-62).

19. Hem, L.J. and Efraimsen, H. (2001). Assimilable organic carbon in molecular weight fractions of natural organic matter. *Water Res*; **35** (4): 1106-1110.

20. Ma, J., Ibekwe, A.M., Leddy, M., Yang, C.H. and Crowley, D.E. (2012). Assimilable organic carbon (AOC) in soil water extracts using *Vibrio harveyi* BB721 and its implication for microbial biomass. *PloS One*; **7** (5): e28519.

21. Kaplan, J.Á. (2010). Biofilm dispersal: mechanisms, clinical implications, and potential therapeutic uses. *J Dent Res*; **89** (3): 205-218.

22. Barraud, N., J Kelso, M., A Rice, S. and Kjelleberg, S. (2015). Nitric oxide: a key mediator of biofilm dispersal with applications in infectious diseases. *Curr Pharm Des*; **21** (1): 31-42.

23. Saavedra, J.E., Southan, G.J., Davies, K.M., Lundell, A., Markou, C., Hanson, S.R., Adrie, C., Hurford, W.E., Zapol, W.M. and Keefer, L.K. (1996). Localizing antithrombotic and vasodilatory activity with a novel, ultrafast nitric oxide donor. *J Med Chem*; **39** (22): 4361-4365.

24. Tansel, B. (2008). New technologies for water and wastewater treatment: A survey of recent patents. *Recent Pat Chem Eng*; **1** (1): 17-26.

25. Sutherland, K. (2008). Drinking water: Pretreatment processes for fresh water. *Filtr Sep*; **45** (2): 22-25.

26. Gaid, K. (2011). A large review of the pre treatment *Expanding issues in desalination*. InTech: London (Ch. 1, pp 3-50).

27. Ramalho, R. (2012). Characterization of domestic and industrial wastewaters. *Introduction to wastewater treatment processes*. Elsevier: London (Ch. 2, pp 26-66).

28. Radjenović, J., Matošić, M., Mijatović, I., Petrović, M. and Barceló, D. (2008). Membrane bioreactor (MBR) as an advanced wastewater treatment technology. *Emerging contaminants from industrial and municipal waste*. Springer: Berlin (Ch. 2, pp 37-101).

29. Le, N.L. and Nunes, S.P. (2016). Materials and membrane technologies for water and energy sustainability. *SM&T*; **7**: 1-28.

30. Krishna, H.J. (2004). Introduction to desalination technologies. *TWDB*; **2**: 1-7.

31. Cicek, N., Franco, J.P., Suidan, M.T. and Urbain, V. (1998). Using a membrane bioreactor to reclaim wastewater. *J Am Water Works Assoc*; **90** (11): 105.

32. Ramesh, A., Lee, D.J., Wang, M.L., Hsu, J.P., Juang, R.S., Hwang, K.J., Liu, J.C. and Tseng, S.J. (2006). Biofouling in membrane bioreactor. *Sep Sci Technol*; **41** (7): 1345-1370.

33. Ahansazan, B., Afrashteh, H., Ahansazan, N. and Ahansazan, Z. (2014). Activated sludge process overview. *Int J Environ Sci Technol*; **5** (1): 81.

34. Verma, M., Brar, S.K., Blais, J.F., Tyagi, R.D. and Surampalli, R.Y. (2006). Aerobic biofiltration processes—Advances in wastewater treatment. *Pract Period Hazard Toxic Radioact Waste Manag*; **10** (4): 264-276.

35. Srivastava, N.K. and Majumder, C.B. (2008). Novel biofiltration methods for the treatment of heavy metals from industrial wastewater. *J Hazard Mater*; **151** (1): 1-8.

36. Chaudhary, D.S., Vigneswaran, S., Ngo, H.H., Shim, W.G. and Moon, H. (2003). Biofilter in water and wastewater treatment. *Korean J Chem Eng*; **20** (6): 1054.

37. Webb, J.S., Givskov, M. and Kjelleberg, S. (2003). Bacterial biofilms: prokaryotic adventures in multicellularity. *Curr Opin Microbiol*; **6** (6): 578-585.

38. Goldberg, J. (2002). Biofilms and antibiotic resistance: a genetic linkage. *Trends Microbiol*; **10** (6): 264.

39. Peng, J.S., Tsai, W.C. and Chou, C.C. (2002). Inactivation and removal of *Bacillus cereus* by sanitizer and detergent. *Int J Food Microbiol*; **77** (1): 11-18.

40. Chen, M.J., Zhang, Z. and Bott, T.R. (1998). Direct measurement of the adhesive strength of biofilms in pipes by micromanipulation. *Biotech*; **12** (12): 875-880.

41. Koch, B., Worm, J., Jensen, L.E., Højberg, O. and Nybroe, O. (2001). Carbon limitation induces ςS-dependent gene expression in *Pseudomonas fluorescens* in soil. *Appl Environ Microbiol*; **67** (8): 3363-3370.

42. Mun, E., Lee, S., Kim, I., Kwon, B., Park, H. and Hong, S. (2013). Measurements of assimilable organic carbon (AOC) in high saline conditions using P17. *Water Sci Technol*; **13** (2): 265-272.

43. Volk, C.J. and LeChevallier, M.W. (1999). Impacts of the reduction of nutrient levels on bacterial water quality in distribution systems. *Appl Environ Microbiol*; **65** (11): 4957-4966.

44. Escobar, I.C., Hong, S. and Randall, A.A. (2000). Removal of assimilable organic carbon and biodegradable dissolved organic carbon by reverse osmosis and nanofiltration membranes. *J Memb Sci*; **175** (1): 1-17.

45. Van Der Kooij, D. (1990). Assimilable organic carbon (AOC) in drinking water. *Drinking water microbiology*. Springer: New York (Ch. 3, pp 57-87).

46. Hammes, F., Berger, C., Köster, O. and Egli, T. (2010). Assessing biological stability of drinking water without disinfectant residuals in a full-scale water supply system. *J Water Supply Res Technol* **59** (1): 31-40.

47. Takada, K., Hashimoto, K., Soda, S., Ike, M., Yamashita, K. and Hashimoto, T. (2014). Characterization of microbial community in membrane bioreactors treating domestic wastewater. *J Water Environ Tech*; **12** (2): 99-107.

48. Kemmy, F.A., Fry, J.C. and Breach, R.A. (1989). Development and operational implementation of a modified and simplified method for determination of assimilable organic carbon (AOC) in drinking water. *Water Sci Technol*; **21** (3): 155-159.

49. Jørgensen, M.K., Bugge, T.V., Larsen, P., Nielsen, P.H. and Christensen, M.L. (2017). Membrane filtration device for studying compression of fouling layers in membrane bioreactors. *PloS One*; **12** (7): e0181652.

50. Boerlage, S.F., Kennedy, M., Aniye, M.P. and Schippers, J.C. (2003). Applications of the MFI-UF to measure and predict particulate fouling in RO systems. *J Memb Sci*; **220** (1): 97-116.

51. Ruiz-García, A., Melián-Martel, N. and Nuez, I. (2017). Short review on predicting fouling in RO desalination. *Membranes*; **7** (4): 62.

52. Leparc, J., Rapenne, S., Courties, C., Lebaron, P., Croue, J.P., Jacquemet, V. and Turner, G. (2007). Water quality and performance evaluation at seawater reverse osmosis plants through the use of advanced analytical tools. *Desalination*; **203** (1-3): 243-255.

53. Alhadidi, A., Kemperman, A.J.B., Blankert, B., Schippers, J.C., Wessling, M. and Van der Meer, W.G.J. (2011). Silt density index and modified fouling index relation, and effect of pressure, temperature and membrane resistance. *Desalination*; **273** (1): 48-56.

54. Unosson, E. (2015). *Antibacterial strategies for Titanium biomaterials*. Uppsala, Sweden; University of Uppsala, Dissertation, 66 pp

55. Fleming, D. and Rumbaugh, K.P. (2017). Approaches to dispersing medical biofilms. *Microorganisms*; **5** (2): 15.

56. Yildiz, F.H. (2008). Cyclic dimeric GMP signaling and regulation of surface-associated developmental programs. *J Bacteriol*; **190** (3): 781-783.

57. Simm, R., Morr, M., Kader, A., Nimtz, M. and Römling, U. (2004). GGDEF and EAL domains inversely regulate cyclic di-GMP levels and transition from sessility to motility. *Mol Microbiol*; **53** (4): 1123-1134.

58. Thormann, K.M., Saville, R.M., Shukla, S. and Spormann, A.M. (2005). Induction of rapid detachment in *Shewanella oneidensis* MR-1 biofilms. *J Bacteriol*; **187** (3): 1014-1021.

59. Thormann, K.M., Duttler, S., Saville, R.M., Hyodo, M., Shukla, S., Hayakawa, Y. and Spormann, A.M. (2006). Control of formation and cellular detachment from *Shewanella oneidensis* MR-1 biofilms by cyclic di-GMP. *J Bacteriol*; **188** (7): 2681-2691.

60. Boehm, A., Steiner, S., Zaehringer, F., Casanova, A., Hamburger, F., Ritz, D., Keck, W., Ackermann, M., Schirmer, T. and Jenal, U. (2009). Second messenger signalling governs *Escherichia coli* biofilm induction upon ribosomal stress. *Mol Microbiol*; **72** (6): 1500-1516.

61. Gjermansen, M., Nilsson, M., Yang, L. and Tolker-Nielsen, T. (2010). Characterization of starvation-induced dispersion in *Pseudomonas putida* biofilms: genetic elements and molecular mechanisms. *Mol Microbiol*; **75** (4): 815-826.

62. Newell, P.D., Monds, R.D. and O'Toole, G.A. (2009). LapD is a bis-(3′, 5′)-cyclic dimeric GMP-binding protein that regulates surface attachment by *Pseudomonas fluorescens* Pf0–1. *Proc Natl Acad Sci* **106** (9): 3461-3466.

63. Yildiz, F.H. and Visick, K.L. (2009). *Vibrio* biofilms: so much the same yet so different. *Trends Microbiol*; **17** (3): 109-118.

64. Barraud, N., Storey, M.V., Moore, Z.P., Webb, J.S., Rice, S.A. and Kjelleberg, S. (2009). Nitric oxide-mediated dispersal in single-and multi-species biofilms of clinically and industrially relevant microorganisms. *Microb Biotechnol*; **2** (3): 370-378.

65. Delgado-Nixon, V.M., Gonzalez, G. and Gilles-Gonzalez, M.A. (2000). Dos, a heme-binding PAS protein from *Escherichia coli*, is a direct oxygen sensor. *Biochemistry*; **39** (10): 2685-2691.

66. Rodionov, D.A., Dubchak, I.L., Arkin, A.P., Alm, E.J. and Gelfand, M.S. (2005). Dissimilatory metabolism of nitrogen oxides in bacteria: comparative reconstruction of transcriptional networks. *PLoS Comput Biol*; **1** (5): e55.

67. Liu, R., Yu, Z., Guo, H., Liu, M., Zhang, H. and Yang, M. (2012). Pyrosequencing analysis of eukaryotic and bacterial communities in faucet biofilms. *Sci Total Environ*; **435**: 124-131.

68. Xu, S., Yao, J., Ainiwaer, M., Hong, Y. and Zhang, Y. (2018). Analysis of Bacterial Community Structure of Activated Sludge from Wastewater Treatment Plants in Winter. *Biomed Res Int*; **2018**: 1-8.

69. Arnal, J.M., García-Fayos, B. and Sancho M. (2011). Membrane cleaning. *Expanding issues in desalination*. InTech: London (Ch. 3, pp 64-79).

70. Tamura, K., Peterson, D., Peterson, N., Stecher, G., Nei, M. and Kumar, S. (2011). MEGA5: molecular evolutionary genetics analysis using maximum likelihood, evolutionary distance, and maximum parsimony methods. *Mol Biol Evol*; **28** (10): 2731-2739.

71. Hall, T. (1999). BioEdit: a user-friendly biological sequence alignment editor and analysis program for Windows 95/98/NT. *Nucleic Acids Res*; **41**: 95-98.

72. Kimura, M. (1980). A simple method for estimating evolutionary rates of base substitutions through comparative studies of nucleotide sequences. *J Mol Evol*; **16**: 111-120.

73. Felsenstein, J. (1985). Confidence limits on phylogenies: an approach using the bootstrap. *Evolution*; **39** (4): 783-791.

74. Villacorte, L.O. (2016). Liquid chromatography: organic carbon detection (LC-OCD). *Springer*: 1100-1102.

75. Huber, S.A., Balz, A., Abert, M. and Pronk, W. (2011). Characterisation of aquatic humic and non-humic matter with size-exclusion chromatography–organic carbon detection–organic nitrogen detection (LC-OCD-OND). *Water Res*; **45** (2): 879-885.

76. Simon, F.X., Penru, Y., Guastalli, A.R., Esplugas, S., Llorens, J. and Baig, S. (2013). NOM characterization by LC-OCD in a SWRO desalination line. *Desalination*; **51** (7-9): 1776-1780.

77. Singh, N., Paterson, D.L., Acar, J., Casewell, M., Freeman, J., Friis, C., Goossens, H., Kronvall, G., Kyriakopoulos, A.M., Matsiota-Bernard, P. and Marinis, E. (2000). Determination of minimum inhibitory concentrations (MICs) of antibacterial agents by agar dilution. *Clin Microbiol Infect*; **6** (9): 453-515.

78. Viswanathan, K., Viswanathan, P. and Kroos, L. (2006). Mutational analysis of the *Myxococcus xanthus* Ω4406 promoter region reveals an upstream negative regulatory element that mediates C-signal dependence. *J Bacteriol*; **188** (2): 515-524.

79. McDougald, D., Rice, S.A. and Kjelleberg, S. (2001). SmcR-Dependent Regulation of Adaptive Phenotypes in *Vibrio vulnificus*. *J Bacteriol*; **183** (2): 758-762.

80. McDougald, D., Srinivasan, S., Rice, S.A. and Kjelleberg, S. (2003). Signal-mediated cross-talk regulates stress adaptation in *Vibrio* species. . *Microbiology*; **149** (7): 1923-1933.

81. Bresan, S., Sznajder, A., Hauf, W., Forchhammer, K., Pfeiffer, D. and Jendrossek, D. (2016). Polyhydroxyalkanoate (PHA) granules have no phospholipids. *Sci Rep*; **6**: 26612.

82. Matz, C., McDougald, D., Moreno, A.M., Yung, P.Y., Yildiz, F.H. and Kjelleberg, S. (2005). Biofilm formation and phenotypic variation enhance predation-driven persistence of *Vibrio cholerae*. *Proc Natl Acad Sci* **102** (46): 16819-16824.

83. Liu, I.R.I.S., Liu, M.A.R.T.H.A. and Shergill, K.A.R.E.N. (2006). The effect of spheroplast formation on the transformation efficiency in *Escherichia coli* DH5α. *J Exp Microbiol Immunol*; **9**: 81-85.

84. Zeaiter, Z., Mapelli, F., Crotti, E. and Borin, S. (2018). Methods for the genetic manipulation of marine bacteria. *Electron J Biotechnol*; **33**: 17-28.

85. Zhao, X., Hu, H., Liu, S., Jiang, F., Shi, X., Li, M. and Xu, X. (2013). Improvement of the assimilable organic carbon (AOC) analytical method for reclaimed water. *Front Environ Sci Eng*; **7** (4): 483-491.

86. Xu, X.W., Wu, Y.H., Wang, C.S., Gao, X.H., Wang, X.G. and Wu, M. (2010). *Pseudoalteromonas lipolytica* sp. nov., isolated from the Yangtze River estuary. *Int J Syst Evol Microbiol*; **60** (9): 2176-2181.

87. Thompson, F.L., Iida, T. and Swings, J. (2004). Biodiversity of vibrios. *Microbiol Mol Biol Rev*; **68** (3): 403-431.

88. Thompson, F.L., Hoste, B., Thompson, C.C., Goris, J., Gomez-Gil, B., Huys, L., De Vos, P. and Swings, J. (2002). *Enterovibrio norvegicus* gen. nov., sp. nov., isolated from the gut of turbot (*Scophthalmus maximus*) larvae: a new member of the family *Vibrionaceae*. *Int J Syst Evol Microbiol*; **52** (6): 2015-2022.

89. Naidu, G., Jeong, S., Vigneswaran, S. and Rice, S.A. (2013). Microbial activity in biofilter used as a pretreatment for seawater desalination. *Desalination*; **309**: 254-260.

90. Glascock, C.B. and Weickert, M.J. (1998). Using chromosomal lacIQ1 to control expression of genes on high-copy-number plasmids in *Escherichia coli*. *Gene*; **223** (1): 221-231.

91. Andreu, N., Zelmer, A., Fletcher, T., Elkington, P.T., Ward, T.H., Ripoll, J., Parish, T., Bancroft, G.J., Schaible, U., Robertson, B.D. and Wiles, S. (2010). Optimisation of bioluminescent reporters for use with mycobacteria. *PloS One*; **5** (5): e10777.

92. Wiles, S., Ferguson, K., Stefanidou, M., Young, D.B. and Robertson, B.D. (2005). Alternative luciferase for monitoring bacterial cells under adverse conditions. *Appl Environ Microbiol*; **71** (7): 3427-3432.

93. Tehrani, G.A., Mirzaahmadi, S., Bandehpour, M., Laloei, F., Eidi, A., Valinasab, T. and Kazemi, B. (2011). Molecular cloning and expression of the luciferase coding genes of *Vibrio fischeri*. *AJB*; **10** (20): 4018-4023.

94. Jablonski, E. and DeLuca, M. (Properties and uses of immobilized light-emitting enzyme systems from *Beneckea harveyi*. *Clin Chem*; **25** (9): 1622-1627.

95. Waidmann, M.S., Bleichrodt, F.S., Laslo, T. and Riedel, C.U. (2011). Bacterial luciferase reporters: the Swiss army knife of molecular biology. *Bioeng Bugs*; **2** (1): 8-16.

96. Kawagishi, I., Okunishi, I., Homma, M. and Imae, Y. (1994). Removal of the periplasmic DNase before electroporation enhances efficiency of transformation in the marine bacterium *Vibrio alginolyticus*. *Microbiology*; **140** (9): 2355-2361.

97. Meighen, E.A. (1991). Molecular biology of bacterial bioluminescence. *Microbiol Rev*; **55** (1): 123-142.

98. Chaudhary, N., Sharma, A.K., Agarwal, P., Gupta, A. and Sharma, V.K. (2015). 16S classifier: a tool for fast and accurate taxonomic classification of 16S rRNA hypervariable regions in metagenomic datasets. *PloS One*; **10** (2): e0116106.

99. Nguyen, N.P., Warnow, T., Pop, M. and White, B. (2016). A perspective on 16S rRNA operational taxonomic unit clustering using sequence similarity. *NPJ Biofilms Microbiomes*; **2**: 16004.

100. Ye, L., Shao, M.F., Zhang, T., Tong, A.H.Y. and Lok, S. (2011). Analysis of the bacterial community in a laboratory-scale nitrification reactor and a wastewater treatment plant by 454-pyrosequencing. *Water Res*; **45** (15): 4390-4398.

101. Boon, N., De Windt, W., Verstraete, W. and Top, E.M. (2002). Evaluation of nested PCR–DGGE (denaturing gradient gel electrophoresis) with group-specific 16S rRNA primers for the analysis of bacterial communities from different wastewater treatment plants. *FEMS Microbiol Ecol*; **39** (2): 101-112.

102. Regan, J.M., Harrington, G.W. and Noguera, D.R. (2002). Ammonia-and nitrite-oxidizing bacterial communities in a pilot-scale chloraminated drinking water distribution system. *Appl Environ Microbiol*; **68** (1): 73-81.

103. Matsumoto, S., Katoku, M., Saeki, G., Terada, A., Aoi, Y., Tsuneda, S., Picioreanu, C. and Van Loosdrecht, M.C. (2010). Microbial community structure in autotrophic nitrifying granules characterized by experimental and simulation analyses. *Environ Microbiol* **12** (1): 192-206.

104. Hao, X., Wang, Q., Zhang, X., Cao, Y. and van Mark Loosdrecht, C.M. (2009). Experimental evaluation of decrease in bacterial activity due to cell death and activity decay in activated sludge. *Water Res*; **43** (14): 3604-3612.

105. Zhang, T., Shao, M.F. and Ye, L. (2012). 454 Pyrosequencing reveals bacterial diversity of activated sludge from 14 sewage treatment plants. *ISME J*; **6** (6): 1137-1147.

106. Margulies, M., Egholm, M., Altman, W.E., Attiya, S., Bader, J.S., Bemben, L.A., Berka, J., Braverman, M.S., Chen, Y.J., Chen, Z. and Dewell, S.B. (2005). Genome sequencing in microfabricated high-density picolitre reactors. *Nature*; **437** (7057): 376-380.

107. Degnan, P.H. and Ochman, H. (2012). Illumina-based analysis of microbial community diversity. *ISME J*; **6** (1): 183-194.

108. Apprill, A., McNally, S., Parsons, R. and Weber, L. (2015). Minor revision to V4 region SSU rRNA 806R gene primer greatly increases detection of SAR11 bacterioplankton. *Aquat Microb Ecol*; **75** (2): 129-137.

109. Parada, A.E., Needham, D.M. and Fuhrman, J.A. (2016). Every base matters: assessing small subunit rRNA primers for marine microbiomes with mock communities, time series and global field samples. *Environ Microbiol* **18** (5): 1403-1414.

110. Caporaso, J.G., Lauber, C.L., Walters, W.A., Berg-Lyons, D., Lozupone, C.A., Turnbaugh, P.J., Fierer, N. and Knight, R. (2011). Global patterns of 16S rRNA diversity at a depth of millions of sequences per sample. *Proc Natl Acad Sci* **108**: 4516-4522.

111. Kuczynski, J., Stombaugh, J., Walters, W.A., González, A., Caporaso, J.G. and Knight, R. (2012). Using QIIME to analyze 16S rRNA gene sequences from microbial communities. *Curr Protoc Microbiol*; **27** (1): 1E-5.

112. Fan, J., Ji, F., Xu, X., Wang, Y., Yan, D., Xu, X., Chen, Q., Xiong, J. and He, Q. (2015). Prediction of the effect of fine grit on the MLVSS/MLSS ratio of activated sludge. *Bioresour Technol*; **190**: 51-56.

113. Zawani, Z., Chuah-Abdullah, L., Ahmadun, F.R. and Abdan, K. (2013). Acclimatization process of microorganisms from activated sludge in Kenaf-Retting wastewater. *Developments in sustainable chemical and bioprocess technology*. Springer: Boston (Ch. 8, pp 59-64).

114. Kodape, S., Sapkal, P., Sapkal, V.S. and Sapkal, R.S. (Performance enhancement of recirculated membrane bioreactor (RMBR) with dual effect of cross flow velocity and operating temperature for wastewater treatment. *Int J Emerging Technol Adv Eng*; **4** (8): 134-140.

115. Guo, W.S., Vigneswaran, S., Ngo, H.H. and Xing, W. (2007). Experimental investigation on acclimatized wastewater for membrane bioreactors. *Desalination*; **207** (1-3): 383-391.

116. Hai, F.I. and Yamamoto, K. (2009). Suitability of Membrane Bioreactor for treatment of recalcitrant textile dye wastewater utilising white-rot fungi. *IJEE*; **2** (1-3): 43-55.

117. Golbabaei Kootenaei, F. and Aminirad, H. (2014). Membrane biological reactors (MBR) and their applications for water reuse. *IJABBR*; **2** (7): 2208-2216.

118. Davis, A.M., Fournier, E.K., Waring, L.E. and Shooshan, R.M. (2013). *Utilizing GAC and MIEX to improve TOC removal from wastewater for discharge to groundwater near drinking water sources*. Massachusetts; Worcester Polytechnic Institute, Dissertation, pp 133

119. Wang, Y.K., Pan, X.R., Geng, Y.K. and Sheng, G.P. (2015). Simultaneous effective carbon and nitrogen removals and phosphorus recovery in an intermittently aerated membrane bioreactor integrated system. *Sci Rep*; **5**: 16281.

120. Jeong, S., Rice, S.A. and Vigneswaran, S. (2014). Long-term effect on membrane fouling in a new membrane bioreactor as a pretreatment to seawater desalination. *Bioresour Technol*; **165**: 60-68.

121. Ammary, B.Y. (2004). Nutrients requirements in biological industrial wastewater treatment. *Afr J Biotechnol*; **3** (4): 236-238.

122. Shen, J., He, R., Han, W., Sun, X., Li, J. and Wang, L. (2009). Biological denitrification of high-nitrate wastewater in a modified anoxic/oxic-membrane bioreactor (A/O-MBR). *J Hazard Mater*; **172** (2-3): 595-600.

123. Wen, J., Liu, Y., Tu, Y. and LeChevallier, M. (2015). Energy and chemical efficient nitrogen removal at a full-scale MBR water reuse facility. *AIMS Environmental Science*; **1** (2): 42-55.

124. Hatamoto, M., Kaneko, T., Takimoto, Y., Ito, T., Miyazato, N., Maki, S., Yamaguchi, T. and Aoi, T. (2017). Microbial Community Structure and Enumeration of *Bacillus* species in Activated Sludge. *JWET*; **15** (6): 233-240.

125. Hu, M., Wang, X., Wen, X. and Xia, Y. (2012). Microbial community structures in different wastewater treatment plants as revealed by 454-pyrosequencing analysis. *Bioresour Technol*; 117: 72-79.

126. Nascimento, A.L., Souza, A.J.D., Andrade, P.A.M.D., Dini-Andreote, F., Gomes, A.R.C., Oliveira, F.C. and Regitano, J.B. (2018). Sewage sludge microbial structures and relations to their sources, treatments, and chemical attributes. *Front Microbiol*; **9**: 1462.

127. Luo, J., Zhang, J., Barnes, R.J., Tan, X., McDougald, D., Fane, A.G., Zhuang, G., Kjelleberg, S., Cohen, Y. and Rice, S.A. (2015). The application of nitric oxide to control biofouling of membrane bioreactors. *Microb Biotechnol*; **8** (3): 549-560.

128. Oh, H.S., Constancias, F., Ramasamy, C., Tang, P.Y.P., Yee, M.O., Fane, A.G., McDougald, D. and Rice, S.A. (2018). Biofouling control in reverse osmosis by nitric oxide treatment and its impact on the bacterial community. *J Memb Sci*; **550**: 313-321.

129. Xia, Y., Kong, Y., Thomsen, T.R. and Nielsen, P.H. (2008). Identification and ecophysiological characterization of epiphytic protein-hydrolyzing *Saprospiraceae* ("*Candidatus Epiflobacter*" spp.) in activated sludge. *Appl Environ Microbiol*; **74** (7): 2229-2238.

130. Oberbeckmann, S., Osborn, A.M. and Duhaime, M.B. (2016). Microbes on a bottle: substrate, season and geography influence community composition of microbes colonizing marine plastic debris. *PLoS One*; **11** (8): e0159289.

131. Canfora, L., Bacci, G., Pinzari, F., Papa, G.L., Dazzi, C. and Benedetti, A. (2014). Salinity and bacterial diversity: to what extent does the concentration of salt affect the bacterial community in a saline soil? *PLoS One*; **9** (9): e106662.

132. Luo, J., Lv, P., Zhang, J., Fane, A.G., McDougald, D. and Rice, S.A. (2017). Succession of biofilm communities responsible for biofouling of membrane bio-reactors (MBRs). *PloS One*; **12** (7): e0179855.

133. Gao, D., Fu, Y. and Ren, N. (2013). Tracing biofouling to the structure of the microbial community and its metabolic products: A study of the three-stage MBR process. *Water Res*; **47** (17): 6680-6690.

134. Kim, N.K., Oh, S. and Liu, W.T. (2016). Enrichment and characterization of microbial consortia degrading soluble microbial products discharged from anaerobic methanogenic bioreactors. *Water Res*; **90**: 395-404.

135. Ju, F. and Zhang, T. (2015). Bacterial assembly and temporal dynamics in activated sludge of a full-scale municipal wastewater treatment plant. *ISME J*; **9** (3): 683.

136. Denner, E.B., Paukner, S., Kämpfer, P., Moore, E.R., Abraham, W.R., Busse, H.J., Wanner, G. and Lubitz, W. (2001). *Sphingomonas pituitosa* sp. nov., an exopolysaccharide-producing bacterium that secretes an unusual type of sphingan. *Int J Syst Evol Microbiol*; **51** (3): 827-841.

137. Matsuyama, H., Katoh, H., Ohkushi, T., Satoh, A., Kawahara, K. and Yumoto, I. (2008). *Sphingobacterium kitahiroshimense* sp. nov., isolated from soil. *Int J Syst Evol Microbiol*; **58** (7): 1576-1579.

138. Bereschenko, L.A., Stams, A.J.M., Euverink, G.J.W. and Van Loosdrecht, M.C.M. (2010). Biofilm formation on reverse osmosis membranes is initiated and dominated by *Sphingomonas* spp. *Appl Environ Microbiol*; **76** (8): 2623-2632.

139. Xia, Y., Kong, Y. and Nielsen, P.H. (2007). In situ detection of protein-hydrolysing microorganisms in activated sludge. *FEMS microbiology ecology*; **60** (1): 156-165.

140. Dang, H. and Lovell, C.R. (2016). Microbial surface colonization and biofilm development in marine environments. *Microbiol Mol Biol Rev*; **80** (1): 91-138.

141. Xue, J., Zhang, Y., Liu, Y. and El-Din, M.G. (2016). Treatment of oil sands process-affected water (OSPW) using a membrane bioreactor with a submerged flat-sheet ceramic microfiltration membrane. *Water Res*; **88**: 1-11.

142. Thomsen, T.R., Kong, Y. and Nielsen, P.H. (2007). Ecophysiology of abundant denitrifying bacteria in activated sludge. *FEMS microbiology ecology*; **60** (3): 370-382.

143. Wu, Y., Shukal, S., Mukherjee, M. and Cao, B. (2015). Involvement in denitrification is beneficial to the biofilm lifestyle of comamonas testosteroni: a mechanistic study and its environmental implications. *Environ Sci Technol* **49**: 11551-11559.